

# **SPECTRUM EFFICIENCY OPTIMIZATION IN CELLULAR PACKET DATA COMMUNICATION**

by

**PETER H. J. CHONG**

B.ENG. (Electrical Engineering), Technical University of Nova Scotia, Canada, 1993

**A THESIS SUBMITTED IN PARTIAL FULFILLMENT OF**

**THE REQUIREMENTS FOR THE DEGREE OF**

**MASTER OF APPLIED SCIENCE**

in

**THE FACULTY OF GRADUATE STUDIES**

**DEPARTMENT OF ELECTRICAL ENGINEERING**

**We accept this thesis as conforming**

**to the required standard**

**THE UNIVERSITY OF BRITISH COLUMBIA**

**April 1996**

**© Peter H.J. Chong , 1996**

In presenting this thesis in partial fulfilment of the requirements for an advanced degree at the University of British Columbia, I agree that the Library shall make it freely available for reference and study. I further agree that permission for extensive copying of this thesis for scholarly purposes may be granted by the head of my department or by his or her representatives. It is understood that copying or publication of this thesis for financial gain shall not be allowed without my written permission.

Department of Electrical Engineering

The University of British Columbia  
Vancouver, Canada

Date April 15, 96

## Abstract

In most studies on the effect of co-channel interferers, the interference is assumed to be Gaussian. In this thesis, a more realistic simulation model of multiple co-channel interferers in a cellular *packet data* communication system using non-coherent frequency shift keying modulation is developed for a non-fading and a fading environment.

The performance of the *packet data* traffic as the number of co-channel interferers increases is investigated in terms of BER and BKER results obtained from the simulation. Other parameters studied are block length, propagation loss exponent, fading rate and background noise level. It is found that as the number of interferers increases, error rates increase except for the BER in slow Rayleigh fading which tends to be independent of the number of interferers. Eventually, the effect of the interference signal can be regarded as similar to that of Gaussian noise.

The spectrum efficiency with different system configurations and parameters is obtained by assuming that the mobile is located near the cell boundary. The influence of the cluster size on spectrum efficiency is investigated. The optimal value,  $K_{opt}$ , of the cluster size is found. In an interference-limited environment, the spectrum efficiency tends to increase with the propagation loss exponent because of the improved SIR value. It is found that the optimal spectrum efficiency can be greatly increased with the use of directional antennas. In most non-fading and very slow fading cases considered,  $K_{opt}$  is typically less than 7. However,  $K_{opt}$  increases with the fading rate. Generally, measures such as FEC taken to counteract the effects of the interference result in a smaller value of  $K_{opt}$ . However, FEC does not necessarily improve the spectrum efficiency.

# Table of Contents

<b>Abstract</b>	<b>ii</b>
<b>List of Tables</b>	<b>vi</b>
<b>List of Figures</b>	<b>ix</b>
<b>Acknowledgment</b>	<b>xiii</b>
<b>Chapter 1 Introduction</b>	<b>1</b>
1.1 Motivation and Scope of the thesis .....	2
1.2 Outline of the thesis .....	3
<b>Chapter 2 Background</b>	<b>5</b>
2.1 Review of error probability formulas.....	5
2.1.1 Non-fading Channel with AWGN .....	6
2.1.2 Fading Channel .....	8
2.2 Basic Concept of Frequency Reuse .....	10
2.2.1 Frequency Reuse Distance.....	11
2.2.2 Signal-to-Interference Ratio (SIR) Models.....	12
A SIR model for an omnidirectional antenna system.....	13
B SIR Model for a Directional Antenna System.....	15
2.2.3 Inclusion of the Second-Tier Co-channel Interferers.....	17
<b>Chapter 3 Design of the Communication System Model</b>	<b>21</b>
3.1 About SPW <sup>TM</sup> .....	21
3.1.1 Basic Tools in SPW <sup>TM</sup> .....	21
3.1.2 DSP Block Library.....	22
3.1.3 How to run SPW <sup>TM</sup> .....	22

3.2	Simulation Model .....	23
3.2.1	Transmitter structure.....	24
3.2.2	Channel Model.....	26
3.2.3	Receiver Structure.....	30
3.2.4	Desired Signal Model .....	31
3.2.5	Co-channel Interference Signals Model.....	33
3.2.6	Parameters.....	33
<b>Chapter 4</b>	<b>Simulation Results and Discussion</b>	<b>36</b>
4.1	Validation of the Simulation Model.....	36
4.1.1	Error Performance for the Basic Model.....	36
4.1.2	Comparison with Previous Results for Tone Interferers.....	39
4.2	Error Performance with Multiple Co-channel Interferers in a Non-fading Environment.....	40
4.2.1	BER Results.....	41
4.2.2	BKER Results.....	43
4.3	Error Performance with Co-channel Interferers in a very slow Rayleigh Fading Environment	
4.3.1	BER Results.....	49
4.3.2	BKER Results.....	50
4.4	Error Performance in a Rayleigh fading Environment .....	55
4.4.1	BER Results.....	55
4.4.2	BKER Results.....	56
4.5	Error Performance with the First and Second-tier Co-channel Interferers.....	57
4.5.1	BER Results.....	58

4.5.2 BKER Results .....	58
<b>Chapter 5 Spectrum Efficiency in Cellular Systems</b>	<b>60</b>
5.1 Analysis of Spectrum Efficiency .....	60
5.2 Spectrum Efficiency in a Non-fading Environment .....	62
5.2.1 Omnidirectional Antennas .....	62
5.2.2 Omnidirectional Antenna System with Forward Error Correction (FEC) .....	65
5.2.3 Directional Antenna System .....	67
5.3 Spectrum Efficiency in a (very slow) Rayleigh Fading Environment .....	70
5.3.1 Omnidirectional Antenna System .....	70
5.3.2 Omnidirectional Antenna System with FEC .....	72
5.3.3 Directional Antenna System .....	74
5.4 Spectrum Efficiency with Different Values of $f_d T_m$ .....	76
5.4.1 Omnidirectional Antenna System .....	77
5.4.2 Directional Antenna System .....	79
5.5 Consideration of the Co-channel Interferers in the Second Tier .....	81
<b>Chapter 6 Conclusions</b>	<b>84</b>
<b>Glossary</b>	<b>87</b>
<b>Bibliography</b>	<b>89</b>
<b>Appendix A Block Diagram of the Simulation Models</b>	<b>93</b>
<b>Appendix B Derivation of BER in Rayleigh Fading</b>	<b>97</b>

## List of Tables

Table 2.1	SIR (dB) for different $K$ with first-tier interferers for $\beta=4$ .....	17
Table 2.2	SIR (dB) for different $K$ with first-tier interferers for $\beta=3$ .....	17
Table 2.3	SIR (dB) with first and second-tier interferers in ideal assumption for $\beta=4$ .....	19
Table 2.4	SIR (dB) with first and second-tier interferers in conservative assumption for $\beta=4$ .....	20
Table 2.5	SIR (dB) with first and second-tier interferers in ideal assumption for $\beta=3$ .....	20
Table 3.1	Summary of the four basic tools in SPW <sup>TM</sup> .....	22
Table 3.2	Summary of DSP block libraries in SPW <sup>TM</sup> .....	23
Table 5.1	The spectrum efficiency of an omnidirectional antenna system in a non-fading environment with 6 co-channel interferers, AWGN at $\frac{E_b}{N_o}=40$ dB and $N=255$ bits.....	62
Table 5.2	The spectrum efficiency of an omnidirectional antenna system in a non-fading environment with AWGN at $\frac{E_b}{N_o}=40$ dB and $N=1023$ bits.....	63
Table 5.3	The spectrum efficiency, $E_s$ , of an omnidirectional antenna system in a non-fading environment with AWGN at $\frac{E_b}{N_o}=20$ dB and $N=255$ bits.....	64
Table 5.4	The spectrum efficiency, $E_s$ , of an omnidirectional antenna system with FEC in a non-fading environment with AWGN at $\frac{E_b}{N_o}=40$ dB and $N=255$ bits.....	65
Table 5.5	The spectrum efficiency, $E_s$ , of an omnidirectional antenna system with FEC in a non-fading environment with AWGN at $\frac{E_b}{N_o}=40$ dB and $N=1023$ .....	66
Table 5.6	The spectrum efficiency, $E_s$ , of an omnidirectional antenna system with FEC in a non-fading environment with AWGN at $\frac{E_b}{N_o}=20$ dB and $N=255$ .....	67
Table 5.7	The spectrum efficiency, $E_s$ , of a directional antenna system in a non-fading	

	environment with $\beta=4$ .....	68
Table 5.8	The spectrum efficiency, $E_s$ , of a directional antenna system in a non-fading environment with $\beta=3$ .....	69
Table 5.9	$E_s$ in an omnidirectional antenna system with very slow Rayleigh fading with AWGN at $\frac{E_b}{N_o}=40$ dB and $N=255$ bits.....	70
Table 5.10	$E_s$ in an omnidirectional antenna system with very slow Rayleigh fading with AWGN at $\frac{E_b}{N_o}=40$ dB and $N=1023$ bits.....	71
Table 5.11	$E_s$ in an omnidirectional antenna system with very slow Rayleigh fading with AWGN at $\frac{E_b}{N_o}=20$ dB and $N=255$ bits.....	72
Table 5.12	$E_s$ in an omnidirectional antenna system with FEC in a very slow Rayleigh fading environment with AWGN at $\frac{E_b}{N_o}=40$ dB and $N=255$ bits.....	73
Table 5.13	$E_s$ in an omnidirectional antenna system with FEC in a very slow Rayleigh fading environment with AWGN at $\frac{E_b}{N_o}=40$ dB and $N=1023$ bits.....	73
Table 5.14	$E_s$ in an omnidirectional antenna system with FEC in a very slow Rayleigh fading environment with AWGN at $\frac{E_b}{N_o}=20$ dB and $N=255$ bits.....	74
Table 5.15	The spectrum efficiency, $E_s$ , of a directional antenna system in a very slow fading environment with $\beta=4$ .....	75
Table 5.16	The spectrum efficiency, $E_s$ , of a directional antenna system in a very slow fading environment with $\beta=3$ .....	75
Table 5.17	The spectrum efficiency, $E_s$ , of a directional antenna system with FEC in a very slow fading environment with $\beta=4$ .....	76
Table 5.18	The spectrum efficiency, $E_s$ , in an omnidirectional antenna system in a fading environment for $f_d T_m \approx 1$ .....	77
Table 5.19	The spectrum efficiency, $E_s$ , in an omnidirectional antenna system with FEC in a fading environment for $f_d T_m \approx 1$ .....	78
Table 5.20	The spectrum efficiency, $E_s$ , in an omnidirectional antenna system in a fading	

	environment for $f_d T_m \approx 5$ .....	79
Table 5.21	The spectrum efficiency, $E_s$ , in a directional antenna system (SIR <sub>5</sub> ) in a fading environment.....	80
Table 5.22	The spectrum efficiency, $E_s$ , in a directional antenna system (SIR <sub>5</sub> ) with FEC in a fading environment.....	81
Table 5.23	$E_s$ in a non-fading environment for $N=255$ and $\frac{E_b}{N_o}=40$ dB.....	82
Table 5.24	$E_s$ in a very slow fading environment for $N=255$ and $\frac{E_b}{N_o}=40$ dB.....	83

## List of Figures

Figure 2.1	Block diagram of (a) a digital communication system (b) AWGN channel.....6	6
Figure 2.2	Locations of base stations (a) Center-excited cells (b) Corner-excited cells. ....10	10
Figure 2.3	The (normalized) Reuse Distance.....11	11
Figure 2.4	Example of downlink situation with six co-channel cells in worst case scenario. 14	14
Figure 2.5	The worst case situation with two co-channel cells in 120° directional antenna system. ....15	15
Figure 2.6	Cellular system with cluster size $K=3$ .....19	19
Figure 3.1	Block diagram of simulated system model.....24	24
Figure 3.2	Block diagram of FSK modulator.....25	25
Figure 3.3	Rayleigh cumulative distribution function.....27	27
Figure 3.4	Normalized level crossing rate of the envelope of the E field. ....28	28
Figure 3.5	Normalized durations of fade of the envelopes of the E field.....29	29
Figure 3.6	Energy detector used to demodulate the binary NCFSK signal. ....30	30
Figure 3.7	The PSD of FSK signal.....32	32
Figure 4.1	BER in a non-fading and Rayleigh fading channel with AWGN. ....37	37
Figure 4.2	BKER as a function of $\frac{E_b}{N_o}$ in a non-fading channel with block length $N=255$ bits.....38	38
Figure 4.3	BKER with no error correction as a function of $f_d T_m$ for (a) $N=255$ bits (b) $N=1023$ bits. ....38	38
Figure 4.4	$P_f(M,N)$ in a very slow Rayleigh fading channel for (a) $P_f(0,255)$ and $P_f(8,255)$ (b) $P_f(0,1023)$ and $P_f(26,1023)$ . ....39	39
Figure 4.5	BER with (a) 1 tone interferer (b) 2 tone interferers. ....40	40
Figure 4.6	BER as a function of SIR for different number of interferers in a non-fading	

	environment with AWGN at $\frac{E_b}{N_o}=40$ dB.....	41
Figure 4.7	BER with interferers in a non-fading environment with AWGN at (a) $\frac{E_b}{N_o}=20$ dB and (b) $\frac{E_b}{N_o}=10$ dB. ....	43
Figure 4.8	BKER in a non-fading environment with $\frac{E_b}{N_o}=20$ dB for $N=255$ bits. ....	45
Figure 4.9	BKER in a non-fading environment with $\frac{E_b}{N_o}=40$ dB for (a) $N=255$ bits (b) $N=1023$ bits.....	45
Figure 4.10	CDF of the number of bit errors in a non-fading environment with $\frac{E_b}{N_o}=20$ dB and SIR=4.5 dB for $N=255$ bits. ....	46
Figure 4.11	CDF of the number of bit errors in a block in a non-fading environment with $\frac{E_b}{N_o}=40$ dB for (a) SIR=3 dB and $N=255$ bits, (b) SIR=3 dB and $N=1023$ bits, (c) SIR=7 dB and $N=255$ bits and (d) SIR=7 dB and $N=1023$ bits.....	47
Figure 4.12	$P(8,255)$ as a function of SIR with $\frac{E_b}{N_o}=40$ dB.....	48
Figure 4.13	$P(26,1023)$ as a function of SIR with $\frac{E_b}{N_o}=40$ dB.....	48
Figure 4.14	BER in a very slow fading environment with AWGN at (a) $\frac{E_b}{N_o}=20$ dB and (b) $\frac{E_b}{N_o}=40$ dB.....	50
Figure 4.15	BKER with interferers in a very slow fading environment with (a) AWGN at $\frac{E_b}{N_o}=40$ dB, $N=255$ bits (b) AWGN at $\frac{E_b}{N_o}=20$ dB, $N=255$ bits and (c) AWGN at $\frac{E_b}{N_o}=40$ dB, $N=1023$ bits. ....	51

Figure 4.16	The CDF of the number of bit errors in a block at $\frac{E_b}{N_o}=40$ dB with different number of interferers for (a) $N=255$ bits and SIR=8 dB, (b) $N=255$ bits and SIR=20 dB, (c) $N=1023$ bits and SIR=8 dB and (d) $N=1023$ bits and SIR=20 dB. ....	53
Figure 4.17	The $P_f(8,255)$ and $P_f(26,1023)$ as a function of SIR in very slow Rayleigh fading with AWGN at $\frac{E_b}{N_o}=40$ dB for (a) theoretical case, (b) 2 interferers, (c) 6 interferers, (d) 12 interferers and (e) 24 interferers. ....	54
Figure 4.18	BER in a Rayleigh fading environment with interferers and AWGN at $\frac{E_b}{N_o}=40$ dB for (a) $f_d=5$ Hz, (b) $f_d=20$ Hz and (c) $f_d=100$ Hz. ....	56
Figure 4.19	BKER in a Rayleigh fading environment with interferers and AWGN at $\frac{E_b}{N_o}=40$ dB for (a) $f_d=5$ Hz and $N=1023$ bits, (b) $f_d=20$ Hz and $N=255$ bits and (c) $f_d=100$ Hz and $N=255$ bits. ....	57
Figure 4.20	BER with the first and second-tier co-channel interferers at $\frac{E_b}{N_o}=40$ dB in (a) a non-fading environment and (b) a slow Rayleigh fading environment. ....	59
Figure 4.21	BKER with first and second-tier co-channel interferers for $N=255$ bits and $\frac{E_b}{N_o}=40$ dB in (a) a non-fading environment and (b) a very slow Rayleigh fading environment. ....	59
Figure A.1	Communication model with no co-channel interferer in a non-fading environment. ....	93
Figure A.2	Communication model with 2 co-channel interferers in a non-fading environment. ....	94
Figure A.3	Communication model with no co-channel interferer in a Rayleigh fading environment. ....	95
Figure A.4	Communication model with 2 co-channel interferers in a Rayleigh fading environment. ....	96

Figure B.1 The BER for one synchronized and unsynchronized co-channel interferer in a slow Rayleigh fading channel with no background noise.....100

## **Acknowledgment**

I would like to thank my supervisor, Dr. C. Leung, for his continuous guidance and encouragement throughout the research work for this thesis. This work was supported by a U.B.C. University Graduate Fellowship, a Motorola Research Grant and NSERC Grant OGP0001731.

# Chapter 1 Introduction

As a result of the limited availability of radio frequency channels for mobile communications, spectrum efficiency is an important factor. One technique to increase this efficiency is based on the *frequency reuse* concept [19]. In frequency reuse, users in different geographic locations (different cells) can use the same frequency channel simultaneously. This way, the same sets of channels used in one coverage area can be reused in another coverage area. Although a frequency reuse scheme can improve the spectrum efficiency, it causes *co-channel interference*.

Since the same set of channels are reused in co-channel cells in the frequency reuse method, base stations or subscribers using the same channel in different cells can interfere with each other. This kind of interference is called *co-channel interference*. The *co-channel interference* can be reduced by (1) increasing the distance between co-channel cells, (2) using directional antennas, (3) lowering the height of antennas at the base station [16]. The other common type of interference in cellular systems is called *adjacent channel interference*. *Adjacent channel interference* arises when signal energy from an adjacent channel spills over into the channel of concern or when the filter on the receiver is too “loose” and captures energy from a broader band. This problem can be reduced by using proper channel assignment or a filter with a sharp falloff slope. Generally speaking, the *co-channel interference* problem is more severe than that caused by *adjacent channel interference* in mobile cellular communication systems.

At present, there is a lot of interest in data communication over cellular systems [1]. In most urban and many suburban areas, multipath fading poses the main threat to reliable data transmission. One commonly used fading model assumes that there is no *line-of-sight* path from the transmitter to the receiver [2,3,4]; this results in the amplitude of the received signal following

the Rayleigh distribution [5] and is termed *Rayleigh fading*. Generally, when a data packet encounters a fade, there is a high probability that transmission errors will occur. In order to improve performance in the presence of multipath fading, error control techniques such as automatic repeat request (ARQ) and forward error correction (FEC) must be used [6].

## 1.1 Motivation and Scope of the thesis

The effect of co-channel interference in land cellular mobile radio systems has been reported in numerous papers, e.g., [7,8,9,10,13]. In these papers, the co-channel interference probability is evaluated, but there is no bit error rate (BER) or block error rate (BKER) analysis. The BER performance has been studied in [11,12], but in these studies, the co-channel interference is assumed to be Gaussian. In [22, 26, 41], the co-channel tone interferences are assumed to be statistically independent and their phases are uniformly distributed from  $-\pi$  to  $\pi$ , but constant during one bit period. However, only the BER in a non-fading environment is studied. In this thesis, a more realistic simulation model of multiple co-channel interferers in a digital system using *non-coherent frequency shift keying* (NCFSK) modulation is developed. The performance in terms of BER and BKER is evaluated using simulation. The interference signals are also NCFSK signals. The simulation model is designed for the outbound (base to mobile) situation in which the interferers are from the fixed base stations in co-channel cells. A similar model has been used in [14,15] with Gaussian minimum shift keying (GMSK) modulation, but where only up to six co-channel interferers were considered. These papers also assume that the channel is very slowly fading (VSF), i.e. the received signal level is constant over a block. However, this simplifying assumption is often not valid in practice. In this thesis, we consider the effect on error performance of increasing the number of co-channel interferers in both non-fading (NF), slow fading

(SF) and VSF environments. In the fading situation, the desired signal and the interference signals from the surrounding co-channel cells are assumed to be subject to Rayleigh fading.

One objective of this thesis is to investigate the effect of co-channel interference in a cellular *packet data* communication system. The effects of changing various parameters, such as number of co-channel interferers, background noise level, packet length, propagation loss exponent and fading rate, are studied in both non-fading and fading environment. The performance criteria are BER, BKER and spectrum efficiency. In a frequency reuse system, the coverage area is divided into a certain number of cell clusters. A second objective is to study the influence of the cluster size on spectrum efficiency for different system configurations. The spectrum efficiency is defined as the average number of user data bits correctly received per second per cell [10, 17]. The optimum cluster size to maximize the spectrum efficiency is determined. The selection of the optimum cluster size for a cellular *voice* communication system has been previously studied [16]. It was found to be 12 for an omnidirectional antenna system and 7 for a three sector directional antenna system [19, 23]. The selection of cluster size for a cellular *packet data* communication system has been done in [17], but the interfering signals were modeled as additive white Gaussian noise (AWGN). The use of error correction and sectorization as means to improve the system performance is also considered.

## 1.2 Outline of the thesis

This thesis is organized as follows. Chapter 2 contains a brief review of some basic error probability results for several common binary modulation schemes as well as the basic concept of frequency reuse. Chapter 3 describes the simulation model which was implemented using Signal Processing Worksystem (SPW<sup>TM</sup>) [33]. The results of the simulation are described in Chapter 4.

In Chapter 5, the optimum cluster size is found for a variety of different system configurations.

The main conclusions and some recommendations for future work appear in Chapter 6.

## Chapter 2 Background

The purpose of this chapter is to present some basic error probability expressions for four different binary modulation schemes, namely *coherent phase-shift keying* (CPSK), *coherent frequency shift keying* (CFSK), *differentially coherent PSK* (DPSK) and *noncoherent FSK* (NCFSK). The formulas are based on a non-fading channel with additive white Gaussian noise (AWGN) and a very slow Rayleigh fading channel. The formulas for NCFSK are used in Chapter 4 to validate the simulation model. The second part of this chapter describes the concept of frequency reuse in a cellular system. Five different *signal-to-interference ratio* (SIR) models are discussed. The optimum cluster size depends on the particular SIR model used.

### 2.1 Review of error probability formulas

A simple block diagram of a *digital data transmission* communication system is shown in Figure 2.1(a). The communication system is referred to as *binary* if the digital signal at the modulator input consists of a sequence of pulses, each of which can take on one of two possible values. In binary digital modulation the binary waveform is superimposed on a carrier; phase modulation and frequency modulation are commonly used [18]. A digital system is referred to as *coherent* if a local phase reference is available for demodulation that is in phase with the transmitted carrier. Otherwise, it is referred to as *non-coherent*. A system is referred to as *synchronous* if a periodic signal (clock) is available at the receiver that is in synchronism with the transmitted digital signal.

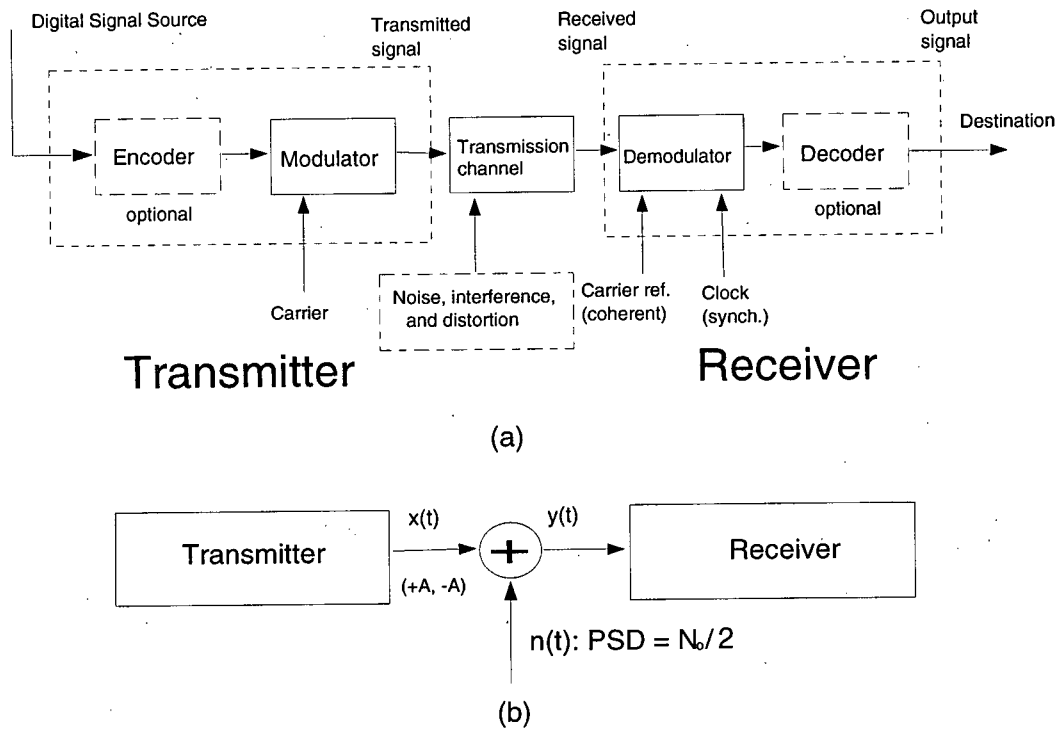


Figure 2.1 Block diagram of (a) a digital communication system (b) AWGN channel

### 2.1.1 Non-fading Channel with AWGN

The binary digital communication system with two values,  $+A$  or  $-A$ , in AWGN is illustrated in Figure 2.1(b). The channel simply adds white Gaussian noise with two-sided power spectral density (PSD)  $N_0/2$  to the signal. The bit error rate (BER) of the four binary modulation techniques are given by [35]

$$CPSK: P_e(\gamma) = \frac{1}{2} \operatorname{erfc}(\sqrt{\gamma}) \quad (2.1)$$

$$CFSK: P_e(\gamma) = \frac{1}{2} \operatorname{erfc}\left(\sqrt{\frac{\gamma}{2}}\right) \quad (2.2)$$

$$DPSK: P_e(\gamma) = \frac{1}{2} \exp(-\gamma) \quad (2.3)$$

$$NCFSK: P_e(\gamma) = \frac{1}{2} \exp\left(-\frac{\gamma}{2}\right) \quad (2.4)$$

where  $\gamma = \frac{E_b}{N_o}$  is the ratio of signal energy per bit to the one sided noise PSD. The complemen-

tary error function  $erfc(x)$  is defined as [30,44]

$$erfc(x) = 1 - \left(\frac{2}{\sqrt{\pi}}\right) \int_0^x e^{-t^2} dt = \left(\frac{2}{\sqrt{\pi}}\right) \int_x^{\infty} e^{-t^2} dt. \quad (2.5)$$

The packet data transmission is based on the transmission of a block of  $N$  bits. The performance with error correction depends on  $P(M,N)$ , the probability of more than  $M$  bit errors in a block of  $N$  bits. For CPSK, CFSK and NCFSK in AWGN, the block error rate (BKER) can be obtained by assuming that the bit errors are independent. However, this assumption is not applicable to the case of DPSK due to bit error correlation. For CPSK, CFSK and NCFSK modulation, the probability of exactly  $m$  errors in a block of  $N$  bits with independent bit errors is given by the binomial distribution

$$\binom{N}{m} P_e(\gamma)^m (1 - P_e(\gamma))^{N-m}. \quad (2.6)$$

The BKER with no error correction,  $P(0,N)$  is given by

$$P(0, N) = 1 - (1 - P_e(\gamma))^N. \quad (2.7)$$

The probability,  $P(M,N)$ , is given by

$$\begin{aligned}
P(M, N) &= \sum_{m=M+1}^N \binom{N}{m} P_e(\gamma)^m (1 - P_e(\gamma))^{N-m} \\
&= 1 - \sum_{m=0}^M \binom{N}{m} P_e(\gamma)^m (1 - P_e(\gamma))^{N-m}.
\end{aligned} \tag{2.8}$$

### 2.1.2 Fading Channel

In a fading environment, the received  $\gamma$  varies. Throughout this thesis, the fading is assumed to be non-frequency-selective (flat in frequency over the spectrum bandwidth) Rayleigh fading with different Doppler frequencies. Some theoretical results for BER in slow fading and BKER in very slow fading have been derived [18,31,35]. The slow fading assumption means that  $\gamma$  is constant over a bit. Then, the average BER,  $P_f$ , in Rayleigh fading is given by

$$P_f(\gamma_o) = \int_0^{\infty} P_e(\gamma) f(\gamma) d\gamma \tag{2.9}$$

where  $f(\gamma)$  is the probability density function (pdf) of Rayleigh fading for the instantaneous signal to noise power and is defined as

$$f(\gamma) = \frac{1}{\gamma_o} \exp\left(-\frac{\gamma}{\gamma_o}\right). \tag{2.10}$$

In (2.10),  $\gamma_o = \frac{E_a}{N_o}$  is the ratio of average energy per bit to noise PSD [18]. Substituting (2.1-2.4)

and (2.10) into (2.9) yields

$$\text{CPSK: } P_f = \frac{1}{2} \left[ 1 - \sqrt{\frac{\gamma_o}{\gamma_o + 1}} \right] \tag{2.11}$$

$$\text{CFSK: } P_f = \frac{1}{2} \left[ 1 - \sqrt{\frac{\gamma_o}{\gamma_o + 2}} \right] \quad (2.12)$$

$$\text{DPSK: } P_f = \frac{1}{2 + 2\gamma_o} \quad (2.13)$$

$$\text{NCFSK: } P_f = \frac{1}{2 + \gamma_o} \quad (2.14)$$

In a very slow fading channel, the signal strength is assumed to be constant over a block of  $N$  bits. The probability,  $P_f(M, N)$ , of more than  $M$  bit errors in a block of  $N$  bits in a very slow Rayleigh fading channel with independent bit errors is given by

$$P_f(M, N) = \int_0^{\infty} P(M, N) f(\gamma) d\gamma. \quad (2.15)$$

The derivation of  $P_f(M, N)$  for all four modulations appears in [21]. In [29], an accurate approximation to  $P_f(M, N)$  for NCFSK has been derived as

$$P_f(M, N) \approx 1 - P_f^c(0, x; r) \sum_{m=0}^M \frac{(r)_m}{m!} \quad (2.16)$$

where

$$(r)_0 = 1, (r)_m = r(r+1)\dots(r+m-1), \quad m = 1, 2, \dots \quad (2.17)$$

and

$$P_f^c(0, x; r) = 2^r \frac{\Gamma(x+1)\Gamma(1+r)}{\Gamma(x+1+r)}. \quad (2.18)$$

In (2.18),  $x$  is the number of bits in a block,  $r = \frac{2}{\gamma_0}$  and  $\Gamma(\bullet)$  denotes the gamma function [30].

## 2.2 Basic Concept of Frequency Reuse

In order to overcome the problem of scarce bandwidth in cellular mobile radio systems, frequency reuse is employed. In a frequency reuse system, a certain number of channels is assigned to a cluster of cells; the same channels can be reused in other clusters to cover different areas which are separated from one another sufficiently to result in acceptable co-channel interference. Each cluster contains the same number of cells. Each cell is viewed as the coverage area of a particular land site and visualized as having the same shape. For design purposes, the shape of the cell can be assumed to be square or hexagonal, but under some conditions the hexagonal coverage areas are expected to provide a better system configuration and has been adopted by Bell Laboratories [19]. The locations of base stations in a cell can be visualized in two different ways:

- (i) the base stations are located at the center of each cell, "center-excited" cells.
- (ii) the base stations are located at half of vertices of each cell, "corner-excited" cells.

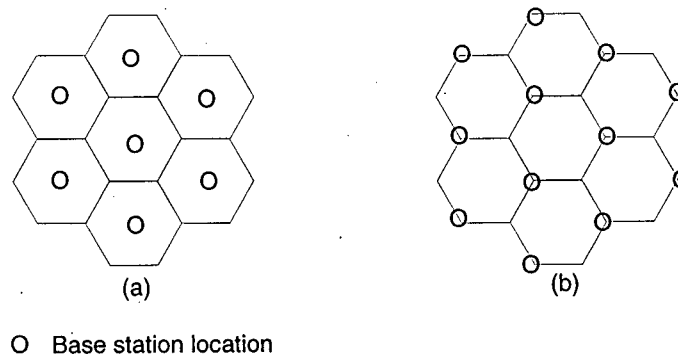


Figure 2.2 Locations of base stations (a) Center-excited cells (b) Corner-excited cells.

These two configurations are shown in Figure 2.2. In this thesis, hexagonal cells with “center excited” base stations are assumed.

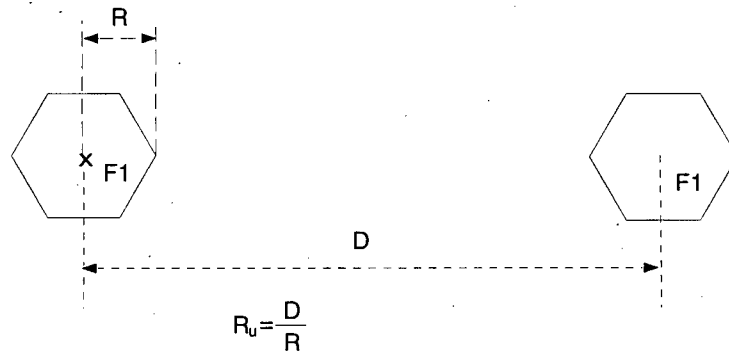


Figure 2.3 The (normalized) Reuse Distance.

### 2.2.1 Frequency Reuse Distance

Co-channel interference is a major impairment in frequency reuse systems. Cells assigned the same channels have to be separated sufficiently to ensure an acceptable level of interference. The minimum distance,  $D$ , which allows the same frequency to be reused is called the frequency reuse distance (see Figure 2.3). The (normalized) reuse distance,  $R_u$ , is defined as

$$R_u = \frac{D}{R} \quad (2.19)$$

where  $R$  is the radius of a cell, i.e. the distance from the center of a cell to any of its vertices.  $R_u$  is also related to the cluster size,  $K$ , as [19]

$$R_u = \sqrt{3K} \quad (2.20)$$

where  $K$  is given by [19]

$$K = i^2 + ij + j^2, \quad i, j=0,1,2,3,\dots \quad (2.21)$$

where  $i, j$ , are termed the “shift parameters”.

### 2.2.2 Signal-to-Interference Ratio (SIR) Models

In this section, five different SIR models will be described. In all SIR models, we consider the worst case scenario in which the mobile unit is at its own desired cell boundary. In this situation, the mobile unit will receive the weakest signal from its own desired cell but strong interference from interfering cells. The first three SIR models are obtained by using omnidirectional antennas. The last two SIR models are based on a sectorization technique using the directional antennas. Since only the outbound situation is considered here, the signal-to-interference (SIR) is defined as the ratio of the desired signal power to the total interfering power at the desired mobile receiver. This SIR can be expressed as

$$SIR = \frac{P_s}{\sum_{i=1}^M I_i} \quad (2.22)$$

where  $P_s$  is the desired signal power at the mobile receiver,  $I_i$  is the interfering power from co-channel cell  $i$  received at the mobile and  $M$  is the total number of interference cells.

In free space, the received signal power varies inversely with the square of distance. However, in mobile communication, ground-wave propagation causes more severe attenuation of the received signal power. The received power  $P_s$  can be approximated by

$$P_s \propto P_{Td} r^{-\beta} \quad (2.23)$$

where  $P_{Td}$  is the transmitted power from the desired base station,  $r$  is the distance from the desired base station to mobile and  $\beta$  is the propagation loss exponent, generally between 2 and 5.

Similarly,  $I_i$  is also inversely proportional to  $d_i^\beta$

$$I_i \propto P_{Ti} d_i^{-\beta} \quad (2.24)$$

where  $P_{Ti}$  is the transmitted power from co-channel cell  $i$  and  $d_i$  is the distance between the interfering base station in co-channel cell  $i$  and the mobile.

In case of UHF propagation in cellular radio, a typical value for  $\beta$  is 4 [20,27] for most urban and suburban areas. The relationship stated above is depicted in Figure 2.4. According to (2.23) and (2.24), the signal-to-interference ratio of (2.22) becomes

$$SIR = \frac{P_{Td} r^{-\beta}}{\sum_{i=1}^6 P_{Ti} d_i^{-\beta}} \quad (2.25)$$

In (2.25), only the six first-tier interferers are considered.

### **A SIR model for an omnidirectional antenna system**

It is shown in [19] that any cell has exactly six equidistant co-channel cells in the first tier. In [16], it is noted that the interference cells from second tier and farther are negligible to first order. Therefore, in this model, only six first-tier co-channel cells are considered and the distances from the six first-tier co-channel interfering cells are shown in Figure 2.4.

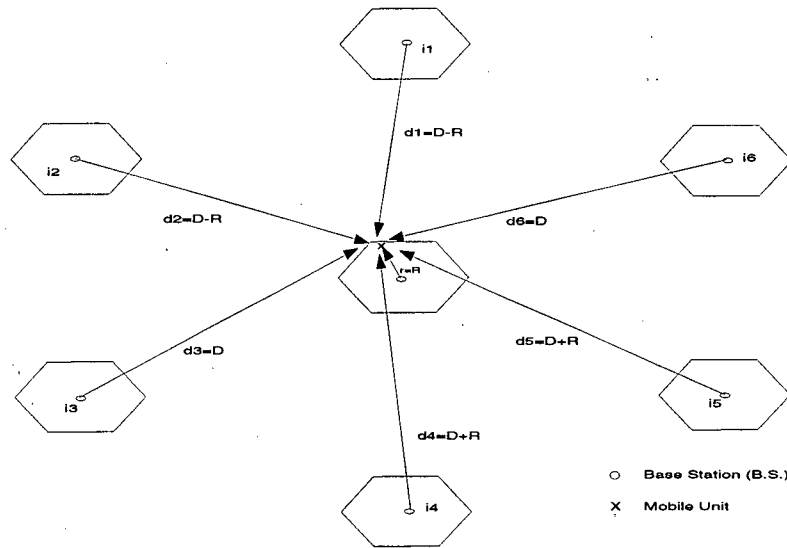


Figure 2.4 Example of downlink situation with six co-channel cells in worst case scenario.

### Model 1:

Since the transmitted power from any base station, either desired or interfering base station, are equal,  $P_{Td}$  is equal to  $P_{Ti}$  in (2.25). According to Figure 2.4, the  $SIR$  of (2.25) can be approximated by

$$SIR_1 = \frac{R^{-\beta}}{2(D-R)^{-\beta} + 2D^{-\beta} + 2(D+R)^{-\beta}}. \quad (2.26)$$

Substituting (2.20) into (2.26),  $SIR_1$  can be expressed in terms of the cluster size,  $K$ , as

$$SIR_1 = \frac{1}{2[(\sqrt{3K}-1)^{-\beta} + (\sqrt{3K})^{-\beta} + (\sqrt{3K}+1)^{-\beta}]}. \quad (2.27)$$

### Model 2:

A conservative approximation for the shortest distance between a first-tier co-channel

interferer and the mobile unit is  $D-R$ . If the shortest distance is used for all six interferers, then  $SIR_2$  is given by

$$\begin{aligned} SIR_2 &= \frac{R^{-\beta}}{6(D-R)^{-\beta}} \\ &= \frac{1}{6(\sqrt{3K}-1)^{-\beta}} \end{aligned} \quad (2.28)$$

### Model 3:

In an ideal assumption, the distance between a first-tier co-channel interferer and the mobile unit is  $D$  and so the  $SIR_3$  is given by

$$SIR_3 = \frac{1}{6(\sqrt{3k})^{-\beta}} \quad (2.29)$$

### B SIR Model for a Directional Antenna System

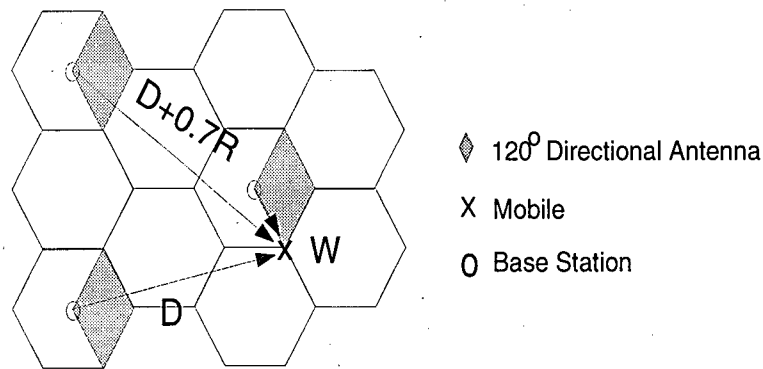


Figure 2.5 The worst case situation with two co-channel cells in  $120^\circ$  directional antenna system.

In this SIR model, a three sector cell is considered. The coverage area in each cell is divided into three sectors using  $120^\circ$  directional antennas. The number of first-tier interfering cells is reduced from six to two. The worst case situation with two interfering cells in a directional

antenna system is illustrated in Figure 2.5.

#### Model 4:

The worst case SIR occurs when the mobile is at the location  $W$  [16]. This is because the mobile receives the weakest signal from its own cell. The distance between the mobile and the two interfering cells are  $D$  and  $D+0.7R$ . The  $SIR_4$  is given by

$$SIR_4 = \frac{R^{-\beta}}{(D + 0.7R)^{-\beta} + D^{-\beta}} \quad (2.30)$$

Substituting Equation (2.20) into (2.30), we have

$$SIR_4 = \frac{1}{(\sqrt{3K} + 0.7)^{-\beta} + (\sqrt{3K})^{-\beta}} \quad (2.31)$$

#### Model 5:

A conservative value for the shortest distance between the mobile and an interfering cell is  $D$ . If this is used, (2.31) becomes

$$\begin{aligned} SIR_5 &= \frac{R^{-\beta}}{2D^{-\beta}} \\ &= \frac{1}{2(\sqrt{3K})^{-\beta}} \end{aligned} \quad (2.32)$$

The SIR values of the five SIR models corresponding to different values of  $K$  with six first-tier co-channel interferers for  $\beta = 4$  are shown in Table 2.1. For  $\beta = 3$ , the SIR values are shown in Table 2.2. It can be seen that the SIR values for  $\beta = 3$  are much smaller than those for

$\beta = 4$ . Therefore, the degradation with co-channel interferers increases for smaller  $\beta$ .

**Table 2.1: SIR (dB) for different  $K$  with first-tier interferers for  $\beta=4$ .**

K	SIR <sub>1</sub>	SIR <sub>2</sub>	SIR <sub>3</sub>	SIR <sub>4</sub>	SIR <sub>5</sub>
1	-8.6	-13.2	1.76	8.5	6.53
3	8.0	4.26	11.3	17.5	16.1
4	11.4	7.88	13.8	19.9	18.6
7	17.3	14.4	18.6	24.5	23.4
9	19.8	17.1	20.8	26.6	25.6
12	22.5	20.2	23.3	29	28.1
13	23.3	21.0	24.0	29.6	28.8
16	25.2	23.1	25.8	31.4	30.6
19	26.8	24.9	27.3	32.8	32.1

**Table 2.2: SIR (dB) for different  $K$  with first-tier interferers for  $\beta=3$ .**

K	SIR <sub>1</sub>	SIR <sub>2</sub>	SIR <sub>3</sub>	SIR <sub>4</sub>	SIR <sub>5</sub>
1	-7.47	-11.85	-0.62	5.82	4.15
3	4.49	1.25	6.53	12.46	11.30
4	6.90	3.97	8.41	14.21	13.18
7	11.2	8.84	12.05	17.65	16.82
9	13.03	10.90	13.69	19.21	18.46
12	15.07	13.19	15.56	21.0	20.33
13	15.63	13.81	16.08	21.49	20.86
16	17.07	15.41	17.44	22.79	22.2
19	18.25	16.71	18.56	23.87	23.33

### 2.2.3 Inclusion of the Second-Tier Co-channel Interferers

In a fully equipped hexagonal-shaped cellular system, there are always six co-channel interferers in each tier as shown in Figure 2.6. It can be shown that the distances between the center of the desired cell and the second-tier cells are approximately equal to  $2D\cos(\frac{\pi}{6})$ . For an

ideal assumption, the maximum distance between the mobile and the second-tier co-channel interferer is approximately equal to  $2D\cos(\frac{\pi}{6})$ . If the six second-tier interferers are included, the SIR can be obtained by adding the term  $6(1.732\sqrt{3K})^{-\beta}$  to the denominator of (2.27), (2.28) and (2.29) in an omnidirectional antenna system. For a directional antenna system, the number of second-tier interferers is reduced from six to two and the SIR is obtained by adding the term  $2(1.732\sqrt{3K})^{-\beta}$  to the denominator of (2.31) and (2.32). For a conservative assumption, the shortest distance between a second-tier co-channel interferer and the mobile is  $2D\cos(\frac{\pi}{6}) - R$  in an omnidirectional antenna system and so the term  $6(1.732\sqrt{3K})^{-\beta}$  is replaced by  $6(1.732\sqrt{3K} - 1)^{-\beta}$ . For a directional antenna system, the shortest distance is approximately equal to  $2D\cos(\frac{\pi}{6})$  and therefore SIR has the same value for both ideal and conservative assumption.

Table 2.3 shows the SIR values for five different models with the first and second tier interferers of the ideal assumption for  $\beta = 4$ . For conservative assumption, the SIR values are shown in Table 2.4. In Table 2.4, only  $SIR_1$ ,  $SIR_2$  and  $SIR_3$  are shown because  $SIR_4$  and  $SIR_5$  have the same values for both ideal and conservative assumption. When the second-tier interferers are considered, the difference between the ideal and conservative assumption is less than 0.5 dB, except for  $K=1$ . The ideal assumption of the SIR values for  $\beta = 3$  is shown in Table 2.5. The SIR values are significantly lower than for  $\beta=4$ . It can be seen that the SIR values in Tables 2.3, 2.4 and 2.5 are less than the SIR values in Tables 2.1 and 2.2 by approximately 1 dB for any  $K$ . Therefore, the effect of the second-tier interferers is quite small and can usually be neglected.

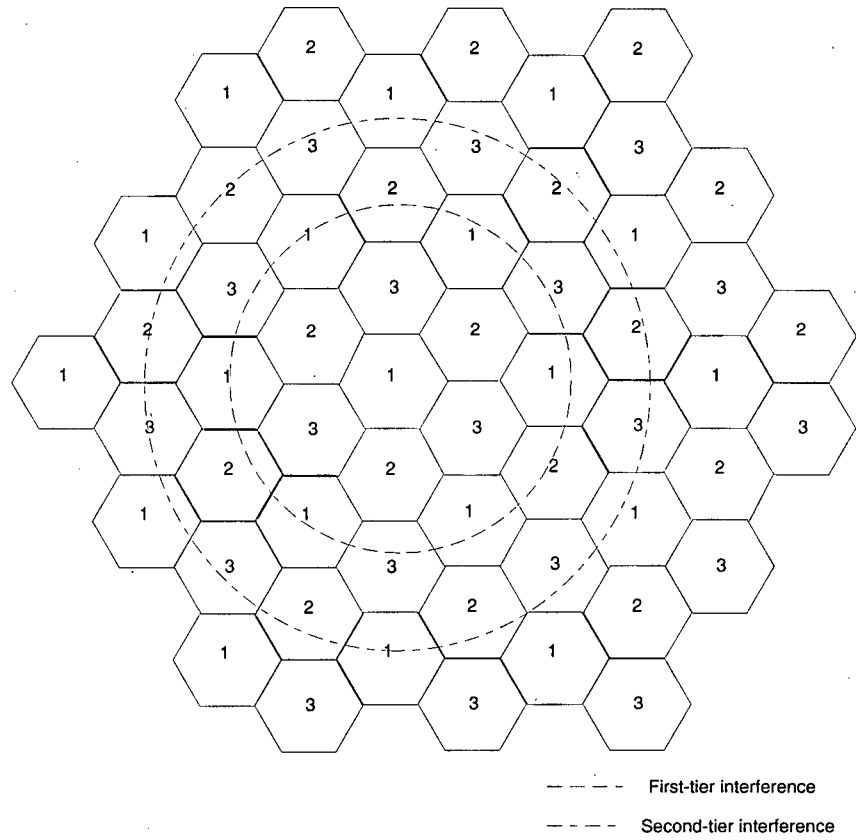


Figure 2.6 Cellular system with cluster size  $K=3$ .

Table 2.3: SIR (dB) with first and second-tier interferers in ideal assumption for  $\beta=4$ .

K	SIR <sub>1</sub>	SIR <sub>2</sub>	SIR <sub>3</sub>	SIR <sub>4</sub>	SIR <sub>5</sub>
1	-8.6	-13.2	1.3	7.8	6.07
3	7.8	4.2	10.8	16.9	15.6
4	11.1	7.8	13.3	19.3	18.1
7	16.9	14.2	18.2	23.9	22.9
9	19.4	16.9	20.4	26.0	25.2
12	22.2	20.0	22.9	28.4	27.7
13	22.9	20.8	23.6	29.1	28.4
16	24.8	22.9	25.4	30.8	30.2
19	26.4	24.6	26.9	32.3	31.6

**Table 2.4: SIR (dB) with first and second-tier interferers in conservative assumption for  $\beta=4$ .**

K	SIR <sub>1</sub>	SIR <sub>2</sub>	SIR <sub>3</sub>
1	-8.8	-13.3	-0.18
3	7.5	4.0	10.3
4	10.8	7.64	12.9
7	16.7	14.1	17.9
9	19.2	16.8	20.1
12	22.0	19.8	22.7
13	22.7	20.7	23.4
16	24.7	22.8	25.2
19	26.3	24.5	26.7

**Table 2.5: SIR (dB) with first and second-tier interferers in ideal assumption for  $\beta=3$ .**

K	SIR <sub>1</sub>	SIR <sub>2</sub>	SIR <sub>3</sub>	SIR <sub>4</sub>	SIR <sub>5</sub>
1	-7.64	-11.91	-1.39	4.74	3.38
3	4.0	1.01	5.77	11.49	10.54
4	6.34	3.68	7.64	13.26	12.41
7	10.57	8.46	11.29	16.74	16.06
9	12.37	10.48	12.92	18.31	17.7
12	14.38	12.73	14.80	20.12	19.57
13	14.94	13.34	15.32	20.62	20.09
16	16.36	14.91	16.67	21.93	21.44
19	17.53	16.19	17.79	23.01	22.56

## **Chapter 3 Design of the Communication System Model**

Two important issues in the design of communication systems are performance evaluation and trade-off analysis. Unfortunately, it is difficult to evaluate the performance of complex systems using analytical techniques unless idealized or oversimplified models are adopted. Thus, computer-aided techniques provide a useful and effective solution to the problem of system performance evaluation. The computer-aided techniques for system analysis and design fall into two categories: formula-based method and simulation-based method. This thesis uses the simulation-based method. The software simulation tool is Signal Processing Worksystem (SPW<sup>TM</sup>) [33]. In this chapter, a brief description of SPW<sup>TM</sup> and its functions is first given. Then, the overall design of the communication system model used in the simulation is described.

### **3.1 About SPW<sup>TM</sup>**

SPW<sup>TM</sup> is a powerful software tool for developing, simulating, debugging, and evaluating digital signal processing (DSP) and communication systems. It provides a graphical user interface for all aspects of system design, simulation and implementation. The software is divided into program modules that run interactively and concurrently under a “windowing” environment on a computer workstation. SPW<sup>TM</sup> provides tools and a DSP library block for users to design DSP systems easily.

#### **3.1.1 Basic Tools in SPW<sup>TM</sup>**

SPW<sup>TM</sup> provides many tools to implement, test, and simulate a communication system. The basic tools are the File Manager, Block Diagram Editor (BDE), Signal Calculator (SigCalc) and Simulate Program Builder (SPB). Table 3.1 summarizes the functions of each tool.

Table 3.1 Summary of the four basic tools in SPW<sup>TM</sup>

Name of tool	Function
File Manager	This tool is a unified “windowing” tool that can manage all types of SPW <sup>TM</sup> data files. The SigCalc, BDE, and other libraries and data files can be selected from the File Manager.
Block Diagram Editor (BDE)	This is the basic design environment of SPW <sup>TM</sup> . The BDE is used to create and edit DSP system models and allows access to signal processing blocks in the DSP block libraries.
Signal Calculator (Sig-Calc)	This tool can create, display, edit, process and analyze signal waveforms. The waveforms can be input or output signals in BDE block diagram. It can handle many signal value types, such as real, complex and vector etc.
Simulation Program Builder (SPB)	SPB is the SPW <sup>TM</sup> simulator. It analyzes the performance of a system design that was created using the BDE along with signals created under SigCalc. The signals are displayed in SigCalc.

In addition to the above basic tools, there are optional tools available in SPW<sup>TM</sup> to increase design versatility. Detail can be found in [34].

### 3.1.2 DSP Block Library

The blocks in the DSP block library can be used in BDE to build models of signal processing systems. Each block can be modified or combined with other blocks to create new functional blocks. The library contains general purpose digital signal processing and communication blocks. The blocks are stored in separate libraries and summarized in Table 3.2. “Custom-coded” blocks can be created if the existing blocks in the libraries are not adequate.

### 3.1.3 How to run SPW<sup>TM</sup>

In order to simulate a system we must first construct a block diagram of the system in BDE by using the functional blocks in DSP libraries. When a block diagram is finished, it is saved in the database. To start a simulation, we recall the block diagram, set parameter values, and use the SPB. The results of a simulation are displayed and analyzed in the SigCalc which provides a

variety of plots including time domain plots, frequency domain plots and other displays.

Table 3.2 Summary of DSP block libraries in SPW<sup>TM</sup>

Library Name	Content
Adaptive (adapt) library	It contains Least-Means Squared (LMS) and Recursive Least Square (RLS) adaptive filter blocks.
Communication (comm) library	It contains a set of blocks for communication design applications: encoders/decoders, modulators/demodulators, estimator etc.
Filter (filt) library	It contains the filter blocks of various types: frequency domain, time domain, Bessel, Chebyshev etc.
Instrument (iil) library	It contains blocks which facilitate the interface of SPW <sup>TM</sup> with HP and Acurex 7000 MDAS devices.
The SPB library	It contains the basic signal processing blocks such as linear and non-linear processing blocks, math processing blocks etc.

### 3.2 Simulation Model

In any communication system, there are three basic components: the transmitter, channel, and receiver as shown in Figure 2.1 (a). A block diagram of various parts of the simulated communication system model is illustrated in Figure 3.1. The output of the data source is generated by a pseudo-random bit generator. The FSK signal is generated by feeding the data into a FSK modulator. It is then transmitted through the mobile radio channel. The channel contains the multiplicative process of Rayleigh fading and the additive processes of co-channel interference and AWGN. Finally, the received signal is supplied to a NCFSK demodulator.

In this section, we describe each component in the simulation model in detail. The block diagram of the model created by the SPW<sup>TM</sup> for four different cases are shown in Appendix A. The four cases are 1) non-fading environment with no interference, 2) non-fading environment with interference, 3) fading environment with no interference and 4) fading environment with interference.

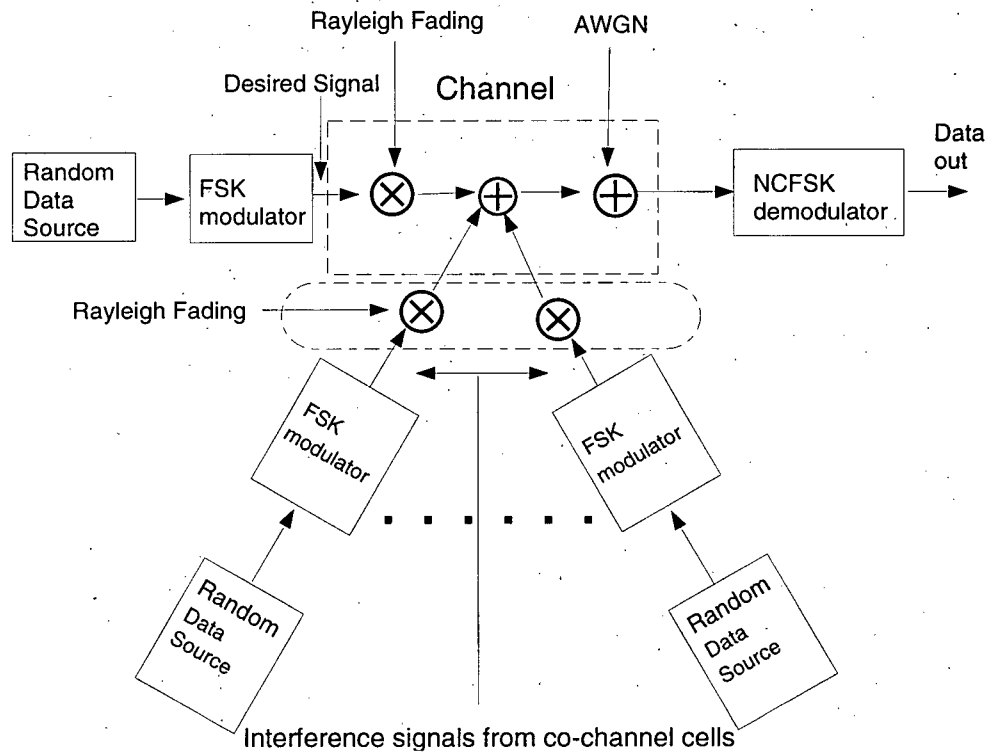


Figure 3.1 Block diagram of simulated system model.

### 3.2.1 Transmitter structure

The transmitter, as shown in Appendix A, consists of two major components, random binary data source and FSK modulator. The functional block, “DATA RANDOM”, from (comm) library generates a random bit stream in the form of a pseudonoise (P.N.) sequence with a period of  $2^n - 1$ , where  $n$  is the order of the shift register (maximum of 34).

In a binary FSK modulation system, two sinusoidal waves of the same amplitude  $A_c$  but different frequencies,  $f_1$ , “mark” frequency and,  $f_2$ , “space” frequency, are used to represent binary symbol 1 and 0 respectively. The FSK signal in this model is generated by switching the transmitter output line between two different oscillators controlled by the digital signal  $x(t)$  as shown in Figure 3.2.

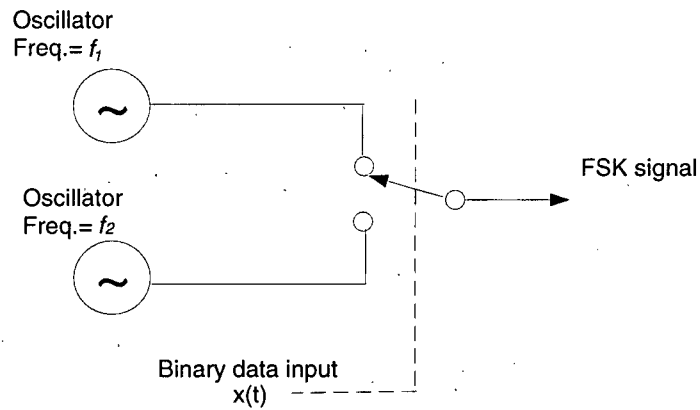


Figure 3.2 Block diagram of FSK modulator.

The modulated signal is called discontinuous-phase FSK since the phase  $\theta(t)$  is discontinuous at the switching times. The general expression for a discontinuous-phase FSK signal  $s(t)$  is given by

$$s(t) = \begin{cases} A_c \cos(2\pi f_1 t + \theta_1), & 0 \leq t \leq T_b \\ A_c \cos(2\pi f_2 t + \theta_2), & 0 \leq t \leq T_b \end{cases} \quad (3.1)$$

where  $T_b = 1/R_b$  is the bit period and  $\theta_1$  and  $\theta_2$  are the initial phases of the two oscillators. The digital frequency modulation index [35] is defined as

$$h = 2f_v T_b \quad (3.2)$$

where  $f_v = f_2 - f_1$  is the peak frequency deviation, assuming that  $f_2 > f_1$ . A continuous-phase FSK signal can be generated if  $h$  is an integer number.

### 3.2.2 Channel Model

The non-fading channel with AWGN is simulated from the functional block “NOISE GENERATOR”. This block generates pseudo-random numbers which conform to a normal distribution. The white Gaussian noise is generated with zero mean, and with variance,  $\sigma^2$ , adjusted to provide the desired  $\frac{E_b}{N_o}$ .

In the fading models, both the desired signal and the interfering signals undergo Rayleigh fading [2,3,4], because we assume that there is no line of sight between the transmitter and receiver in the cellular mobile radio system. In Appendix A, the ‘custom-coded’ functional block “Rayleigh” used in the model implements a non-frequency-selective (flat) Rayleigh fading channel. The Rayleigh fading waveform that arises due to multipath propagation is generated using the method of ‘filtered Gaussian noise’ [36,37]. This method is to construct a fading signal from in-phase and quadrature Gaussian noise sources. Because the envelope of a complex Gaussian noise process has a Rayleigh probability density function (pdf), the output of such a simulator accurately simulates Rayleigh fading. The output of the block “Rayleigh” is generated by passing in-phase and quadrature white Gaussian noise through a fading filter, and then interpolating the output of the fading filter. The frequency response of the fading filter, also known as the spectrum shaping filter, is based on Jakes’ model [25] and given by

$$H(f) = \begin{cases} \left[1 - \left(\frac{f - f_c}{f_d}\right)^2\right]^{-\frac{1}{2}} & \text{for } |f| \leq f_d \\ 0 & \text{for } |f| > f_d \end{cases} \quad (3.3)$$

where  $f_c$  is the carrier frequency and  $f_d$  is the Doppler frequency.

The Rayleigh pdf for the signal amplitude,  $r$ , is represented by

$$p(r) = \frac{r}{\bar{r}^2/2} \exp\left(-\frac{r^2}{\bar{r}^2}\right) \quad (3.4)$$

where  $\bar{r}^2$  is the mean signal power. The Rayleigh cumulative distribution function (CDF) is obtained by integrating (3.4):

$$P(r \leq R) = \int_0^R p(r) dr = 1 - \exp\left(-\frac{R^2}{\bar{r}^2}\right). \quad (3.5)$$

The simulation results obtained from the functional block “Rayleigh” and the theoretical curve of (3.5) for Rayleigh CDF are illustrated in Figure 3.3. It can be seen that the simulation results agree closely with the theoretical curve.

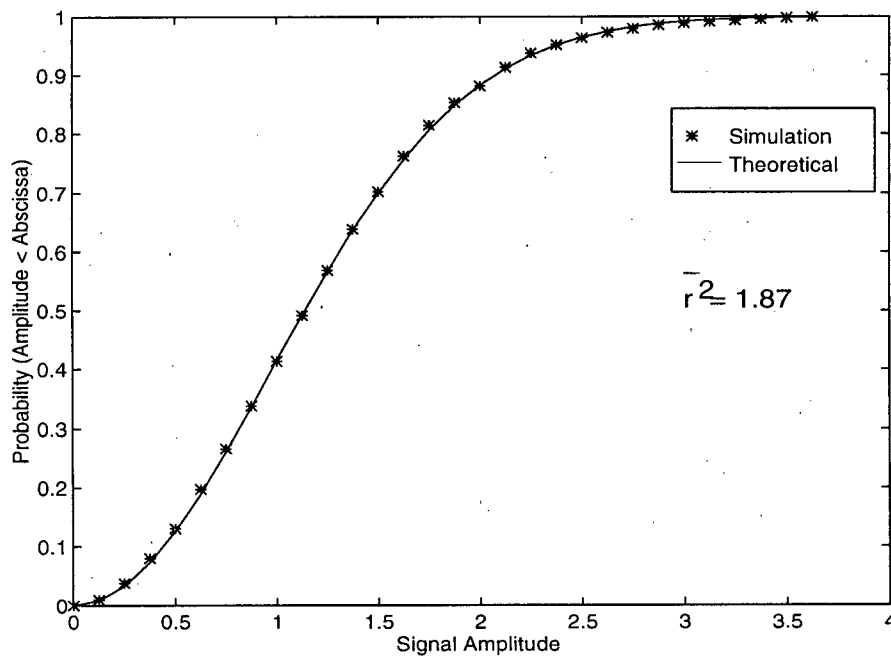


Figure 3.3 Rayleigh cumulative distribution function.

The CDF is a first-order statistic because it is not a function of time [27]. Second order statistics include the level crossing rate (LCR) and average fade duration (AFD) which are related to vehicle speeds. The LCR,  $N_R$ , is defined as the expected rate which the envelope crosses a specified signal level,  $r=R$ , in the positive direction. The expression for the LCR of the envelope of an  $E_Z$  field signal is [25]

$$N_R = \sqrt{2\pi} f_d \rho \exp(-\rho^2), \quad (3.6)$$

where  $f_d$  is the Doppler frequency and

$$\rho = \frac{R}{R_{rms}}. \quad (3.7)$$

The expression in (3.6) for LCR is plotted in Figure 3.4 along with results from the simulation. In Figure 3.4,  $R_{rms}$  is 1.367 and  $f_d$  is 40 Hz.

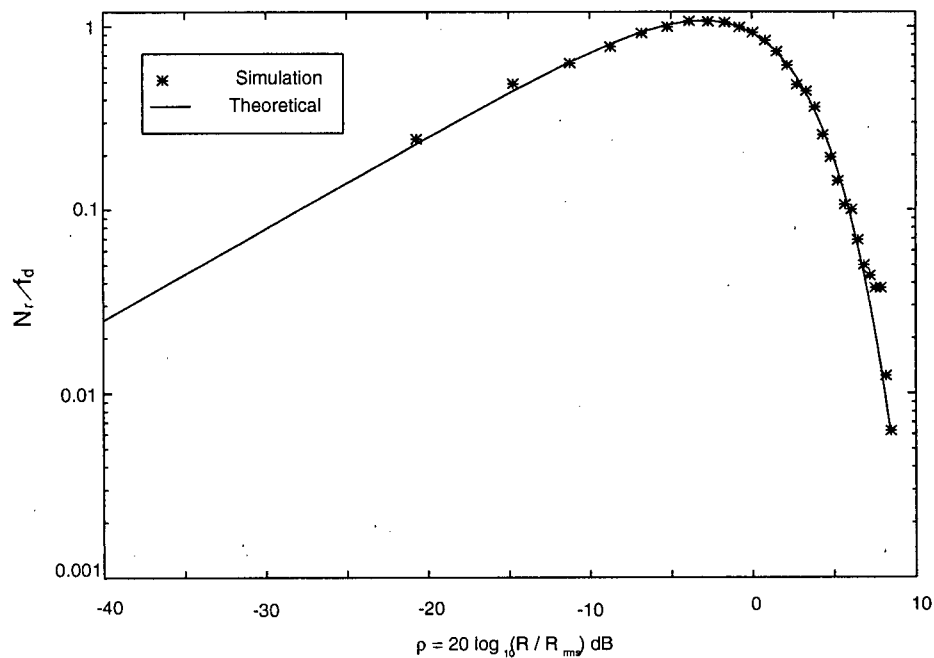


Figure 3.4 Normalized level crossing rate of the envelope of the  $E_Z$  field.

The AFD is defined as the average duration of fades below a signal level  $r < R$ . The AFD,  $\bar{\tau}$ , of the  $E_Z$  field is [25]

$$\bar{\tau} = \frac{\exp(\rho^2) - 1}{\rho f_d \sqrt{2\pi}}. \quad (3.8)$$

The expression in (3.8) for AFD and the simulation results are plotted in Figure 3.5.

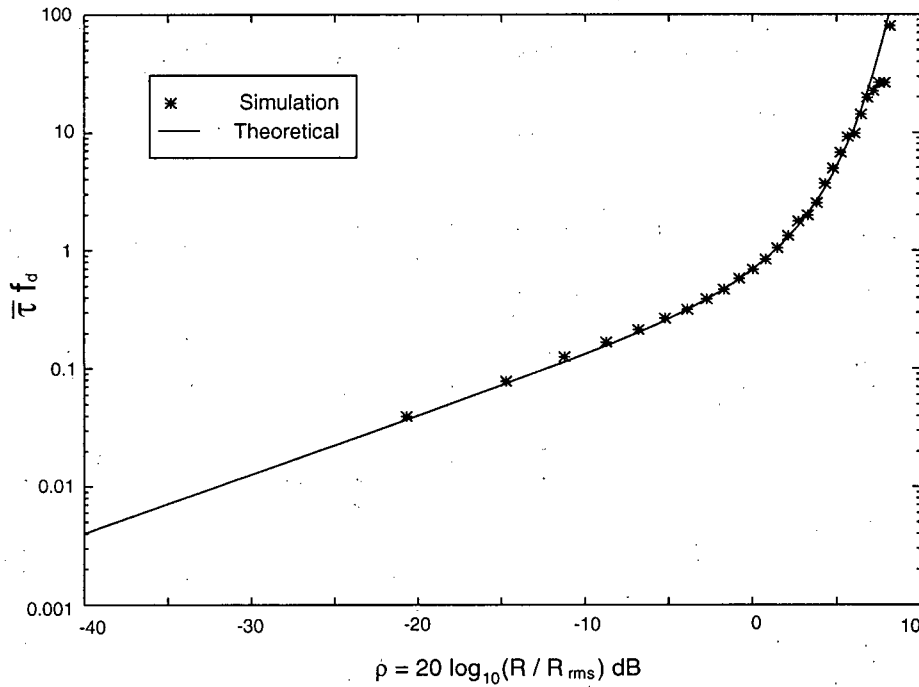


Figure 3.5 Normalized durations of fade of the envelopes of the  $E_Z$  field.

First order and second order statistics of the functional block “Rayleigh” obtained from the simulation were compared with theoretical results. It was found that the simulation results agree very well with the theoretical results.

### 3.2.3 Receiver Structure

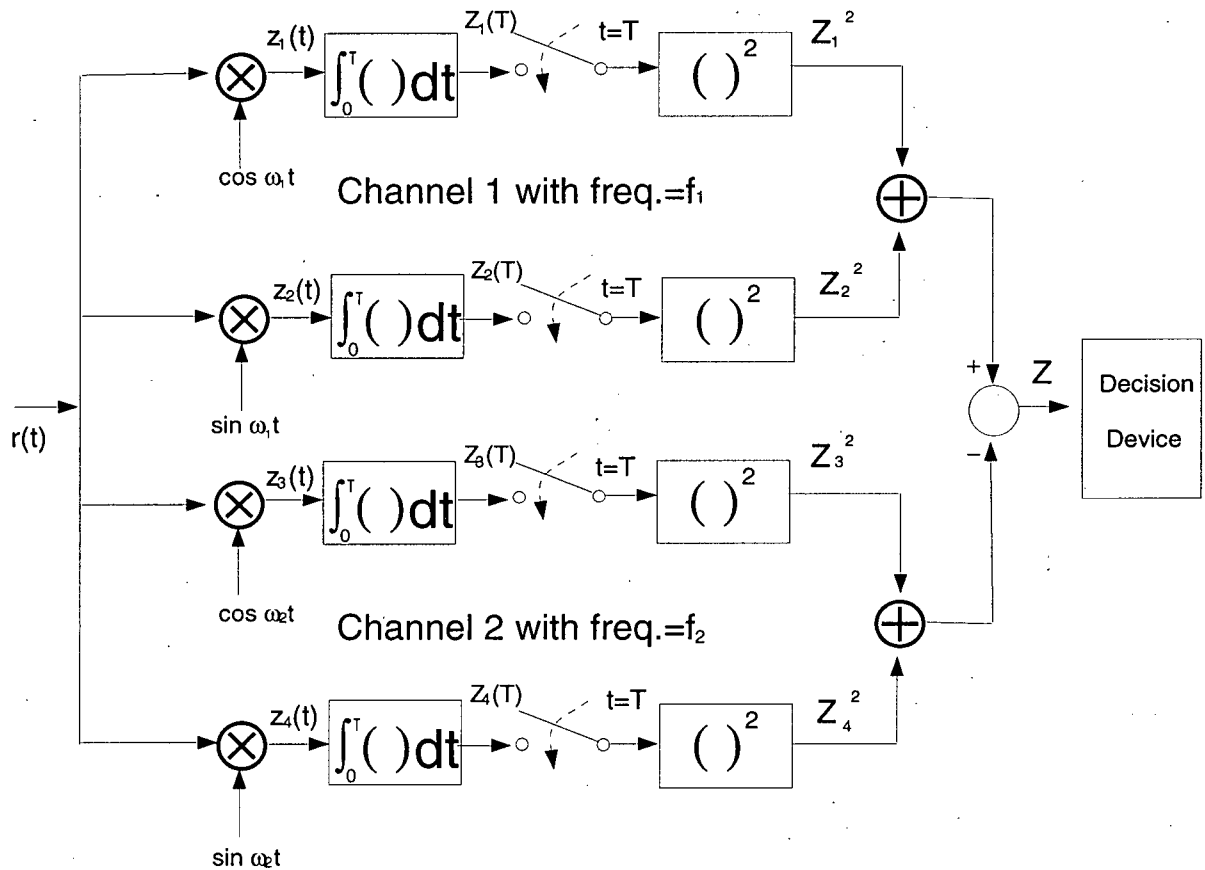


Figure 3.6 Energy detector used to demodulate the binary NCFSK signal.

The FSK signal is demodulated using an energy detector as shown in Figure 3.6. The energy detector is implemented by a correlator and a squarer. With no co-channel interference and noise distortion, the received signal corresponding to “mark” is given by

$$r(t) = A_c \sin(\omega_1 t + \theta_1). \quad (3.9)$$

Referring to Figure 3.6, we have

$$\begin{aligned} z_1(t) &= \cos(\omega_1 t) A_c \sin(\omega_1 t + \theta_1) \\ &= \frac{A_c}{2} [\sin \theta_1 + \sin(2\omega_1 t + \theta_1)]. \end{aligned} \quad (3.10)$$

Also,

$$\begin{aligned} Z_1(T) &= \frac{A_c}{2} \int_0^T \sin\theta_1 + \sin(2\omega_1 t + \theta_1) dt \\ &= \frac{A_c T}{2} \sin\theta_1, \end{aligned} \quad (3.11)$$

where  $T$  is equal to  $T_b$ . The value of the output of the squarer is

$$Z_1^2 = \frac{A_c^2 T^2}{4} (\sin\theta_1)^2. \quad (3.12)$$

In a similar way, the value of  $Z_2^2$ ,  $Z_3^2$  and  $Z_4^2$  can be obtained as  $\frac{A_c^2 T^2}{4} (\cos\theta_1)^2$ , 0 and 0 respec-

tively. The resulting value of  $Z$  is equal to  $\frac{A_c^2 T^2}{4}$ , which is independent of the phase of the received signal. The energy detector can thus be used as a non-coherent demodulator for a binary NCFSK signal.

### 3.2.4 Desired Signal Model

Since the non-coherent demodulator is used, the phase information of the desired signal is not important for the demodulation. With co-channel interference, the error performance depends on the relative phase angle between the co-channel interference and the desired signal. Without loss of generality, the phase of the desired signal is arbitrary chosen as 0 at  $t = 0$ . The transmitter will send a stream of data, 0 or 1. There is no delay for the desired signal from the transmitter to receiver. We assume that the receiver is bit synchronized with the transmitter.

The exact PSD for FSK signals is difficult to evaluate for the case of random data modulation so that it is difficult to accurately determine the bandwidth. In [24], it is stated that the bandwidth requirement of FSK is somewhat larger than that of binary PSK. The bandwidth containing 90% of the total power of binary PSK is about  $2R_b$  [18,24]. The PSD of the FSK signal obtained from the simulation is shown in Figure 3.7. The values of  $f_1$  and  $f_2$  are 20 and 40 kHz respectively. The bit rate,  $R_b$ , is 5 kbit/s. It is found that the 90% bandwidth per channel is about  $1.1R_b$ . Therefore, the total 90% bandwidth is about  $2.2R_b$ . Throughout this thesis, we assume the bandwidth of the FSK signal to be  $2.2R_b$ .

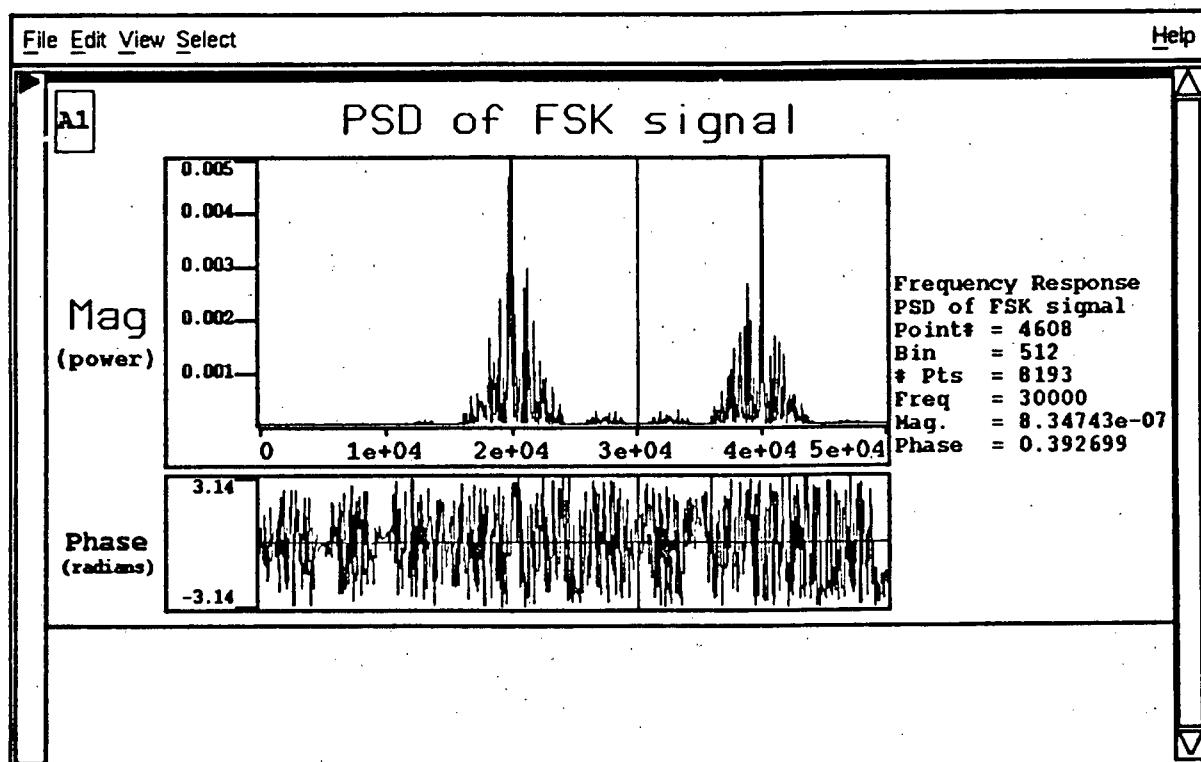


Figure 3.7 The PSD of FSK signal.

### 3.2.5 Co-channel Interference Signals Model

The co-channel interference signals, like the desired signal, are also FSK signals. The data bits for each co-channel interferer are assumed to be independent. All transmitters send data in blocks of  $N$  bits. The arrival times of data blocks at the receiver are independent and delayed relative to the desired block by a random amount which is uniformly distributed between 0 and  $T_b$ . The fading channel for each interference signal is assumed to be independent because the signals are transmitted from co-channel interferers in different locations. Hence, in the simulation model in Figure A.4, each co-channel interferer is transmitted through an uncorrelated (Rayleigh) fading channel. The power of each interference signal is attenuated as a function of the distance between the mobile in the desired cell and the base station of the interfering cell.

### 3.2.6 Parameters

In this section, the function and description of each parameter used in the simulation are explained.

#### (1) sampling freq

The '*sampling freq*' is the number of samples per second. In our model, '*sampling freq*' is set at 480000 samples per second (e.g., see Figure A.1).

#### (2) freq 1

The '*freq 1*' is the "mark" channel frequency used to represent symbol 1. The value of '*freq 1*' is set at 20 kHz in the model (e.g., see Figure A.1).

**(3) freq 2**

The 'freq 2' is the "space" channel frequency used to represent symbol 0. The value of 'freq 2' is set at 40 kHz in the model.

**(4) var (ref. Figure A.1)**

The 'var' is the variance of the Gaussian noise with zero mean. In this thesis, error rates are usually expressed in terms of  $\frac{E_b}{N_o}$ . The relationship between the 'E<sub>b</sub>/N<sub>o</sub>' and 'signal-to-noise' power ratio (SNR) is

$$\frac{P_s}{\sigma^2} = \frac{E_b R_b}{N_o B_n} \quad (3.13)$$

where  $P_s$  is the signal power,  $\sigma^2$  is the noise power,  $R_b$  is the bit rate and  $B_n$  is the equivalent noise bandwidth in the receiver. In the simulation,  $B_n$  is equal to half of the sampling frequency. Thus, the power of the Gaussian noise used in the simulation can be calculated as

$$\sigma^2 = \frac{P_s B_n}{R_b (E_b/N_o)} \quad (3.14)$$

**(5) bit rate**

The 'bit rate',  $R_b$ , refers to the bit rate for the both desired and interference signals. In our model, the bit rate is 5 kbit/second. Therefore, the number of samples per bit is 96 samples/bit.

**(6) bit/bk**

The 'bit/bk' is the total number,  $N$ , of bits in a data block.

**(7) signal power**

The 'signal power' is the desired signal power received at the mobile.

**(8) tot inter power**

The 'tot inter power' is the total interference power received at the mobile.

**(9) doppler freq (see. Figure A.3)**

The 'doppler freq' is the Doppler frequency,  $f_d$ , defined as

$$f_d = \frac{V}{\lambda} \quad (3.15)$$

where  $V$  is the vehicle speed in meter/second, and  $\lambda$  is carrier wavelength in meters. For example, at  $f_c=900$  MHz and  $V=60$  km/s,  $f_d=50$  Hz.

Although the simulation is done at baseband, the error performance is the same as at the carrier frequency since the error performance does not depend on the carrier frequency. For a given ' $E_b/N_o$ ', the variance of the Gaussian noise can be obtained using (3.14). The 'signal-to-

interference' power ratio (SIR) is given by  $SIR = \frac{\text{Signal Power}}{\text{Total Interference Power}}$ .

## Chapter 4 Simulation Results and Discussion

Initially, it is necessary to provide a validation of the simulation process. Thus, the simulation model is first validated in this chapter. Then, the simulation results for four cases as mentioned in Chapter 3 will be presented and analyzed. The results presented include the BER, BKER without and with error correction and the CDF of the number of bit errors in a block. For most of the simulation points obtained, the 99% confidence interval is within  $\pm 5\%$  of the average values shown. The worst case is within  $\pm 8\%$ .

### 4.1 Validation of the Simulation Model

In the first part of this section, the BER and BKER obtained from the basic model<sup>1</sup> in both non-fading and Rayleigh fading channels are compared with the theoretical results from Chapter 2. Then, the BER with multiple co-channel interferers in a non-fading channel, as shown in Figure A.2, is compared with results from [22,26].

#### 4.1.1 Error Performance for the Basic Model

The BER values obtained from the simulation are shown in Figure 4.1 for both a non-fading and a slow fading channel with AWGN. The theoretical results for the non-fading and fading channels are obtained from (2.4) and (2.14) respectively. The slow fading condition implies that  $f_d T_b \ll 1$  [31] so that the signal strength remains constant over a bit. In Figure 4.1, the parameter  $f_d$  used for the simulation is equal to 40 Hz and so  $f_d T_b = 0.008$ . The simulation results agree closely with the theoretical curves.

---

<sup>1</sup> The basic model refers to the communication model without co-channel interferer as shown in Figure A.1 and Figure A.3.

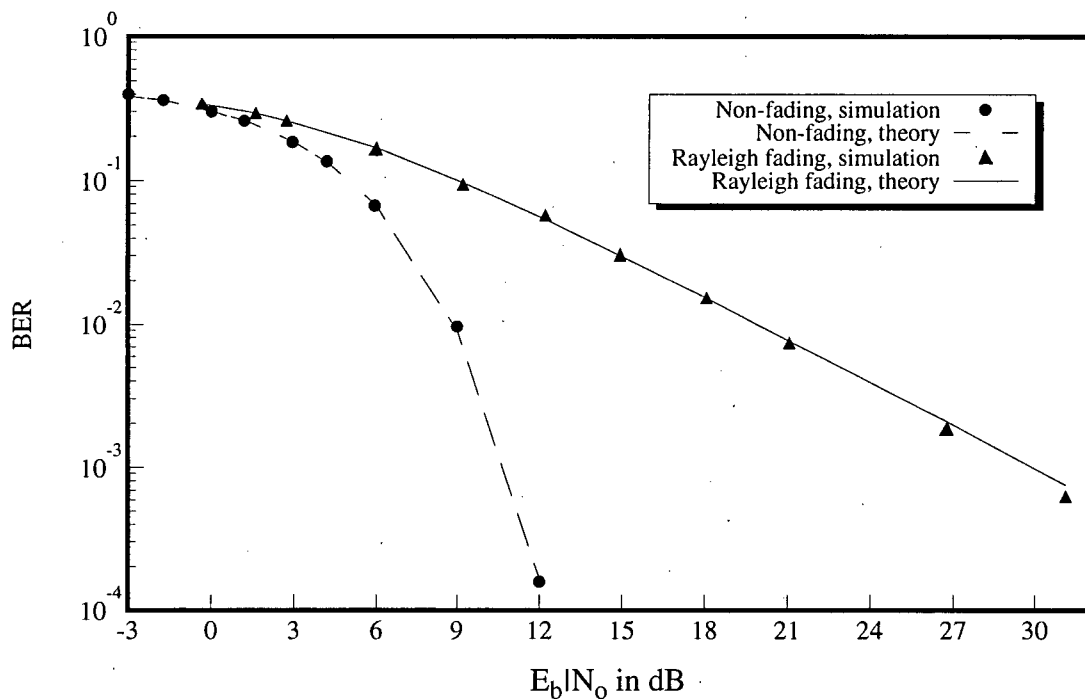


Figure 4.1 BER in a non-fading and Rayleigh fading channel with AWGN.

The BKER assuming correction of up to  $M$  bit errors in a block of length  $N$  bits is given by  $P(M, N)$ . The curves for  $P(0, 255)$ ,  $P(1, 255)$  and  $P(2, 255)$  obtained from simulation and (2.7) and (2.8) in a non-fading channel with AWGN are depicted in Figure 4.2. In a very slow fading channel, the product of  $f_d T_m$ , where  $T_m$  is time duration for a block of data, must be much less than 1 so that the signal can be assumed to be constant over a block. The BKER as a function of  $f_d T_m$  for  $\frac{E_b}{N_0} \approx 18$  dB are plotted in Figure 4.3 (a) and (b) for  $N=255$  and 1023 bits respectively.

The theoretical BKER in very slow fading is obtained from (2.16). In Figures 4.3 (a) and (b), the simulation results are close to the curve from (2.16) for  $f_d T_m < 0.05$ . Since the bit rate is 5000 bit/s, the corresponding values of  $f_d$  for  $N=255$  and 1023 bits must be less than 1 Hz and 0.25 Hz respectively.

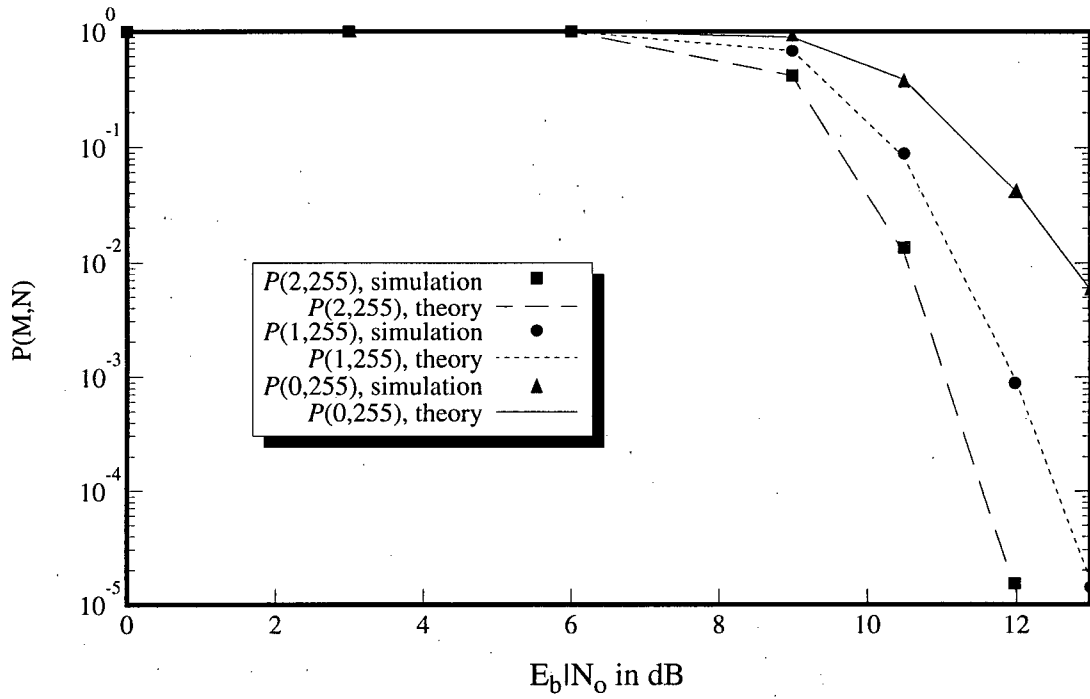


Figure 4.2 BER as a function of  $\frac{E_b}{N_0}$  in a non-fading channel with block length  $N=255$  bits.

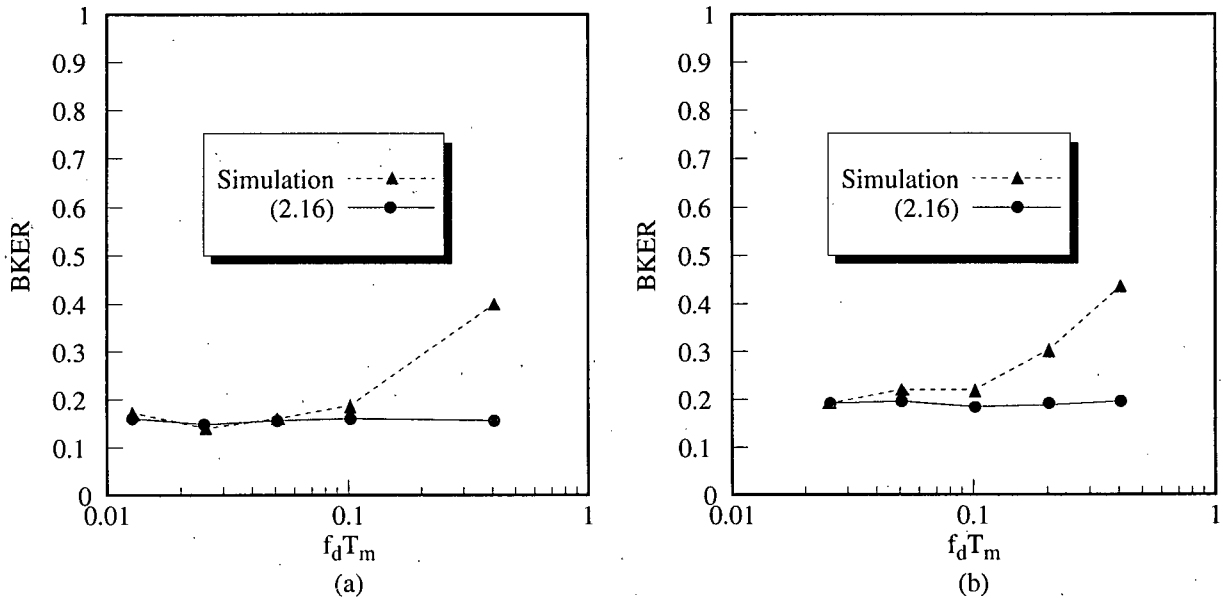


Figure 4.3 BER with no error correction as a function of  $f_d T_m$  for (a)  $N=255$  bits (b)  $N=1023$  bits.

The probability,  $P_f(M,N)$ , in very slow Rayleigh fading are shown in Figure 4.4 (a) and (b). The  $f_d$  used for  $N=255$  and 1023 bits are 0.5 Hz and 0.15 Hz respectively. The number of errors to be corrected for  $N=255$  and 1023 bits are 8 and 26 respectively. The theoretical results are obtained from (2.16). It can be seen that the simulation results agree closely with the theoretical results.

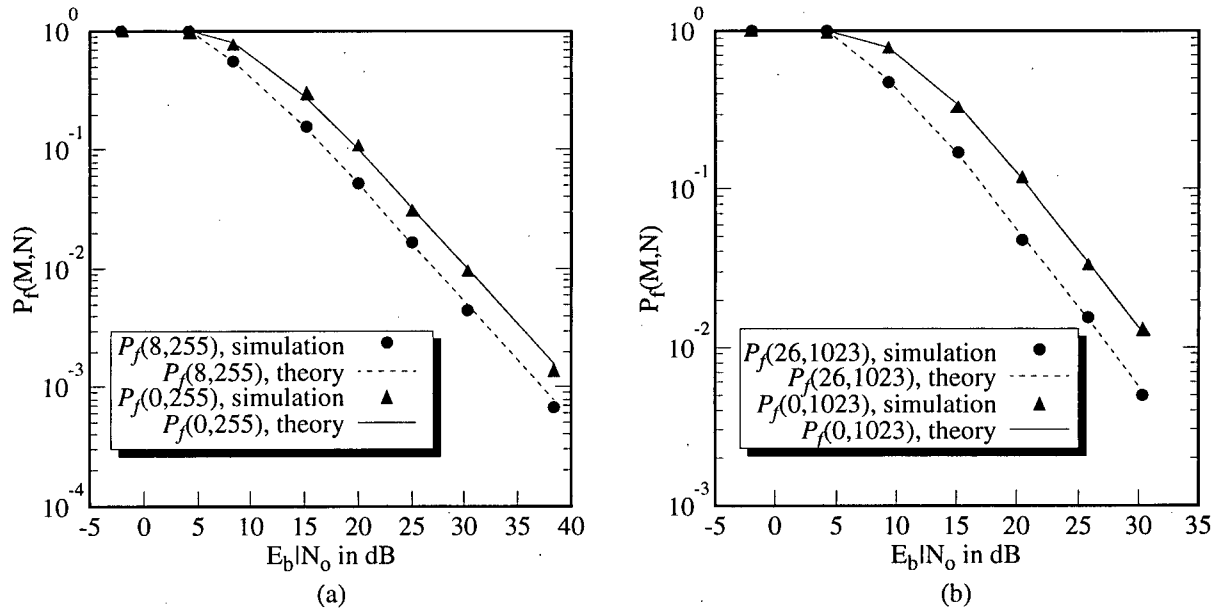


Figure 4.4  $P_f(M,N)$  in a very slow Rayleigh fading channel for (a)  $P_f(0,255)$  and  $P_f(8,255)$  (b)  $P_f(0,1023)$  and  $P_f(26,1023)$ .

#### 4.1.2 Comparison with Previous Results for Tone Interferers

In this section, the simulation BER results with tone interferers in a non-fading environment are compared with the results in [22,26]. In these papers, it is assumed that a (tone) interferer transmits only one frequency signal, either  $f_1$  or  $f_2$ . In [22,26],  $B_n$  is assumed to be  $R_b$  and therefore the “signal-to-noise” (SNR) power ratio is equal to  $E_b/N_o$  from (3.13). Since the bit rate of the interference signal is equal to that of the desired signal, the “interference-to-signal” (ISR) power ratio in [26] is equal to  $I_b/E_b$ , where  $I_b$  is the interference signal energy per bit. The

“interference per channel-to-noise” (JNR) power ratio in [22] is equal to  $(I_b/2)/N_o$  from (3.13) by substituting  $I_b$  for  $E_b$ . The BER with 1 tone interferer at  $I_b/E_b=-2$  dB is shown in Figure 4.5(a). Figure 4.5 (b) shows the BER with 2 tone interferers at  $(I_b/2)/N_o=10$  dB. These simulation results agree closely with results given in [22,26] (with ISR, SNR and JNR replaced by  $I_b/E_b$ ,  $E_b/N_o$  and  $I_b/2N_o$  respectively).

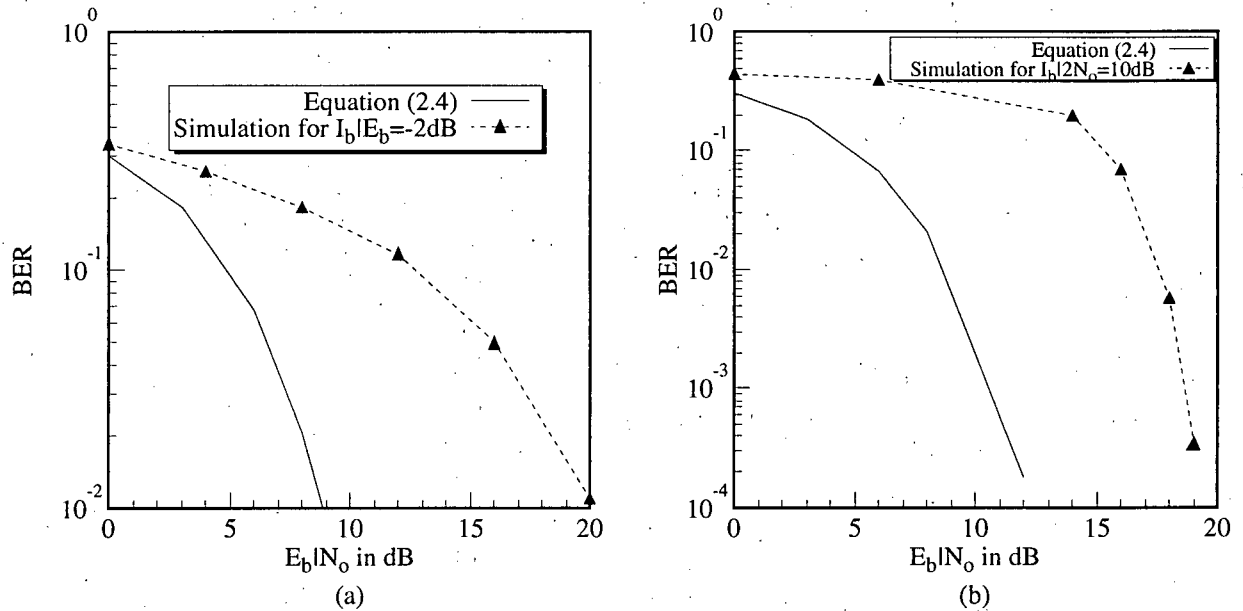


Figure 4.5 BER with (a) 1 tone interferer (b) 2 tone interferers.

## 4.2 Error Performance with Multiple Co-channel Interferers in a Non-fading Environment

In this section, it is assumed that the received power at the mobile from each co-channel interferer is equal. The effects of different background noise levels, block lengths and number of co-channel interferers as well as error correction are investigated.

### 4.2.1 BER Results

Usually the background noise power is much smaller than the co-channel interference power [16,27]. The BER vs. SIR (defined as the signal power-to-total interference power received at the mobile) curves for different number of interferers in a non-fading environment with AWGN

at  $\frac{E_b}{N_o} = 40$  dB are presented in Figure 4.6.

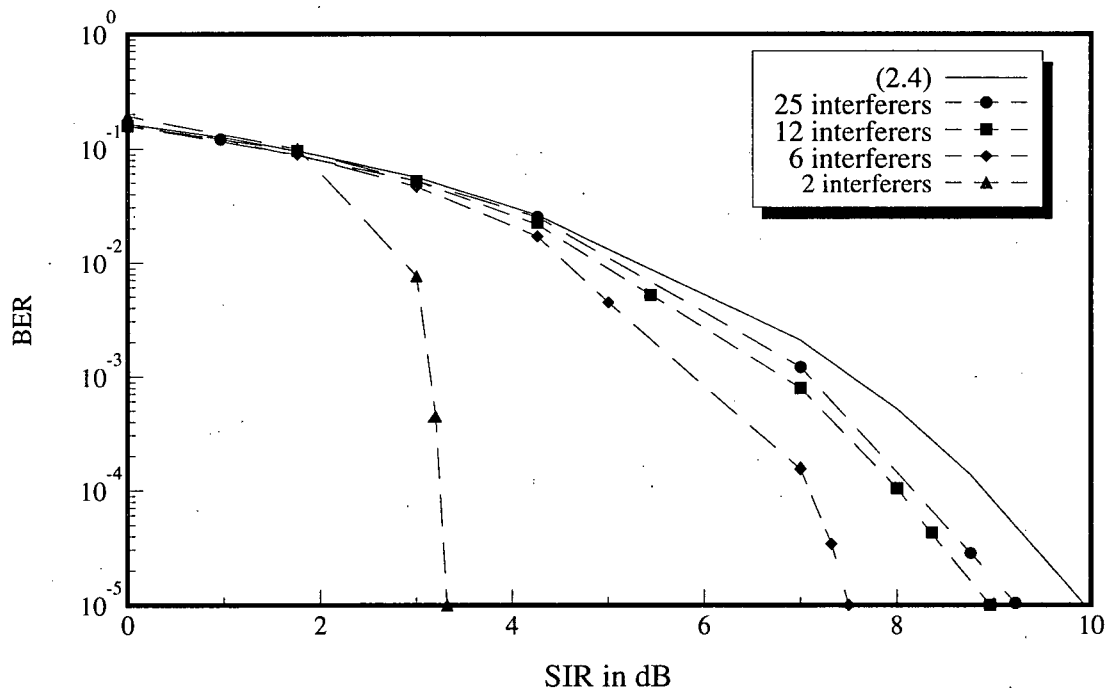


Figure 4.6 BER as a function of SIR for different number of interferers in a non-fading environment with AWGN at  $\frac{E_b}{N_o} = 40$  dB.

In the figure, when the SIR is less than 2 dB, the BER decreases with the number of co-channel interferers,  $n_I$ . However, the BER increases with  $n_I$  for SIR values above 2 dB. The incremental increase becomes smaller with increasing  $n_I$ . Eventually, the curves approach to the theoretical BER curve for binary NCFSK, obtained using (2.4). The one-sided PSD,  $N_o$ , of the Gaussian noise used in (2.4) in calculating the theoretical curve is replaced by the sum,  $N_{o+i}$ , of

the PSD of the *Gaussian* background noise and that of the interference signal. Hence, the joint co-channel interference-plus-noise signal is assumed to have a Gaussian distribution. Figure 4.6 shows that as  $n_I$  increases, the co-channel interference signal can be modeled as Gaussian. The PSD,  $I_o$ , of the interference signal is obtained by

$$I_o = \frac{P_i}{B_i} \quad (4.1)$$

where  $P_i$  is the total received interference power and  $B_i$  is the bandwidth of the interference signal. As discussed in Chapter 3, we use the 90% bandwidth of the interference signal i.e.  $B_i=2.2 R_b$ . For a large  $n_I$ , the BER can be accurately estimated by replacing the interference signal power,  $P_i$ , by bandlimited Gaussian noise of power

$$N_e = \frac{B_n}{B_i} P_i \quad (4.2)$$

The BER with higher Gaussian background noise levels of  $\frac{E_b}{N_o} = 20$  dB and 10 dB are depicted in Figure 4.7 (a) and (b) respectively. It can be seen that as  $n_I$  increases, the BER curves approach (2.4). The curves in Figure 4.7(b) are not as sensitive to  $n_I$  because the background noise is more dominant. In fact, for SIR > 15 dB, the BER is more or less independent of  $n_I$ . As expected, a higher background noise level results in a higher irreducible BER.

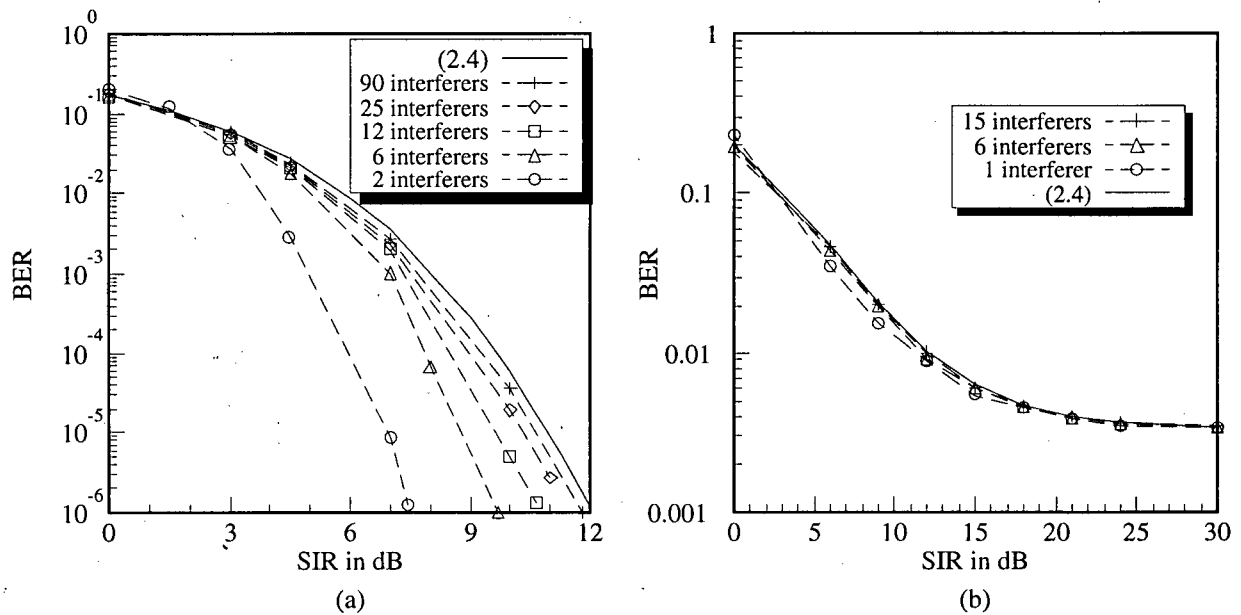


Figure 4.7 BER with interferers in a non-fading environment with AWGN at (a)  $\frac{E_b}{N_o} = 20$  dB and (b)

$$\frac{E_b}{N_o} = 10 \text{ dB.}$$

### 4.2.2 BKER Results

The BKER results in the presence of co-channel interferers in a non-fading environment are presented next. The block lengths used in the simulation are  $N=255$  and 1023 bits with AWGN

at  $\frac{E_b}{N_o} = 20$  dB and 40 dB. The BKER (with no error correction) curves with  $\frac{E_b}{N_o} = 20$  dB and  $N=255$

bits are shown in Figure 4.8. Figures 4.9 (a) and (b) show the BKER (with no error correction)

with  $\frac{E_b}{N_o} = 40$  dB, for  $N=255$  and 1023 bits respectively. Unlike BER, the BKER increases with  $n_I$

for all SIR values considered. The incremental increase becomes very small and the BKER is upperbounded by the theoretical BKER curve, obtained from (2.7) by assuming that bit errors are independent with a BER value obtained from the theoretical BER curve using (2.4). With a large

value of  $n_I$ , the BER is approximately equal to the BER from (2.4) as noted in the previous section. However, the BKER with co-channel interference can be significantly lower than (2.7). The reason is that the errors occur in a more bursty manner with co-channel interference as opposed to (2.7) in which bit errors are assumed to be independent [28]. For high SIR values, the BKER should be close to (2.7) because the co-channel interference is very small compared with the background noise.

The probability,  $P(M,N)$ , is an important quantity when using block coding in an error control scheme. The CDF of the number of bit errors in a block with different number of interferers at  $\frac{E_b}{N_o} = 20$  dB and SIR=4.5 dB for  $N=255$  bits is shown in Figure 4.10. The Gaussian CDF is given by

$$Pr\{\text{number of errors} \leq M\} = 1 - P(M, N) \quad (4.3)$$

where  $P(M,N)$  is obtained from (2.8) with a BER calculated as discussed in Section 4.2.1. In Figure 4.10, it can be seen that the CDF is about the same for a large number of interferers and is quite different from the Gaussian CDF. It can be observed that the probability of more than 10 bit errors in a block with 6 or more co-channel interferers is larger than that obtained with the Gaussian CDF. This is because errors occur in a more bursty manner with interferers. For 2 interferers, the  $P(M,N)$  is much lower than that obtained from (2.8), because the BER is much smaller than the BER from (2.4). The CDF of the number of bit errors in a block at  $\frac{E_b}{N_o} = 40$  dB with different SIR values and block lengths are presented in Figure 4.11(a)-(d).

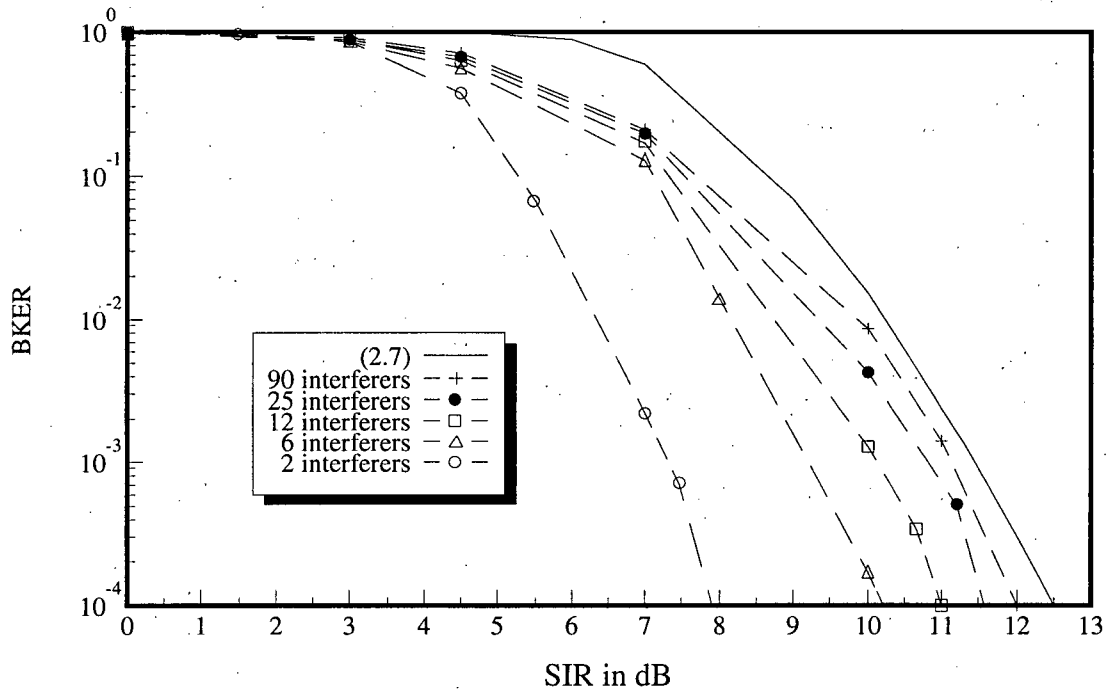


Figure 4.8 BER in a non-fading environment with  $\frac{E_b}{N_o} = 20$  dB for  $N=255$  bits.

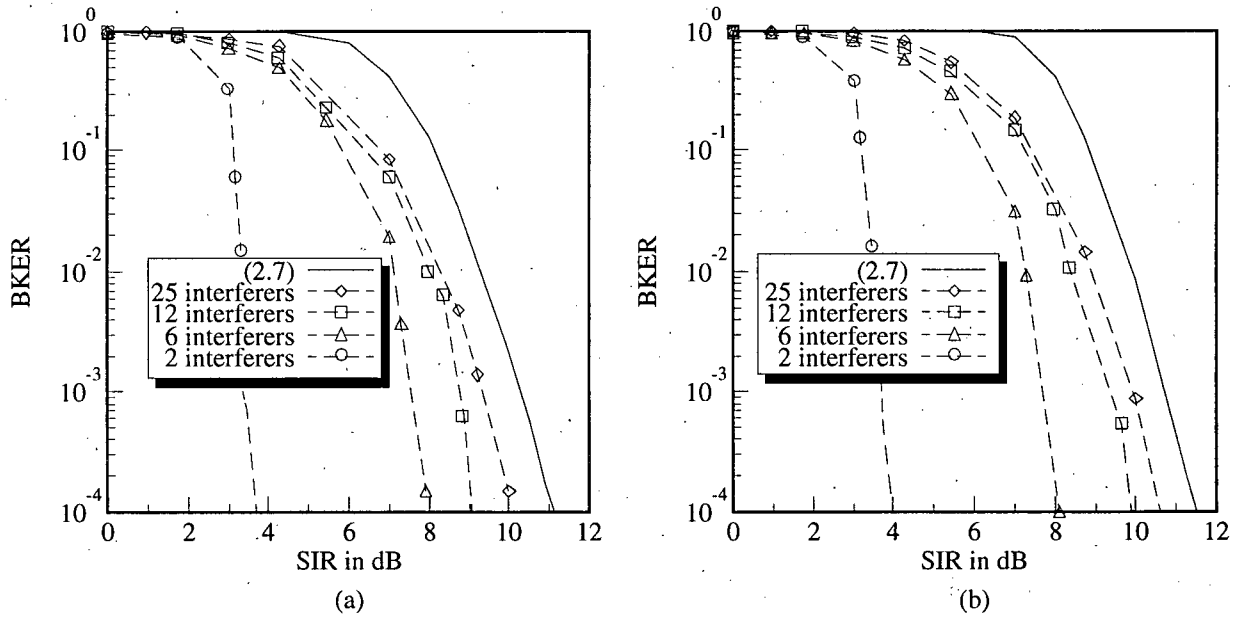


Figure 4.9 BER in a non-fading environment with  $\frac{E_b}{N_o} = 40$  dB for (a)  $N=255$  bits (b)  $N=1023$  bits.

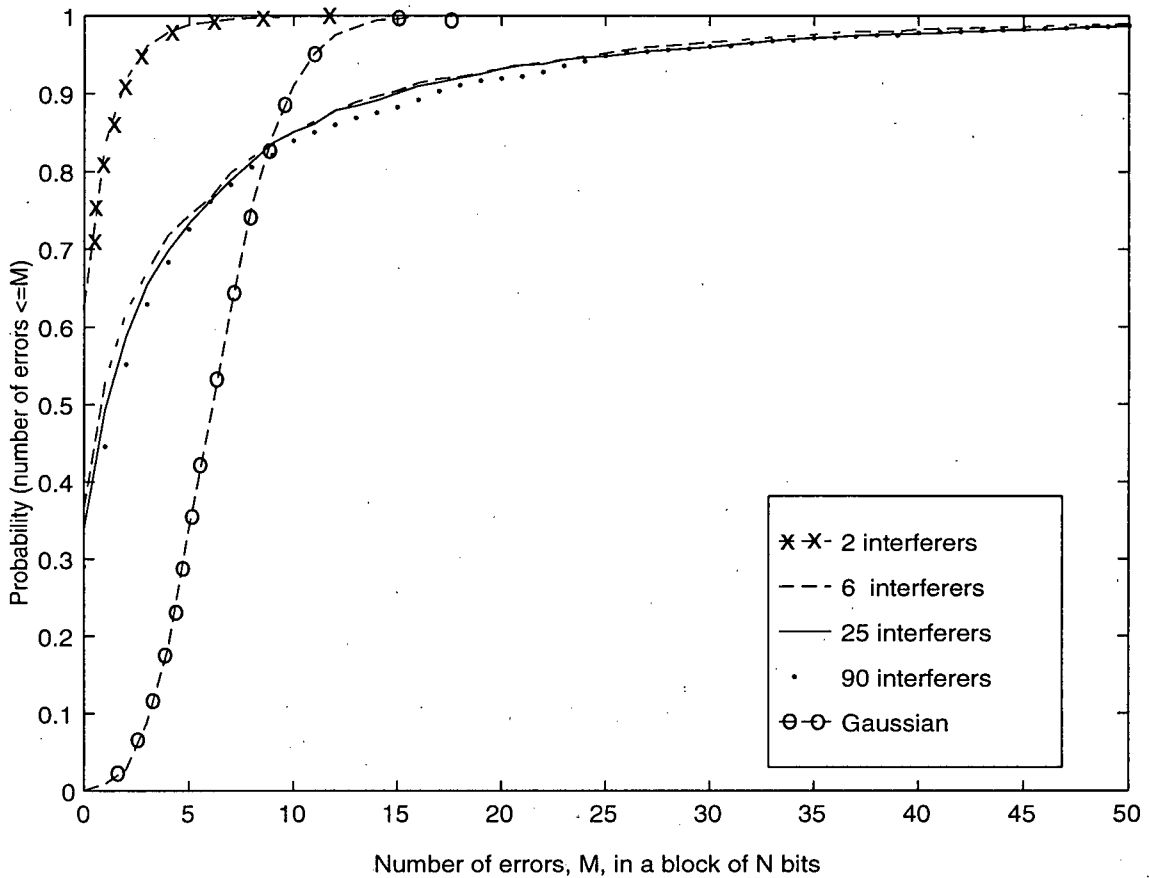


Figure 4.10 CDF of the number of bit errors in a non-fading environment with  $\frac{E_b}{N_o} = 20$  dB and SIR=4.5 dB for  $N=255$  bits.

The probability,  $P(M,N)$ , with error correction are presented in Figure 4.12, for  $M=8$ ,  $N=255$  bits and  $\frac{E_b}{N_o} = 40$  dB. Figure 4.13 shows  $P(M,N)$  for  $M=26$ ,  $N=1023$  bits and  $\frac{E_b}{N_o} = 40$  dB.

With error correction, the improvement of the Gaussian case using (2.8) is greater than with the co-channel interferers in both figures, because the channel with interferers is more bursty. The improvement for 6 or more co-channel interferers is greater than for 2 co-channel interferers. This is because the errors occur in a less bursty manner with a larger number of the co-channel interferers.

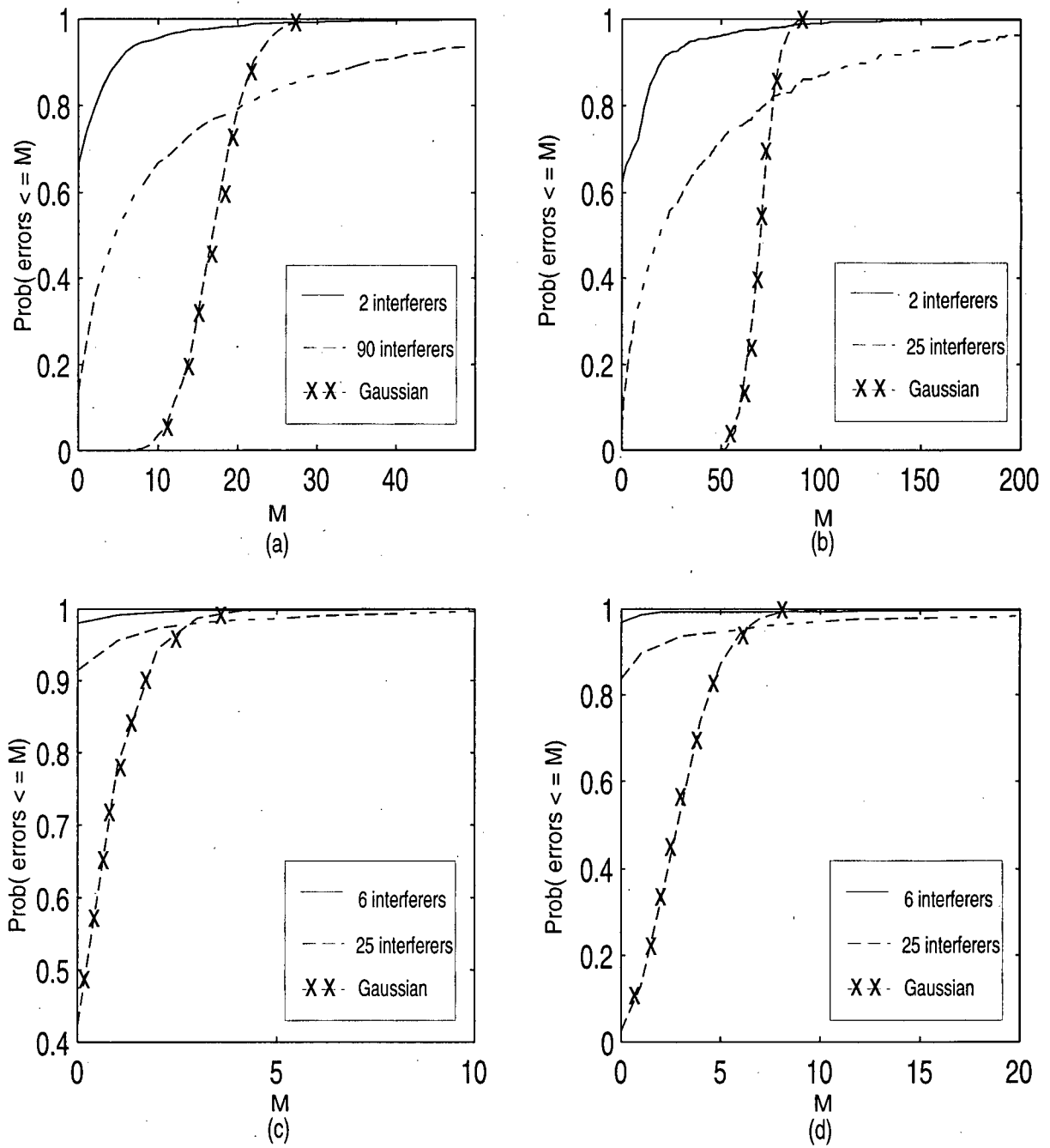


Figure 4.11 CDF of the number of bit errors in a block in a non-fading environment with  $\frac{E_b}{N_o} = 40$  dB for (a) SIR=3 dB and  $N=255$  bits, (b) SIR=3 dB and  $N=1023$  bits, (c) SIR=7 dB and  $N=255$  bits and (d) SIR=7 dB and  $N=1023$  bits.

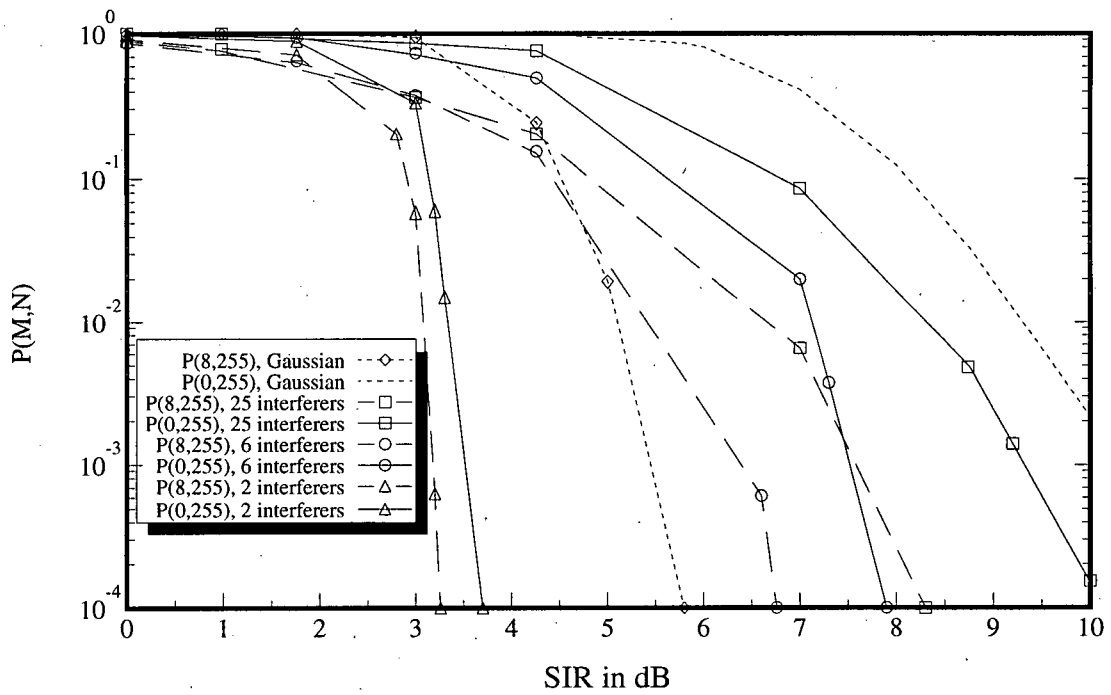


Figure 4.12  $P(8,255)$  as a function of SIR with  $\frac{E_b}{N_o} = 40$  dB.

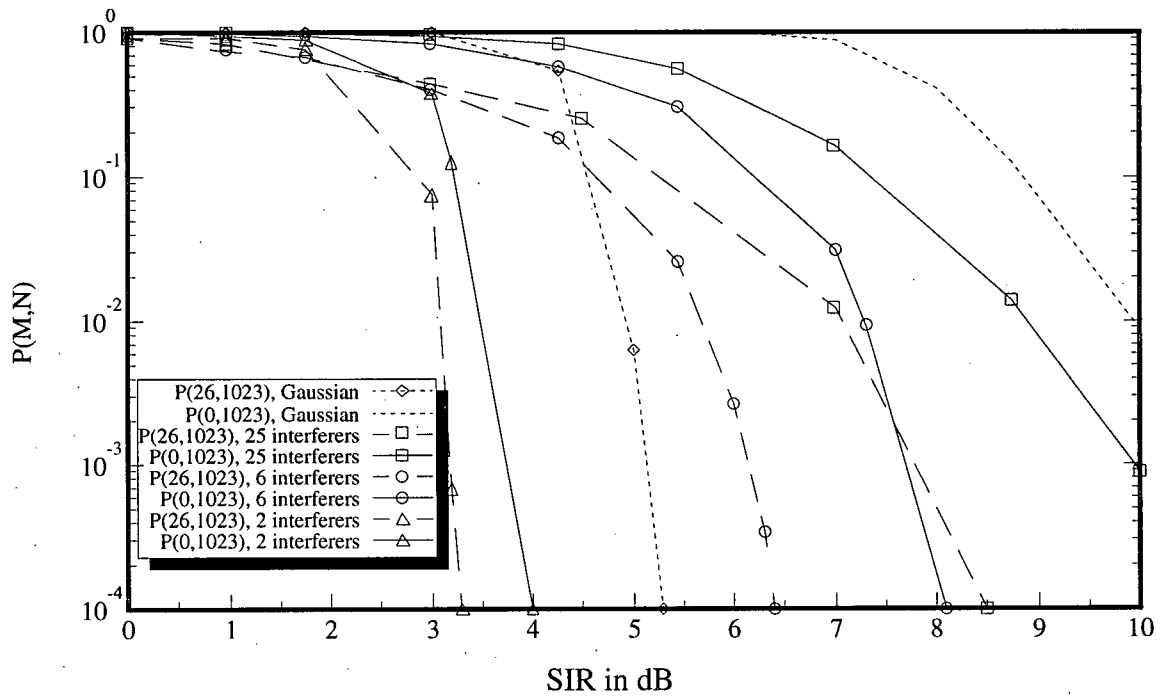


Figure 4.13  $P(26,1023)$  as a function of SIR with  $\frac{E_b}{N_o} = 40$  dB.

### 4.3 Error Performance with Co-channel Interferers in a Very Slow Rayleigh Fading Environment

In this section, the system with multiple co-channel interferers is studied in a very slow Rayleigh fading environment. The values of  $f_d$  are chosen to be 0.5 Hz and 0.15 Hz for  $N=255$  and 1023 bits respectively. The received power at the mobile is assumed to be the same from each co-channel interferer.

#### 4.3.1 BER Results

The BER simulation results with multiple co-channel interferers in a very slow fading environment are presented in Figures 4.14 (a) and (b), with AWGN at  $\frac{E_b}{N_o} = 20$  dB and 40 dB respectively. It can be seen that the BER is more or less independent of the number of co-channel interferers and is well approximated by the theoretical BER curve for binary NCFSK in slow Rayleigh fading. The theoretical BER in slow fading is obtained from (2.14) as a function of  $\gamma_o = \frac{E_b}{N_o}$ . The one sided PSD,  $N_o$ , of Gaussian noise in (2.14) to calculate the theoretical curve is replaced by the sum,  $N_{o+i}$ , of the PSD of the Gaussian background noise and that of interference signal. In terms of bit error performance in a very slow fading environment, it can be assumed that the co-channel interference signal has a Gaussian distribution regardless of the number of interferers and the interference signal power can be well approximated by  $N_e$  as given in (4.2). An expression for the BER for multiple co-channel interferers with bit synchronized in a slow Rayleigh fading environment is derived in Appendix B.

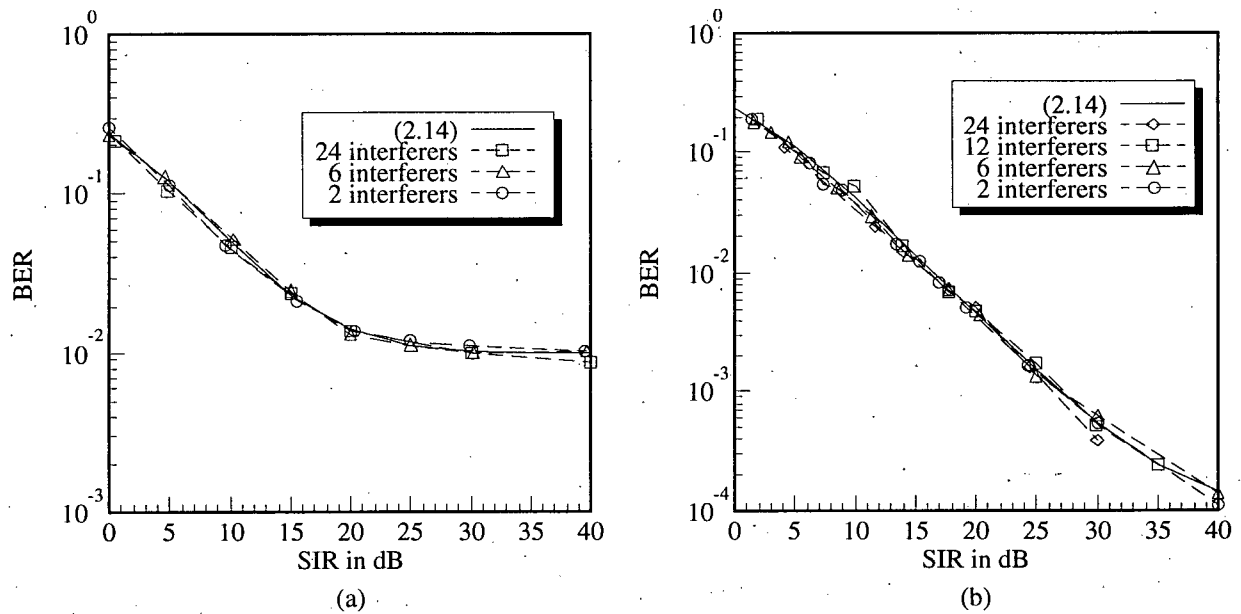


Figure 4.14 BER in a very slow fading environment with AWGN at (a)  $\frac{E_b}{N_o} = 20$  dB and (b)  $\frac{E_b}{N_o} = 40$  dB.

### 4.3.2 BKER Results

The BKER simulation results in very slow Rayleigh fading with different background noise levels and block lengths are shown in Figures 4.15(a)-(c). As  $n_f$  increases, the BKER increases towards the theoretical BKER for NCFSK in very slow Rayleigh fading given by (2.16). The value of  $N_o$  in (2.16) is replaced by  $N_{o+i}$ . In Figure 4.15(a) the simulation BKER is lower than (2.16) by 20 to 50% for  $3 < \text{SIR} < 20$  dB, but for  $\text{SIR} > 25$  dB, the difference is less than 5%. In Figure 4.15(b), the simulation BKER is lower than (2.16) by 10 to 30% for  $3 < \text{SIR} < 20$  dB. The BKER is approximately equal to (2.16) for large SIR values because the background (Gaussian) noise is dominant. The BKER for  $N=1023$  (Figure 4.15(c)) is only slightly lower than for  $N=255$  (Figure 4.15(a)). This is because the BKER for both values of  $N$  is close to 1 for SIR values below 5 dB. For higher SIR values, the BKER for  $N=1023$  can be up to 4 times that for  $N=255$ , but both BKER's will be quite small.

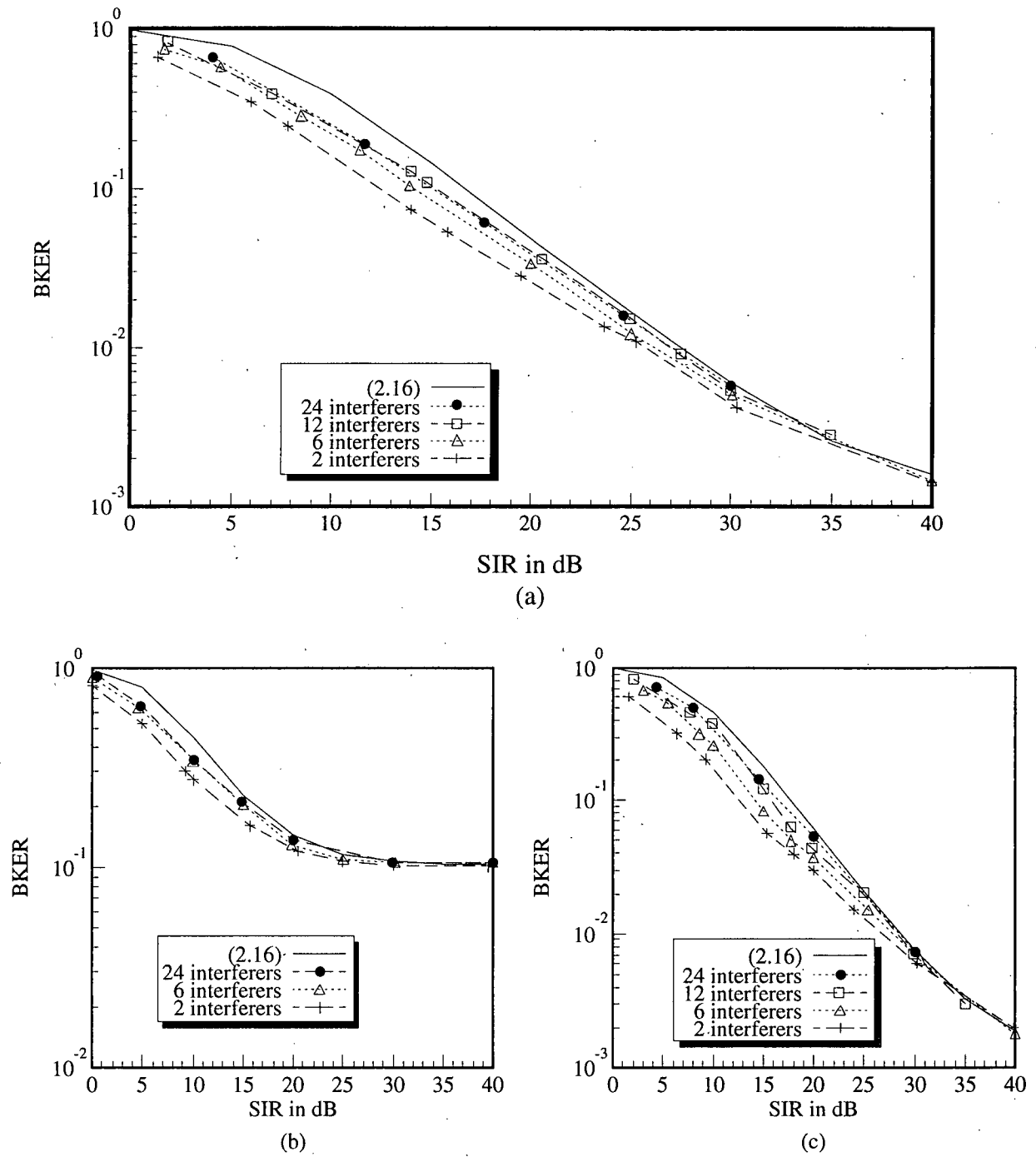


Figure 4.15 BER with interferers in a very slow fading environment with (a) AWGN at  $\frac{E_b}{N_o} = 40$  dB,

$N=255$  bits (b) AWGN at  $\frac{E_b}{N_o} = 20$  dB,  $N=255$  bits and (c) AWGN at  $\frac{E_b}{N_o} = 40$  dB,

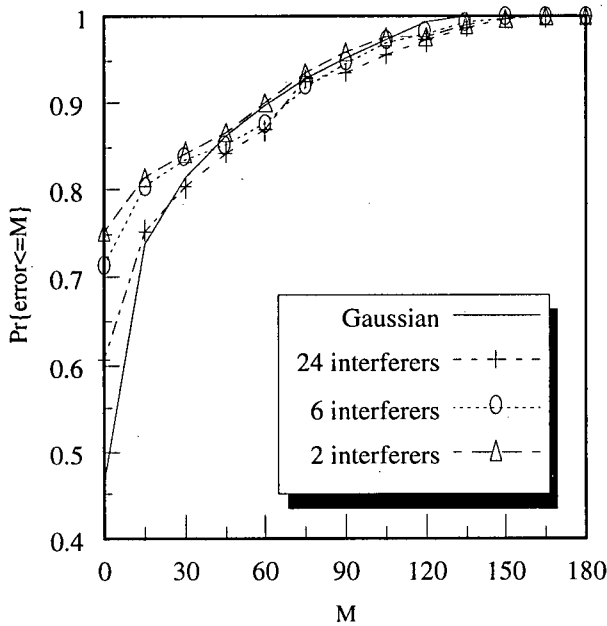
$N=1023$  bits.

The CDF of the number of bit errors in a block are presented in Figures 4.16 (a)-(d), for  $N=255$  and 1023 bits and SIR=8 dB and 20 dB, with AWGN at  $\frac{E_b}{N_o}=40$  dB. The Gaussian CDF is given by

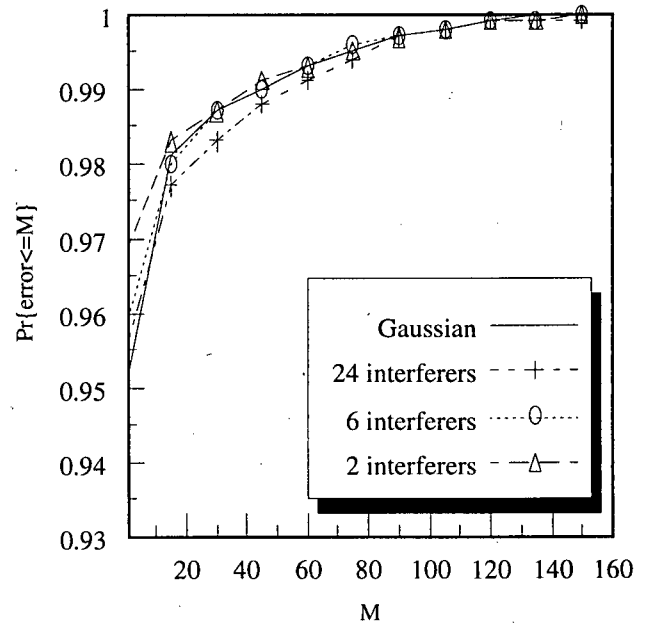
$$Pr\{\text{number of errors} \leq M\} = 1 - P_f(M, N) \quad (4.4)$$

where  $P_f(M, N)$  is obtained from (2.16) by replacing the  $N_o$  in (2.16) by  $N_{o+i}$ . As  $n_I$  increases,  $Pr\{\text{errors} \leq M\}$  decreases gradually. The shapes of the CDF curves look similar to that of the Gaussian CDF.

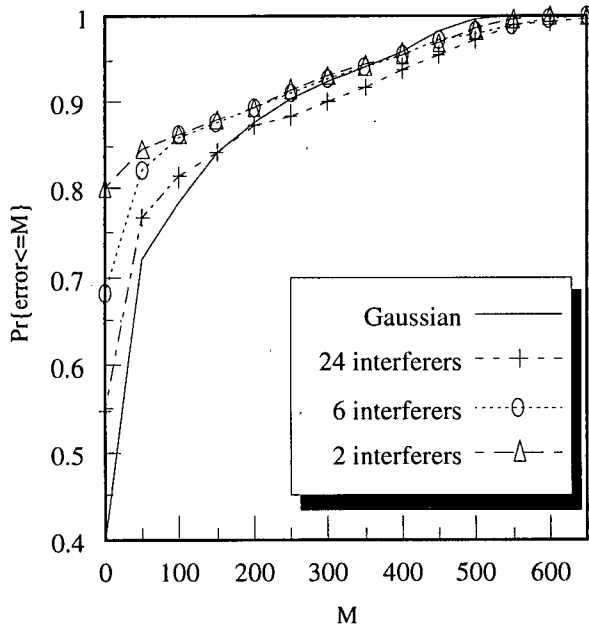
The probability,  $P_f(M, N)$ , with a BCH code of rate approximately equal to 0.75 with AWGN at  $\frac{E_b}{N_o}=40$  dB and different number of interferers are shown in Figures 4.17(a)-(e). The number of errors,  $M$ , to be corrected are 8 and 26 for  $N=255$  and 1023 bits respectively. With error correction, the improvement for the Gaussian case using (2.16) is greater than that for co-channel interferers. For a small number of interferers, say 2 or 6, the improvement is very small for low SIR values. But for high SIR, the improvement becomes as good as the Gaussian case because the background noise is dominant and the interference-plus-noise signal becomes more Gaussian. Also, the improvement increases with  $n_I$ . This occurs because the channel becomes less bursty as  $n_I$  increases.



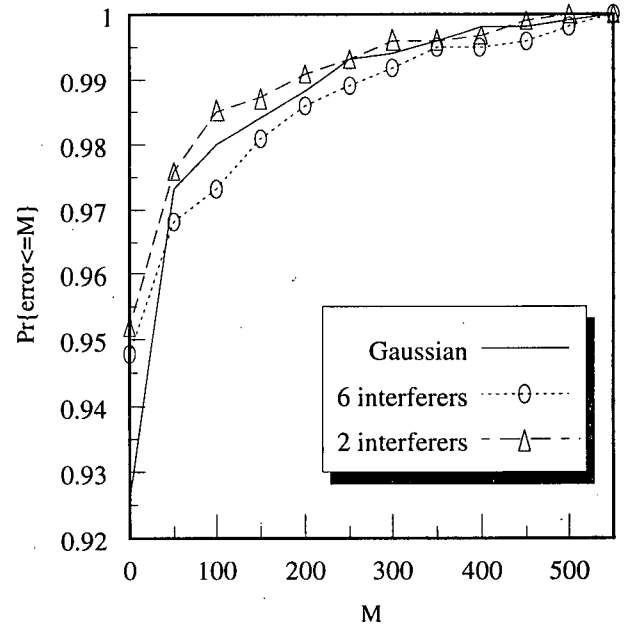
(a)



(b)



(c)



(d)

Figure 4.16 The CDF of the number of bit errors in a block at  $\frac{E_b}{N_o}=40$  dB with different number of interferers for (a)  $N=255$  bits and  $SIR=8$  dB, (b)  $N=255$  bits and  $SIR=20$  dB, (c)  $N=1023$  bits and  $SIR=8$  dB and (d)  $N=1023$  bits and  $SIR=20$  dB.

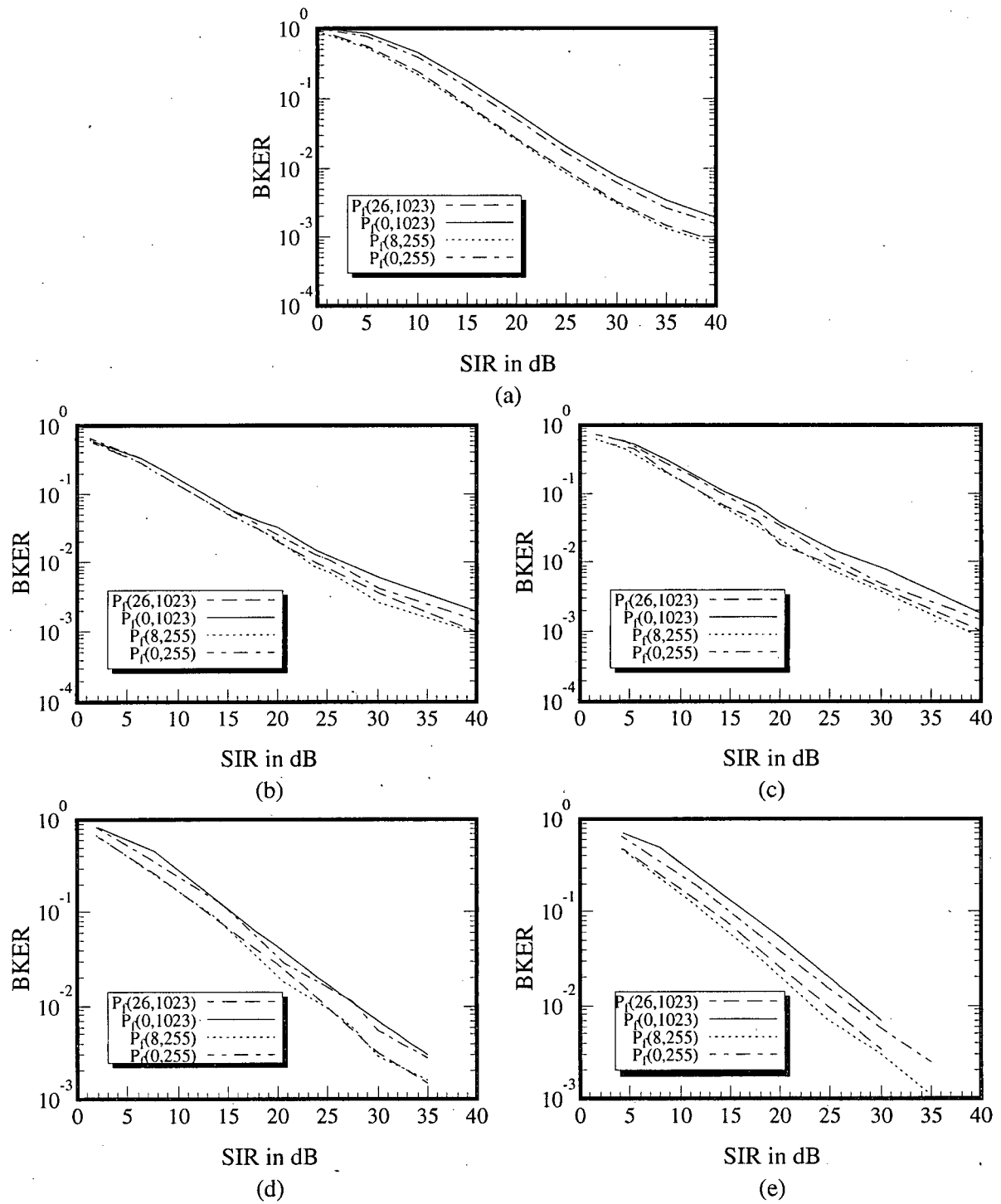


Figure 4.17 The  $P_f(8,255)$  and  $P_f(26,1023)$  as a function of SIR in very slow Rayleigh fading with AWGN at  $\frac{E_b}{N_o} = 40$  dB for (a) Gaussian case, (b) 2 interferers, (c) 6 interferers, (d) 12 interferers and (e) 24 interferers.

## 4.4 Error Performance in a Rayleigh fading Environment

In the past, expressions for BKER have been obtained assuming a very slow Rayleigh fading [21,29]. Unfortunately this assumption is not always valid in practice. In this section, the error performance with multiple co-channel interferers in a Rayleigh fading environment which is not very slowly fading is presented. The received power at the mobile is assumed to be the same from each co-channel interferer.

### 4.4.1 BER Results

The BER with co-channel interferers and AWGN at  $\frac{E_b}{N_o} = 40$  dB is presented in Figure 4.18 (a)-(c), for  $f_d = 5, 20$  and  $100$  Hz corresponding at  $900$  MHz to vehicle speeds of  $6$  km/hr,  $24$  km/hr and  $120$  km/hr respectively. The product of  $f_d T_b$  for  $f_d = 5, 20, 100$  Hz are  $0.001, 0.004$  and  $0.02$  respectively. It can be seen that the BER is independent of number of interferers. In Figure 4.18 (a) and (b), the BER can be well approximated by the theoretical curve obtained from (2.14) for very slow fading. In Figure 4.18 (c), the curve labelled "Gaussian noise" is obtained from simulation by using Gaussian noise of the same PSD value in place of the interference signals. It can be seen that the BER becomes lower than the value obtained from (2.14); when SIR exceeds about  $20$  dB. This indicates that channel for  $f_d = 100$  Hz can not be described as slow fading. The reason is that  $f_d T_b$  is not small enough so that the signal strength can no longer be assumed constant over a bit.

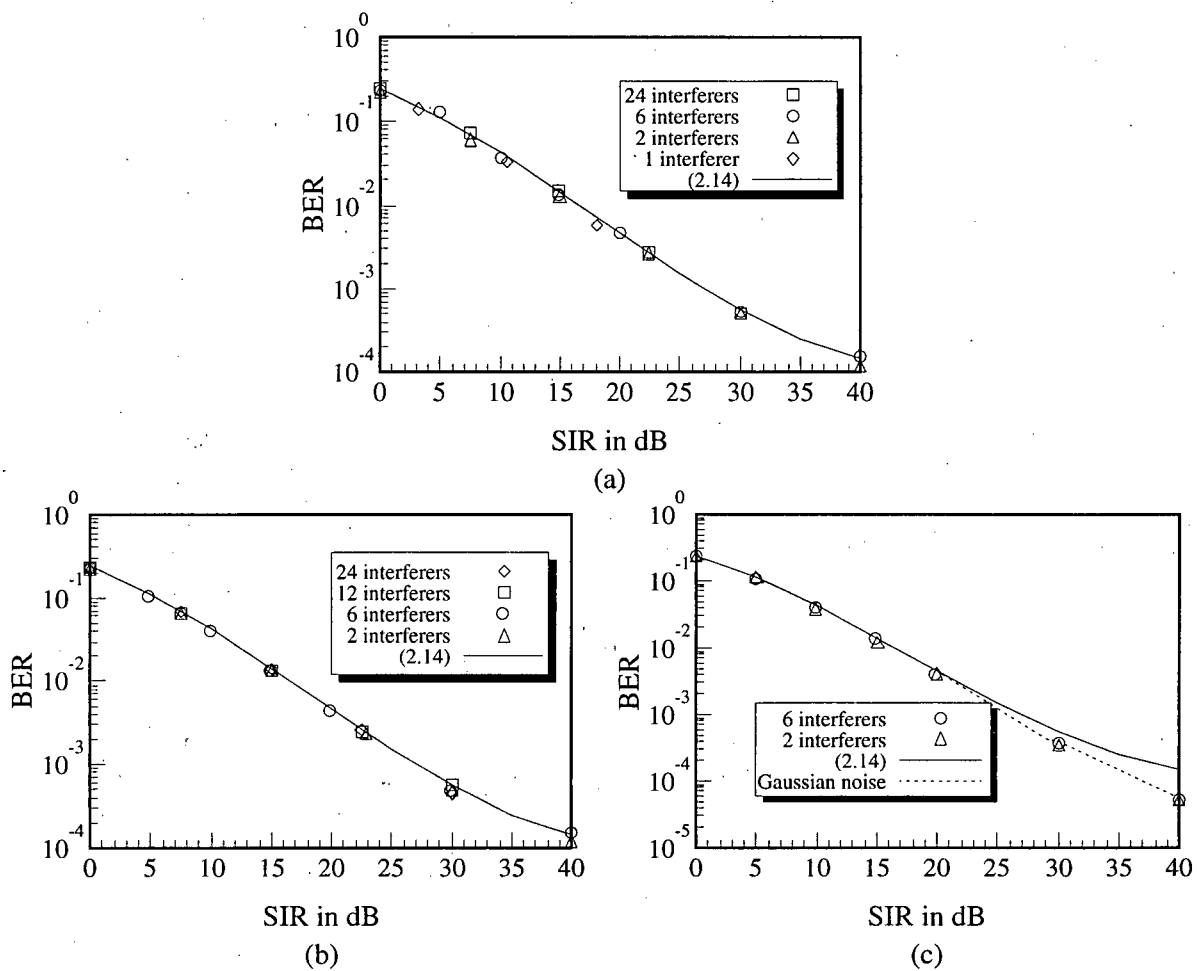


Figure 4.18 BER in a Rayleigh fading environment with interferers and AWGN at  $\frac{E_b}{N_0} = 40$  dB for

(a)  $f_d = 5$  Hz, (b)  $f_d = 20$  Hz and (c)  $f_d = 100$  Hz.

#### 4.4.2 BKER Results

The BKER results with co-channel interferers in a Rayleigh fading environment are shown in Figure 4.19(a)-(c), for  $f_d = 5, 20, 100$  Hz, with AWGN at  $\frac{E_b}{N_0} = 40$  dB. As  $n_I$  increases, the

BKER increases towards the “Gaussian noise” curves which is obtained from simulation by using Gaussian noise of the same PSD in place of interference signals. For large  $n_I$ , the interference

signal can be modeled as Gaussian noise of the same PSD value.

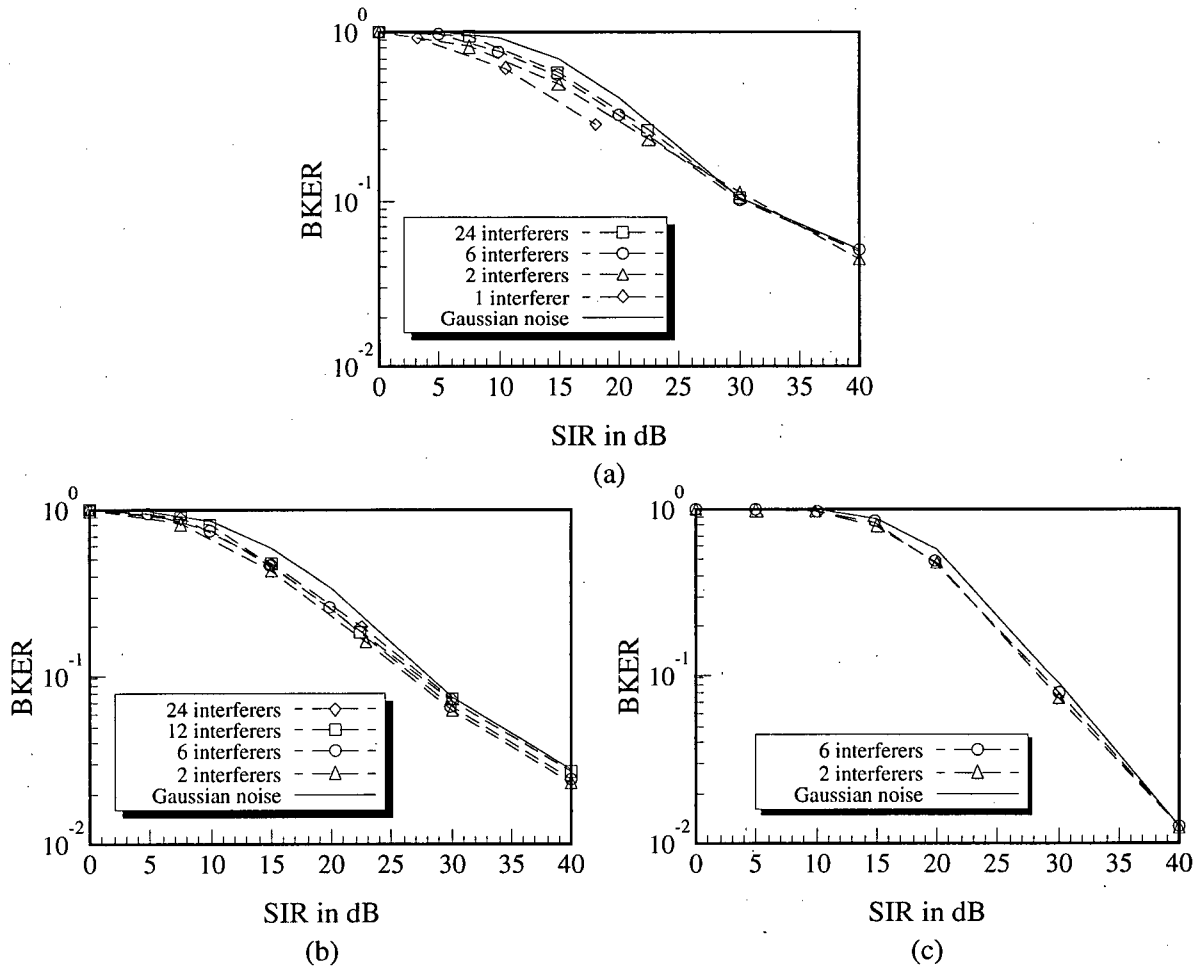


Figure 4.19 BER in a Rayleigh fading environment with interferers and AWGN at  $\frac{E_b}{N_o} = 40$  dB for (a)  $f_d = 5$  Hz and  $N = 1023$  bits, (b)  $f_d = 20$  Hz and  $N = 255$  bits and (c)  $f_d = 100$  Hz and  $N = 255$  bits.

### 4.5 Error Performance with the First and Second-tier Co-channel Interferers

In this section, the co-channel interferers in the first and second tier are considered. Each tier has six co-channel interferers. For simplicity, the distances from a first-tier and second-tier co-channel cell to the mobile are assumed to be  $D$  and  $\sqrt{3}D$ , as described in section 2.2.3. The received powers from the first-tier and second-tier co-channel interferers are proportional to  $D^{-\beta}$

and  $(\sqrt{3}D)^{-\beta}$  respectively. This is in contrast to previous sections in which the received powers are equal from all interferers. The propagation loss exponent,  $\beta$ , is assumed to be 4. Thus, the *SIR* is given by

$$SIR = \frac{R^{-4}}{6D^{-4} + 6(1.732D)^{-4}} \quad (4.5)$$

### 4.5.1 BER Results

The BER results with co-channel interferers in 2 tiers in a non-fading and a slow Rayleigh fading environment with AWGN at  $\frac{E_b}{N_o} = 40$  dB are presented in Figure 4.20 (a) and (b). In Figure 4.20(a), the BER with 6 and 12 interferers in the first tier with equal power are compared. It can be seen that the BER with 6 co-channel interferers in tier 1 and 6 in tier 2 is between the two curves. In Figure 4.20 (b), the BER is approximately equal to the theoretical curve from (2.14) as well as to the BER with different number of interferers in the first tier. Thus, in a fading environment, the BER's are the same for interferers with equal or different powers. This is consistent with the observation in [15,32].

### 4.5.2 BKER Results

The BKER with co-channel interferers in 2 tiers in a non-fading and a very slow Rayleigh fading environment are shown in Figure 4.21(a) and (b), for  $N=255$  bits and AWGN at  $\frac{E_b}{N_o} = 40$  dB. In both figures, this BKER lies between the BKER with 12 interferers and 6 interferers in the first tier.

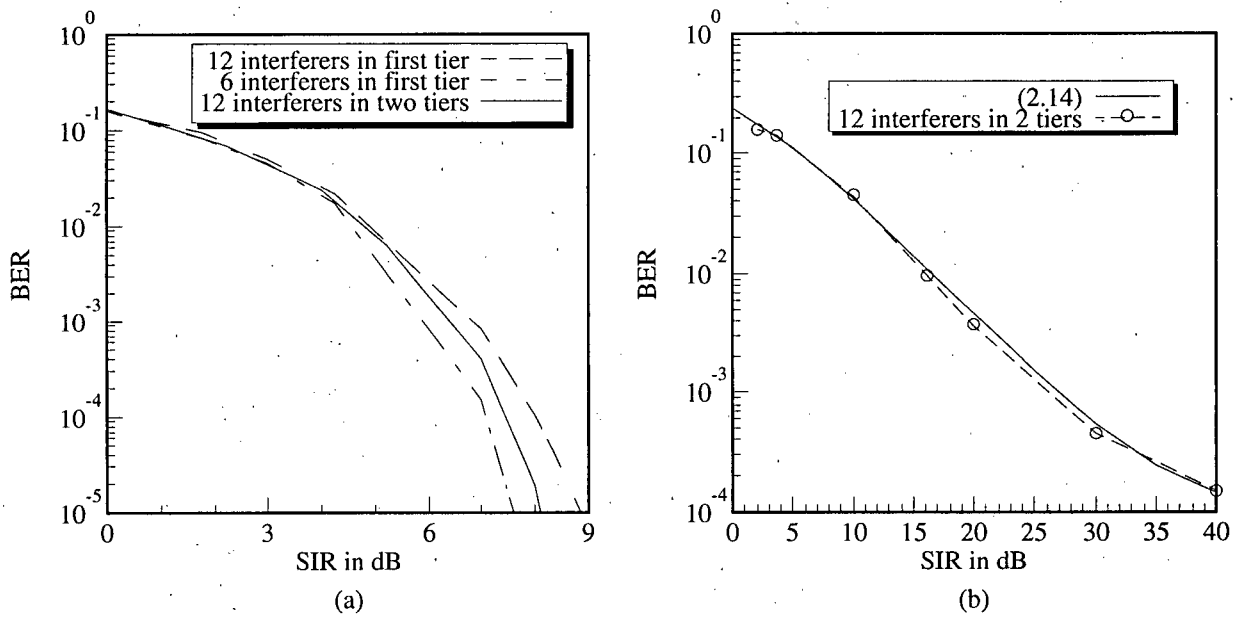


Figure 4.20 BER with the first and second-tier co-channel interferers at  $\frac{E_b}{N_o} = 40$  dB in (a) a non-fading environment and (b) a slow Rayleigh fading environment.

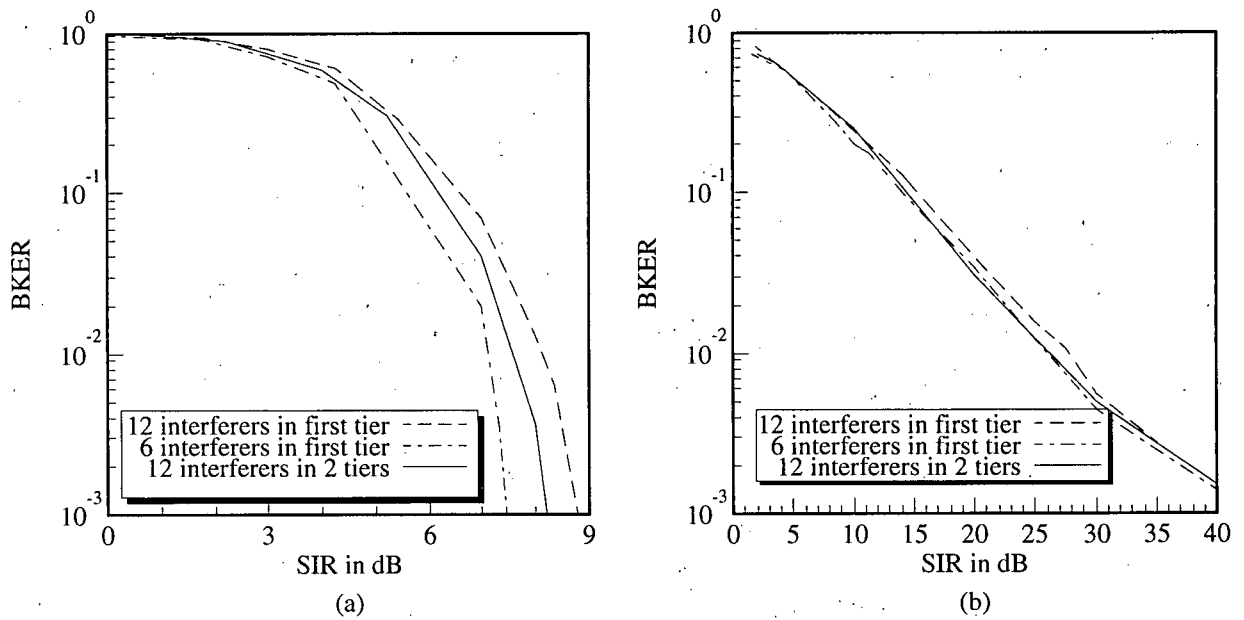


Figure 4.21 BKER with first and second-tier co-channel interferers for  $N=255$  bits and  $\frac{E_b}{N_o} = 40$  dB in (a) a non-fading environment and (b) a very slow Rayleigh fading environment.

## Chapter 5 Spectrum Efficiency in Cellular Systems

The definition of spectrum efficiency as in [10,17] is used. This spectrum efficiency depends on the cluster size  $K$  as well as the probability of successful packet reception. In this chapter, the spectrum efficiencies for different values of  $K$  in a cellular *packet data* communication system for various system configurations and parameters are obtained, i.e., different SIR models, block lengths, background noise levels, propagation loss exponents and fading rates. Values of the cluster size which maximize the spectrum efficiency are found. The probability of successful packet reception is obtained from the BKER results presented in Chapter 4.

### 5.1 Analysis of Spectrum Efficiency

The unnormalized spectrum efficiency,  $E$ , is defined as the throughput (average number of user data bits correctly received per second) per cell. The average packet throughput,  $\eta_p$ , is defined as

$$\eta_p = P_s \times R_p \quad (5.1)$$

where  $P_s$  is the probability of successful packet reception and  $R_p$  is packet transmission rate. The packets are assumed to be  $N$  bits long, each packet consisting of  $I$  information bits,  $p$  bits for error correction and  $b$  overhead bits for synchronization, addressing, etc., i.e.  $I=N-p-b$ . The average user bit throughput,  $\eta_b$ , is

$$\begin{aligned} \eta_b &= P_s \times R_p \times I \\ &= P_s \times R_p \times \frac{N-p-b}{N} \end{aligned} \quad (5.2)$$

where  $R_b = N \times R_p$  is the bit rate. Assuming that the total system bandwidth is  $B$  and the bandwidth per channel is  $B_t$ , the number of channels available in the system is given by  $A = B/B_t$ . With a cluster size of  $K$  cells, the number of channels per cell is  $A/K$ . Thus, we can write

$$\begin{aligned} E &= \eta_b \times \frac{A}{K} \\ &= \frac{B}{K} \times \frac{N-p-b}{N} \times \frac{R_b}{B_t} \times P_s. \end{aligned} \quad (5.3)$$

For convenience, we set the ratio of  $R_b/B_t$  to unity as in [10,17]. In reality, this ratio will depend on the modulation scheme used [39]. However, its value does not affect the optimum value of  $K$  or the relative spectrum efficiency values. The (normalized) spectrum efficiency,  $E_s$ , is defined as

$$\begin{aligned} E_s &= \frac{E}{B} \\ &= \frac{N-p-b}{N} \times \frac{P_s}{K}. \end{aligned} \quad (5.4)$$

In the numerical results to be presented, an overhead of  $b=100$  bits/packet is assumed. In the following sections, the values of  $E_s$  for five different SIR models (as described in Chapter 2) in a non-fading and a Rayleigh fading environment are calculated. (For SIR<sub>2</sub>, SIR<sub>3</sub> and SIR<sub>5</sub>, the  $P_s$  values can be obtained from the BKER results in Chapter 4 which assume that the received powers from all interferers are equal. But for SIR<sub>1</sub> and SIR<sub>4</sub>, the received powers are not assumed to be equal from all interferers, and the BKER is obtained from a separate simulation.) The use of BCH codes [38] of approximate rates 0.75 for error correction is also studied.

## 5.2 Spectrum Efficiency in a Non-fading Environment

In this section, only the first-tier co-channel interferers are considered. Both omnidirectional as well as directional antennas are examined.

### 5.2.1 Omnidirectional Antennas

The six first-tier co-channel interferers in an omnidirectional antenna system are considered. The SIR models are SIR<sub>1</sub>, SIR<sub>2</sub> and SIR<sub>3</sub> (see Chapter 2). Table 5.1 shows the spectrum efficiency for different values of  $K$  and  $\beta$  with AWGN at  $\frac{E_b}{N_o} = 40$  dB and  $N=255$  bits. In this and subsequent tables,  $\sim 0$  is used to represent a value less than  $10^{-10}$ .

**Table 5.1: The spectrum efficiency of an omnidirectional antenna system in a non-fading environment with 6 co-channel interferers, AWGN at  $\frac{E_b}{N_o} = 40$  dB and  $N=255$  bits.**

$K$	$\beta = 4$			$\beta = 3$		
	SIR <sub>1</sub>	SIR <sub>2</sub>	SIR <sub>3</sub>	SIR <sub>1</sub>	SIR <sub>2</sub>	SIR <sub>3</sub>
1	$\sim 0$	$\sim 0$	$4.25 \times 10^{-2}$	$\sim 0$	$\sim 0$	$6.08 \times 10^{-4}$
3	0.203	0.100	0.203	0.130	$1.01 \times 10^{-2}$	0.195
4	0.152	0.152	0.152	0.151	$7.14 \times 10^{-2}$	0.152
7	$8.68 \times 10^{-2}$					
9	$6.75 \times 10^{-2}$					
12	$5.06 \times 10^{-2}$					

In SIR<sub>1</sub> and SIR<sub>2</sub>, for  $K=1$ ,  $E_s$  is quite small because SIR values (see Table 2.1) is negative; in other words, the total interference power is greater than the desired signal power. The optimal value of  $K$  is higher in SIR<sub>2</sub> than in SIR<sub>1</sub> and SIR<sub>3</sub> because SIR<sub>2</sub> results in greater

interference than the others. Note that  $E_s$  has the same value in all models for  $K \geq 4$  with  $\beta=4$  and  $K \geq 7$  with  $\beta=3$ . The reason is that for these cases,  $P_s$  is nearly equal to 1 because the interference signals become negligible. For  $K \leq 4$ ,  $E_s$  with  $\beta=3$  is lower than with  $\beta=4$  because the interference for  $\beta=3$  is greater (see Tables 2.1 and 2.2). For  $K \geq 7$ ,  $E_s$  has the same value for both values of  $\beta$  because the effect of co-channel interference is very small and  $P_s$  is nearly equal to 1. The optimal value,  $K_{opt}$ , of  $K$  in SIR<sub>1</sub> and SIR<sub>2</sub> with  $\beta=3$  is higher than with  $\beta=4$ .

Corresponding results for  $N=1023$  bits (instead of 255 bits) are shown in Table 5.2.

**Table 5.2: The spectrum efficiency of an omnidirectional antenna system in a non-fading environment with AWGN at  $\frac{E_b}{N_o}=40$  dB and  $N=1023$  bits.**

K	$\beta=4$			$\beta=3$		
	SIR <sub>1</sub>	SIR <sub>2</sub>	SIR <sub>3</sub>	SIR <sub>1</sub>	SIR <sub>2</sub>	SIR <sub>3</sub>
1	~0	~0	$4.78 \times 10^{-2}$	~0	~0	$9.02 \times 10^{-6}$
3	0.301	0.129	0.301	0.166	$1.42 \times 10^{-2}$	0.281
4	0.226	0.226	0.226	0.218	$8.57 \times 10^{-2}$	0.226
7	0.129	0.129	0.129	0.129	0.129	0.129
9	0.100	0.100	0.100	0.100	0.100	0.100
12	$7.52 \times 10^{-2}$					

The value of  $K_{opt}$  for SIR<sub>2</sub> is higher than for the other SIR models. Similarly,  $E_s$  with  $\beta=4$  is higher than with  $\beta=3$  for  $K \leq 4$  due to the greater interference with  $\beta=3$ . Compared to Table 5.1,  $K_{opt}$  is the same for both  $N=255$  and 1023 in all SIR models. From the results in previous chapter, BKER with  $N=1023$  is higher than with  $N=255$  bits for the SIR values with  $K \leq 4$  so that for  $K \leq 4$ ,  $P_s$  with  $N=1023$  is lower than with  $N=255$ . For  $K > 4$ ,  $P_s$  is nearly equal

to 1 for both  $N$  because BKER is nearly equal to 0. However, from Table 5.1 and 5.2, it can be seen that  $E_s$  with  $N=1023$  is always higher than with  $N=255$  for all  $K$  because the factor,  $I/N$ , in (5.4) increases the spectrum efficiency with increasing  $N$ .

The spectrum efficiency of SIR<sub>1</sub>, SIR<sub>2</sub> and SIR<sub>3</sub> for different values of  $K$  and  $\beta$  with AWGN at  $\frac{E_b}{N_o}=20$  dB and  $N=255$  bits are shown in Table 5.3.

**Table 5.3: The spectrum efficiency,  $E_s$ , of an omnidirectional antenna system in a non-fading environment with AWGN at  $\frac{E_b}{N_o}=20$  dB and  $N=255$  bits.**

$K$	$\beta=4$			$\beta=3$		
	SIR <sub>1</sub>	SIR <sub>2</sub>	SIR <sub>3</sub>	SIR <sub>1</sub>	SIR <sub>2</sub>	SIR <sub>3</sub>
1	~0	~0	$2.12 \times 10^{-2}$	~0	~0	$6.08 \times 10^{-7}$
3	0.201	$8.51 \times 10^{-2}$	0.203	$8.87 \times 10^{-2}$	$3.04 \times 10^{-3}$	0.169
4	0.152	0.149	0.152	0.138	$5.17 \times 10^{-2}$	0.151
7	$8.68 \times 10^{-2}$	$8.68 \times 10^{-2}$	$8.68 \times 10^{-2}$	$8.68 \times 10^{-2}$	$8.64 \times 10^{-2}$	$8.68 \times 10^{-2}$
9	$6.75 \times 10^{-2}$					
12	$5.06 \times 10^{-2}$					

Similar to previous observations,  $E_s$  with  $\beta=4$  is higher than with  $\beta=3$  due to greater interference with  $\beta=3$ .  $K_{opt}$  with  $\beta=3$  is also higher than with  $\beta=4$  in SIR<sub>1</sub> and SIR<sub>2</sub>. Compared to Table 5.1,  $E_s$  is lower (for  $K \leq 4$ ) because of the greater Gaussian background noise. For  $K \geq 7$ ,  $E_s$  has the same value in Table 5.1 and 5.3 because  $P_s$  approaches to 1. Compared to the results of case 1 and case 2 in [17], the values of  $K_{opt}$  in SIR<sub>2</sub> and SIR<sub>3</sub> with  $\beta=4$  in Tables 5.1 and 5.2 are somewhat lower. This is because the error performance for a given interference power

calculated with the model in [17] is higher than that obtained from the simulations or theoretical model in Section 4.2.2. The SIR value needed to obtain a given BKER is about  $10 \log_{10} 2.2$  dB lower than in [17].

### 5.2.2 Omnidirectional Antenna System with Forward Error Correction (FEC)

FEC can be used to improve the error performance. Here, BCH codes [38] of rate approximately equal to 0.75 are employed. The parameters  $(n, k, t)$  for  $N=255$  and 1023 bits are  $(255, 191, 8)$  and  $(1023, 768, 26)$ , i.e. the number of bit errors to be corrected for  $N=255$  and 1023 bits are 8 and 26 respectively. The values of  $p$  are 64 and 255 respectively. The spectrum efficiency of an omnidirectional antenna system with FEC is shown in Table 5.4, for different values of  $K$  and  $\beta$  with AWGN at  $\frac{E_b}{N_o} = 40$  dB and  $N=255$  bits.

**Table 5.4: The spectrum efficiency,  $E_s$ , of an omnidirectional antenna system with FEC in a non-fading environment with AWGN at  $\frac{E_b}{N_o} = 40$  dB and  $N=255$  bits.**

$K$	$\beta=4$			$\beta=3$		
	SIR <sub>1</sub>	SIR <sub>2</sub>	SIR <sub>3</sub>	SIR <sub>1</sub>	SIR <sub>2</sub>	SIR <sub>3</sub>
1	~0	~0	0.128	~0	~0	$3.20 \times 10^{-2}$
3	0.119	0.102	0.119	0.109	$3.57 \times 10^{-2}$	0.119
4	$8.92 \times 10^{-2}$	$8.92 \times 10^{-2}$	$8.92 \times 10^{-2}$	$8.92 \times 10^{-2}$	$7.32 \times 10^{-2}$	$8.92 \times 10^{-2}$
7	$5.10 \times 10^{-2}$					
9	$3.97 \times 10^{-2}$					
12	$2.97 \times 10^{-2}$					

With the use of FEC,  $K_{opt}$  decreases slightly from 4 to 3 in SIR<sub>2</sub> and 3 to 1 in SIR<sub>3</sub> with

$\beta=4$ . For  $\beta=3$ ,  $K_{opt}$  decreases from 4 to 3 in SIR<sub>1</sub> and 7 to 4 in SIR<sub>2</sub>. Compared to Table 5.1,  $E_s$  is higher in SIR<sub>2</sub> for  $K=3$  and in SIR<sub>3</sub> for  $K=1$  and  $\beta=4$ . For  $\beta=3$ ,  $E_s$  is higher in SIR<sub>2</sub> for  $K=3,4$  and in SIR<sub>3</sub> for  $K=1$ . However, for other values of  $K$ ,  $E_s$  is lower because  $P_s$  is nearly equal to 1 even with no FEC and  $E_s$  with FEC is reduced due to the overhead bits used for error correction.

Table 5.5 shows  $E_s$  for different values of  $K$  and  $\beta$  with AWGN at  $\frac{E_b}{N_o}=40$  dB and  $N=1023$  bits.

**Table 5.5: The spectrum efficiency,  $E_s$ , of an omnidirectional antenna system with FEC in a non-fading environment with AWGN at  $\frac{E_b}{N_o}=40$  dB and  $N=1023$ .**

$K$	$\beta=4$			$\beta=3$		
	SIR <sub>1</sub>	SIR <sub>2</sub>	SIR <sub>3</sub>	SIR <sub>1</sub>	SIR <sub>2</sub>	SIR <sub>3</sub>
1	~0	~0	0.221	~0	~0	$4.24 \times 10^{-2}$
3	0.218	0.178	0.218	0.195	$6.31 \times 10^{-2}$	0.218
4	0.163	0.163	0.163	0.163	0.127	0.163
7	$9.33 \times 10^{-2}$					
9	$7.26 \times 10^{-2}$					
12	$5.44 \times 10^{-2}$					

It can be seen that  $K_{opt}$  has the same value for  $N=255$  and 1023 bits.  $E_s$  is higher than the corresponding values for  $N=255$  in Table 5.4 due to the factor  $I/N$ . Compared to Table 5.2,  $K_{opt}$  decreases slightly and  $E_s$  is improved for low values of  $K$  in some SIR models.

Table 5.6 shows  $E_s$  for different values of  $K$  and  $\beta$  with AWGN at  $\frac{E_b}{N_o}=20$  dB and  $N=255$ .

As expected,  $E_s$  with higher background noise is lower. Compared to Table 5.3,  $K_{opt}$  decreases slightly and  $E_s$  is improved only for small values of  $K$  in some SIR models. Although FEC reduces block error rates, it does not necessarily improve the spectrum efficiency. Typically, FEC can improve  $E_s$  for values of  $K$  which are lower than the  $K_{opt}$  value with no FEC.

**Table 5.6: The spectrum efficiency,  $E_s$ , of an omnidirectional antenna system with FEC in a non-fading environment with AWGN at  $\frac{E_b}{N_o} = 20$  dB and  $N=255$ .**

$K$	$\beta = 4$			$\beta = 3$		
	SIR <sub>1</sub>	SIR <sub>2</sub>	SIR <sub>3</sub>	SIR <sub>1</sub>	SIR <sub>2</sub>	SIR <sub>3</sub>
1	~0	~0	0.125	~0	~0	$3.57 \times 10^{-2}$
3	0.119	$9.75 \times 10^{-2}$	0.119	0.101	$2.97 \times 10^{-2}$	0.118
4	$8.92 \times 10^{-2}$	$8.91 \times 10^{-2}$	$8.92 \times 10^{-2}$	$8.91 \times 10^{-2}$	$6.96 \times 10^{-2}$	$8.92 \times 10^{-2}$
7	$5.10 \times 10^{-2}$					
9	$3.97 \times 10^{-2}$					
12	$2.97 \times 10^{-2}$					

### 5.2.3 Directional Antenna System

In a  $120^\circ$  directional antenna system, each cell is divided into three sectors. The number of co-channel interferers is reduced from six to two. Two SIR models, SIR<sub>4</sub> and SIR<sub>5</sub> (see Chapter 2), are considered. For error correction, BCH codes with rate of approximately 0.75 are again assumed.

The spectrum efficiencies in a directional antenna system with different values of  $K$ ,  $N$  and background noise levels for  $\beta = 4$  are shown in Table 5.7.

**Table 5.7: The spectrum efficiency,  $E_s$ , of a directional antenna system in a non-fading environment with  $\beta=4$ .**

$K$	$\frac{E_b}{N_o} = 40 \text{ dB}$				$\frac{E_b}{N_o} = 20 \text{ dB}$	
	$N=1023 \text{ bits}$		$N=255 \text{ bits}$		$N=255 \text{ bits}$	
	SIR <sub>4</sub>	SIR <sub>5</sub>	SIR <sub>4</sub>	SIR <sub>5</sub>	SIR <sub>4</sub>	SIR <sub>5</sub>
1	0.902	0.902	0.608	0.608	0.608	0.605
3	0.301	0.301	0.203	0.203	0.203	0.203
4	0.226	0.226	0.152	0.152	0.152	0.152
7	0.129	0.129	$8.68 \times 10^{-2}$	$8.68 \times 10^{-2}$	$8.68 \times 10^{-2}$	$8.68 \times 10^{-2}$
9	0.100	0.100	$6.75 \times 10^{-2}$	$6.75 \times 10^{-2}$	$6.75 \times 10^{-2}$	$6.75 \times 10^{-2}$
12	$7.52 \times 10^{-2}$	$7.52 \times 10^{-2}$	$5.06 \times 10^{-2}$	$5.06 \times 10^{-2}$	$5.06 \times 10^{-2}$	$5.06 \times 10^{-2}$

It can be seen that the optimal value,  $K_{opt}$ , of  $K$  in SIR<sub>4</sub> and SIR<sub>5</sub> is 1. The spectrum efficiency,  $E_s$ , has the same value in both SIR models because from Section 4.2.2, the BKER for 2 interferers in a non-fading environment is very low for the SIR values corresponding to  $K \geq 1$ . Therefore,  $P_s$  is nearly equal to 1 for all  $K$  in both SIR models.  $E_s$  for  $K=1$  is at least 3 times higher than that for  $K>1$ . The spectrum efficiency in a directional antenna system is improved greatly as compared with  $E_s$  in an omnidirectional antenna system. The reasons are that (1) the BKER is much lower with 2 interferers than with 6 interferers even for a given SIR value (2) the corresponding SIR values with 2 interferers for each  $K$  is higher i.e. the interference is much smaller. However, for  $K \geq 7$ ,  $E_s$  has the same value in both systems because  $P_s$  is almost equal to 1.

Corresponding results for  $\beta=3$  (instead of  $\beta=4$ ) are shown in Table 5.8. With  $\beta=3$ ,  $K_{opt}$

is still equal to 1. In Table 5.7 and 5.8,  $E_s$  has the same value with AWGN at  $\frac{E_b}{N_o} = 40$  dB although the interference for  $\beta = 4$  is lesser than for  $\beta = 3$ . This is because BKER is quite small for the corresponding SIR values and  $P_s$  is nearly equal to 1.

**Table 5.8: The spectrum efficiency,  $E_s$ , of a directional antenna system in a non-fading environment with  $\beta = 3$ .**

$K$	$\frac{E_b}{N_o} = 40$ dB				$\frac{E_b}{N_o} = 20$ dB	
	$N=1023$ bits		$N=255$ bits		$N=255$ bits	
	SIR <sub>4</sub>	SIR <sub>5</sub>	SIR <sub>4</sub>	SIR <sub>5</sub>	SIR <sub>4</sub>	SIR <sub>5</sub>
1	0.902	0.902	0.608	0.608	0.591	0.316
3	0.301	0.301	0.203	0.203	0.203	0.203
4	0.226	0.226	0.152	0.152	0.152	0.152
7	0.129	0.129	$8.68 \times 10^{-2}$	$8.68 \times 10^{-2}$	$8.68 \times 10^{-2}$	$8.68 \times 10^{-2}$
9	0.100	0.100	$6.75 \times 10^{-2}$	$6.75 \times 10^{-2}$	$6.75 \times 10^{-2}$	$6.75 \times 10^{-2}$
12	$7.52 \times 10^{-2}$	$7.52 \times 10^{-2}$	$5.06 \times 10^{-2}$	$5.06 \times 10^{-2}$	$5.06 \times 10^{-2}$	$5.06 \times 10^{-2}$

In a directional antenna system with no FEC,  $P_s$  is very close to 1 for all cases (except for  $K=1$ ,  $\beta = 3$  and  $\frac{E_b}{N_o} = 20$  dB) so that there is no benefit to using FEC. With FEC,  $P_s$  is nearly equal to 1 in all cases in Tables 5.7 and 5.8. The corresponding  $E_s$  values in both tables are reduced by the factor  $I/N$  due to the effect of the overhead correction bits. Compared to the omnidirectional antenna system, the optimal value of  $E_s$  is about three times higher.

### 5.3 Spectrum Efficiency in a (very slow) Rayleigh Fading Environment

In this section, the spectrum efficiency in a very slow Rayleigh fading environment is obtained. Only the first-tier co-channel interferers are considered as well.

#### 5.3.1 Omnidirectional Antenna System

The spectrum efficiency,  $E_s$ , in an omnidirectional system is shown in Table 5.9, for different  $K$  and  $\beta$  with AWGN at  $\frac{E_b}{N_o} = 40$  dB and  $N=255$  bits.

**Table 5.9:  $E_s$  in an omnidirectional antenna system with very slow Rayleigh fading with AWGN at  $\frac{E_b}{N_o} = 40$  dB and  $N=255$  bits.**

$K$	$\beta = 4$			$\beta = 3$		
	SIR <sub>1</sub>	SIR <sub>2</sub>	SIR <sub>3</sub>	SIR <sub>1</sub>	SIR <sub>2</sub>	SIR <sub>3</sub>
1	-0	-0	0.158	-0	-0	$7.29 \times 10^{-2}$
3	0.151	$8.31 \times 10^{-2}$	0.171	0.101	$4.46 \times 10^{-2}$	0.122
4	0.127	0.105	0.137	$9.57 \times 10^{-2}$	$6.08 \times 10^{-2}$	0.109
7	$8.28 \times 10^{-2}$	$7.88 \times 10^{-2}$	$8.31 \times 10^{-2}$	$6.99 \times 10^{-2}$	$6.47 \times 10^{-2}$	$7.77 \times 10^{-2}$
9	$6.53 \times 10^{-2}$	$6.36 \times 10^{-2}$	$6.56 \times 10^{-2}$	$6.00 \times 10^{-2}$	$5.61 \times 10^{-2}$	$6.21 \times 10^{-2}$
12	$4.96 \times 10^{-2}$	$4.9 \times 10^{-2}$	$4.98 \times 10^{-2}$	$4.64 \times 10^{-2}$	$4.48 \times 10^{-2}$	$4.68 \times 10^{-2}$
13	$4.60 \times 10^{-2}$	$4.54 \times 10^{-2}$	$4.61 \times 10^{-2}$	$4.33 \times 10^{-2}$	$4.18 \times 10^{-2}$	$4.35 \times 10^{-2}$
16	$3.76 \times 10^{-2}$	$3.73 \times 10^{-2}$	$3.76 \times 10^{-2}$	$3.57 \times 10^{-2}$	$3.50 \times 10^{-2}$	$3.65 \times 10^{-2}$

$E_s$  for SIR<sub>2</sub> is lower than for other SIR models and  $K_{opt}$  for SIR<sub>2</sub> is higher than for other SIR models due to greater interference. For  $K \geq 12$ ,  $E_s$  in all SIR models is very close to each other because the interference level is negligible. Compared to the non-fading case in Table 5.1,  $E_s$  is lower because  $P_s$  is lower in very slow fading. Compared to [17],  $E_s$  is higher for all  $K$

because in [17] the errors occurring on the Rayleigh fading environment are assumed to be independent (idealized (infinite) interleaving assumption) and so the BKER is higher.

Table 5.10 shows  $E_s$  for  $N=1023$  bits. Compared to Table 5.9,  $K_{opt}$  is unchanged. In Tables 5.9 and 5.10,  $K_{opt}$  increases slightly only for  $SIR_2$  (from 4 to 7) when  $\beta$  is reduced to 3. Therefore,  $\beta$  does not greatly affect the optimal value of  $K$ . For both non-fading and fading environments,  $K_{opt}$  has the same value for  $N=255$  and 1023 bits. Thus  $K_{opt}$  is not very sensitive to block length.

**Table 5.10:  $E_s$  in an omnidirectional antenna system with very slow Rayleigh fading with AWGN at  $\frac{E_b}{N_o}=40$  dB and  $N=1023$  bits.**

$K$	$\beta = 4$			$\beta = 3$		
	$SIR_1$	$SIR_2$	$SIR_3$	$SIR_1$	$SIR_2$	$SIR_3$
1	~0	~0	0.230	~0	~0	0.122
3	0.215	0.120	0.244	0.138	$6.62 \times 10^{-2}$	0.165
4	0.180	0.156	0.206	0.127	$8.91 \times 10^{-2}$	0.156
7	0.120	0.117	0.123	0.117	$8.96 \times 10^{-2}$	0.108
9	$9.64 \times 10^{-2}$	$9.44 \times 10^{-2}$	$9.71 \times 10^{-2}$	$8.72 \times 10^{-2}$	$8.00 \times 10^{-2}$	$8.92 \times 10^{-2}$
12	$7.35 \times 10^{-2}$	$7.24 \times 10^{-2}$	$7.36 \times 10^{-2}$	$6.89 \times 10^{-2}$	$6.62 \times 10^{-2}$	$6.96 \times 10^{-2}$
13	$6.80 \times 10^{-2}$	$6.73 \times 10^{-2}$	$6.81 \times 10^{-2}$	$6.44 \times 10^{-2}$	$6.19 \times 10^{-2}$	$6.45 \times 10^{-2}$
16	$5.55 \times 10^{-2}$	$5.52 \times 10^{-2}$	$5.56 \times 10^{-2}$	$5.31 \times 10^{-2}$	$5.22 \times 10^{-2}$	$5.35 \times 10^{-2}$

Table 5.11 shows  $E_s$  with higher Gaussian background noise at  $\frac{E_b}{N_o} = 20$  dB and  $N=255$  bits. For  $\beta = 3$ , the  $E_s$  values are obtained only for  $SIR_2$  and  $SIR_3$  because the simulation results for  $SIR_1$  were not available due to time constraints.

**Table 5.11:  $E_s$  in an omnidirectional antenna system with very slow Rayleigh fading with AWGN at  $\frac{E_b}{N_o} = 20$  dB and  $N=255$  bits.**

$K$	$\beta = 4$			$\beta = 3$	
	SIR <sub>1</sub>	SIR <sub>2</sub>	SIR <sub>3</sub>	SIR <sub>2</sub>	SIR <sub>3</sub>
1	~0	~0	0.131	~0	$3.95 \times 10^{-2}$
3	0.124	$7.29 \times 10^{-2}$	0.162	$4.01 \times 10^{-2}$	$9.93 \times 10^{-2}$
4	0.109	$9.27 \times 10^{-2}$	0.119	$6.89 \times 10^{-2}$	$9.12 \times 10^{-2}$
7	$7.35 \times 10^{-2}$	$6.90 \times 10^{-2}$	$7.47 \times 10^{-2}$	$5.30 \times 10^{-2}$	$6.34 \times 10^{-2}$
9	$5.84 \times 10^{-2}$	$5.67 \times 10^{-2}$	$5.89 \times 10^{-2}$	$4.69 \times 10^{-2}$	$5.27 \times 10^{-2}$
12	$4.48 \times 10^{-2}$	$4.41 \times 10^{-2}$	$4.50 \times 10^{-2}$	$3.90 \times 10^{-2}$	$4.10 \times 10^{-2}$

Compared to the non-fading case in Table 5.3,  $E_s$  is lower, but  $K_{opt}$  has the same value except that  $K_{opt}$  is reduced from 7 to 4 in SIR<sub>2</sub> for  $\beta = 3$ . Even though BKER is higher in the very slow fading environment,  $K_{opt}$  is not increased.

Compared to the non-fading environment, for  $K > 1$ ,  $E_s$  is lower due to the higher BKER. However, for  $K=1$ ,  $E_s$  is higher in SIR<sub>3</sub> (for SIR<sub>1</sub> and SIR<sub>2</sub>,  $E_s$  is very small in both environments). The reason is that for  $K=1$ , the SIR value is less than about 2 dB as seen in Tables 2.1 and 2.2. In a non-fading environment, the BKER is nearly equal to 1, but the BKER in fading is less than 1 due to the bursty nature of the errors.

### 5.3.2 Omnidirectional Antenna System with FEC

The effect of using approximate rate 0.75 BCH codes was considered. The  $E_s$  values are

shown in Table 5.12, with AWGN at  $\frac{E_b}{N_o}=40$  dB and  $N=255$  bits. Table 5.13 shows  $E_s$  with

AWGN at  $\frac{E_b}{N_o}=40$  dB and  $N=1023$  bits. Table 5.14 shows  $E_s$  with AWGN at  $\frac{E_b}{N_o}=20$  dB and

$N=255$  bits.

**Table 5.12:  $E_s$  in an omnidirectional antenna system with FEC in a very slow**

**Rayleigh fading environment with AWGN at  $\frac{E_b}{N_o}=40$  dB and  $N=255$  bits.**

K	$\beta = 4$			$\beta = 3$		
	SIR <sub>1</sub>	SIR <sub>2</sub>	SIR <sub>3</sub>	SIR <sub>1</sub>	SIR <sub>2</sub>	SIR <sub>3</sub>
1	~0	~0	0.136	~0	~0	$9.65 \times 10^{-2}$
3	$9.64 \times 10^{-2}$	$6.66 \times 10^{-2}$	0.105	$7.11 \times 10^{-2}$	$3.93 \times 10^{-2}$	$8.33 \times 10^{-2}$
4	$7.85 \times 10^{-2}$	$6.91 \times 10^{-2}$	$8.31 \times 10^{-2}$	$6.38 \times 10^{-2}$	$4.56 \times 10^{-2}$	$8.03 \times 10^{-2}$
7	$4.95 \times 10^{-2}$	$4.79 \times 10^{-2}$	$4.96 \times 10^{-2}$	$4.39 \times 10^{-2}$	$4.05 \times 10^{-2}$	$4.59 \times 10^{-2}$
9	$3.88 \times 10^{-2}$	$3.82 \times 10^{-2}$	$3.89 \times 10^{-2}$	$3.64 \times 10^{-2}$	$3.43 \times 10^{-2}$	$3.69 \times 10^{-2}$
12	$2.94 \times 10^{-2}$	$2.91 \times 10^{-2}$	$2.94 \times 10^{-2}$	$2.81 \times 10^{-2}$	$2.74 \times 10^{-2}$	$2.83 \times 10^{-2}$

**Table 5.13:  $E_s$  in an omnidirectional antenna system with FEC in a very slow**

**Rayleigh fading environment with AWGN at  $\frac{E_b}{N_o}=40$  dB and  $N=1023$  bits.**

K	$\beta = 4$			$\beta = 3$		
	SIR <sub>1</sub>	SIR <sub>2</sub>	SIR <sub>3</sub>	SIR <sub>1</sub>	SIR <sub>2</sub>	SIR <sub>3</sub>
1	~0	~0	0.271	~0	~0	0.245
3	0.173	0.112	0.194	0.132	$8.16 \times 10^{-2}$	0.141
4	0.140	0.122	0.153	0.110	$8.71 \times 10^{-2}$	0.129
7	$8.91 \times 10^{-2}$	$8.81 \times 10^{-2}$	$9.17 \times 10^{-2}$	$8.76 \times 10^{-2}$	$7.56 \times 10^{-2}$	$8.49 \times 10^{-2}$
9	$7.11 \times 10^{-2}$	$6.99 \times 10^{-2}$	$7.13 \times 10^{-2}$	$6.73 \times 10^{-2}$	$6.42 \times 10^{-2}$	$6.80 \times 10^{-2}$
12	$5.56 \times 10^{-2}$	$5.34 \times 10^{-2}$	$5.37 \times 10^{-2}$	$5.16 \times 10^{-2}$	$5.06 \times 10^{-2}$	$5.20 \times 10^{-2}$

**Table 5.14:  $E_s$  in an omnidirectional antenna system with FEC in a very slow Rayleigh fading environment with AWGN at  $\frac{E_b}{N_o}=20$  dB and  $N=255$  bits.**

$K$	$\beta = 4$			$\beta = 3$	
	SIR <sub>1</sub>	SIR <sub>2</sub>	SIR <sub>3</sub>	SIR <sub>2</sub>	SIR <sub>3</sub>
1	~0	~0	0.114	~0	$6.07 \times 10^{-2}$
3	$8.89 \times 10^{-2}$	$5.83 \times 10^{-2}$	$9.64 \times 10^{-2}$	$3.63 \times 10^{-2}$	$7.43 \times 10^{-2}$
4	$7.34 \times 10^{-2}$	$6.20 \times 10^{-2}$	$7.63 \times 10^{-2}$	$4.28 \times 10^{-2}$	$6.43 \times 10^{-2}$
7	$4.66 \times 10^{-2}$	$4.49 \times 10^{-2}$	$4.72 \times 10^{-2}$	$3.70 \times 10^{-2}$	$4.21 \times 10^{-2}$
9	$3.71 \times 10^{-2}$	$3.61 \times 10^{-2}$	$3.71 \times 10^{-2}$	$3.17 \times 10^{-2}$	$3.41 \times 10^{-2}$
12	$2.80 \times 10^{-2}$	$2.78 \times 10^{-2}$	$2.80 \times 10^{-2}$	$2.56 \times 10^{-2}$	$2.66 \times 10^{-2}$

The spectrum efficiency,  $E_s$ , is higher for  $N=1023$  bits than that for  $N=255$  bits due to a higher factor  $I/N$ . The longer block length  $N$  or higher background noise level does not change  $K_{opt}$ . Compared to no FEC,  $K_{opt}$  is reduced for SIR<sub>2</sub> for  $\beta = 3$  and SIR<sub>3</sub> because FEC improves the error performance; however, FEC does not generally improve  $E_s$ .

### 5.3.3 Directional Antenna System

The  $E_s$  values for SIR<sub>4</sub> and SIR<sub>5</sub> in a directional antenna system with different values of  $K$ ,  $N$  and background noise levels for  $\beta = 4$  are shown in Table 5.15. Values for  $\beta = 3$  are shown in Table 5.16. It can be seen that in both tables the optimal value of  $K$  is 1. The spectrum efficiency,  $E_s$ , in SIR<sub>5</sub> is lower than that in SIR<sub>4</sub> because the interference is greater.  $E_s$  for  $K=1$  is about two times higher than that for  $K > 1$ . The  $E_s$  value in Table 5.15 for  $K=1$  and  $N=255$  at  $E_b/N_o=20$  dB is higher than that in Table 5.16 at  $E_b/N_o=40$  dB because of the increased interference with the lower  $\beta$ . For  $K > 1$ , the lower background noise becomes more important. For  $K \geq 9$ ,  $E_s$  are about

the same because the effect of the interference is negligible. Compared to no fading, the  $E_s$  values are lower, but  $K_{opt}$  does not change.

**Table 5.15: The spectrum efficiency,  $E_s$ , of a directional antenna system in a very slow fading environment with  $\beta=4$ .**

$K$	$\frac{E_b}{N_o} = 40 \text{ dB}$				$\frac{E_b}{N_o} = 20 \text{ dB}$	
	$N=1023 \text{ bits}$		$N=255 \text{ bits}$		$N=255 \text{ bits}$	
	SIR <sub>4</sub>	SIR <sub>5</sub>	SIR <sub>4</sub>	SIR <sub>5</sub>	SIR <sub>4</sub>	SIR <sub>5</sub>
1	0.663	0.623	0.496	0.419	0.414	0.356
3	0.290	0.286	0.194	0.192	0.169	0.165
4	0.218	0.217	0.147	0.146	0.128	0.127
7	0.127	0.126	$8.57 \times 10^{-2}$	$8.56 \times 10^{-2}$	$7.73 \times 10^{-2}$	$7.68 \times 10^{-2}$
9	$9.91 \times 10^{-2}$	$9.88 \times 10^{-2}$	$6.70 \times 10^{-2}$	$6.68 \times 10^{-2}$	$6.02 \times 10^{-2}$	$6.02 \times 10^{-2}$
12	$7.46 \times 10^{-2}$	$7.45 \times 10^{-2}$	$5.04 \times 10^{-2}$	$5.03 \times 10^{-2}$	$4.53 \times 10^{-2}$	$4.53 \times 10^{-2}$
13	$6.89 \times 10^{-2}$	$6.89 \times 10^{-2}$	$4.65 \times 10^{-2}$	$4.65 \times 10^{-2}$	$4.18 \times 10^{-2}$	$4.18 \times 10^{-2}$

**Table 5.16: The spectrum efficiency,  $E_s$ , of a directional antenna system in a very slow fading environment with  $\beta=3$ .**

$K$	$\frac{E_b}{N_o} = 40 \text{ dB}$				$\frac{E_b}{N_o} = 20 \text{ dB}$
	$N=1023 \text{ bits}$		$N=255 \text{ bits}$		$N=255 \text{ bits}$
	SIR <sub>4</sub>	SIR <sub>5</sub>	SIR <sub>4</sub>	SIR <sub>5</sub>	SIR <sub>5</sub>
1	0.548	0.532	0.368	0.346	0.267
3	0.271	0.248	0.181	0.176	0.154
4	0.208	0.206	0.140	0.139	0.122
7	0.123	0.123	$8.44 \times 10^{-2}$	$8.29 \times 10^{-2}$	$7.25 \times 10^{-2}$
9	$9.70 \times 10^{-2}$	$9.65 \times 10^{-2}$	$6.56 \times 10^{-2}$	$6.56 \times 10^{-2}$	$5.84 \times 10^{-2}$
12	$7.33 \times 10^{-2}$	$7.31 \times 10^{-2}$	$5.01 \times 10^{-2}$	$4.95 \times 10^{-2}$	$4.46 \times 10^{-2}$
13	$6.78 \times 10^{-2}$	$6.75 \times 10^{-2}$	$4.58 \times 10^{-2}$	$4.58 \times 10^{-2}$	$4.09 \times 10^{-2}$

The spectrum efficiency in a directional antenna system with FEC for  $\beta = 4$  is shown in Table 5.17. With FEC,  $K_{opt}$  is still equal to 1 in all SIR models. Compared to no FEC, the spectrum efficiency is reduced although  $P_s$  is increased because of the overhead (FEC) bits. Compared to the omnidirectional antenna system, the optimal  $E_s$  in the directional antenna system is much higher.

**Table 5.17: The spectrum efficiency,  $E_s$ , of a directional antenna system with FEC in a very slow fading environment with  $\beta = 4$ .**

K	$\frac{E_b}{N_o} = 40$ dB				$\frac{E_b}{N_o} = 20$ dB	
	N=1023 bits		N=255 bits		N=255 bits	
	SIR <sub>4</sub>	SIR <sub>5</sub>	SIR <sub>4</sub>	SIR <sub>5</sub>	SIR <sub>4</sub>	SIR <sub>5</sub>
1	0.520	0.464	0.303	0.257	0.280	0.236
3	0.212	0.209	0.115	0.113	0.109	0.108
4	0.160	0.157	$8.72 \times 10^{-2}$	$8.67 \times 10^{-2}$	$8.25 \times 10^{-2}$	$8.23 \times 10^{-2}$
7	$9.25 \times 10^{-2}$	$9.24 \times 10^{-2}$	$5.05 \times 10^{-2}$	$5.05 \times 10^{-2}$	$4.81 \times 10^{-2}$	$4.80 \times 10^{-2}$
9	$7.22 \times 10^{-2}$	$7.21 \times 10^{-2}$	$3.94 \times 10^{-2}$	$3.94 \times 10^{-2}$	$3.75 \times 10^{-2}$	$3.75 \times 10^{-2}$
12	$5.42 \times 10^{-2}$	$5.42 \times 10^{-2}$	$2.96 \times 10^{-2}$	$2.96 \times 10^{-2}$	$2.82 \times 10^{-2}$	$2.82 \times 10^{-2}$

#### 5.4 Spectrum Efficiency with Different Values of $f_d T_m$

In this section, the spectrum efficiency in a Rayleigh fading environment which cannot be characterized as very slow fading, i.e. the parameter  $f_d T_m$  is not much less than 1, is obtained. Values of  $f_d T_m \approx 1$  and 5 are used. Only the six and two co-channel interferers in the first tier are considered in an omnidirectional and a directional antenna system respectively.

### 5.4.1 Omnidirectional Antenna System

For the omnidirectional antenna system,  $E_s$  in SIR<sub>2</sub> and SIR<sub>3</sub> are obtained. Table 5.18 shows the values of  $E_s$  for  $f_d T_m \approx 1$  with different  $K$ ,  $N$ ,  $\beta$  and AWGN at  $\frac{E_b}{N_o} = 40$  dB. The values of  $f_d$  for  $N=255$  and 1023 bits are set to be 20 and 5 Hz respectively.

**Table 5.18: The spectrum efficiency,  $E_s$ , in an omnidirectional antenna system in a fading environment for  $f_d T_m \approx 1$ .**

K	N=255 bits				N=1023 bits			
	$\beta = 4$		$\beta = 3$		$\beta = 4$		$\beta = 3$	
	SIR <sub>2</sub>	SIR <sub>3</sub>						
1	-0	$1.22 \times 10^{-2}$	-0	$6.78 \times 10^{-5}$	-0	$9.02 \times 10^{-4}$	-0	$9.02 \times 10^{-6}$
3	$1.11 \times 10^{-2}$	$7.09 \times 10^{-2}$	$2.03 \times 10^{-3}$	$2.74 \times 10^{-2}$	$4.51 \times 10^{-3}$	$8.96 \times 10^{-2}$	$1.50 \times 10^{-4}$	$3.01 \times 10^{-2}$
4	$2.89 \times 10^{-2}$	$7.37 \times 10^{-2}$	$7.60 \times 10^{-3}$	$3.04 \times 10^{-2}$	$3.38 \times 10^{-2}$	$9.02 \times 10^{-2}$	$3.38 \times 10^{-3}$	$3.72 \times 10^{-2}$
7	$4.47 \times 10^{-2}$	$6.12 \times 10^{-2}$	$1.91 \times 10^{-2}$	$3.43 \times 10^{-2}$	$5.48 \times 10^{-2}$	$7.99 \times 10^{-2}$	$2.55 \times 10^{-2}$	$4.12 \times 10^{-2}$
9	$4.32 \times 10^{-2}$	$5.20 \times 10^{-2}$	$2.16 \times 10^{-2}$	$3.24 \times 10^{-2}$	$5.56 \times 10^{-2}$	$7.08 \times 10^{-2}$	$2.91 \times 10^{-2}$	$4.01 \times 10^{-2}$
12	$3.80 \times 10^{-2}$	$4.20 \times 10^{-2}$	$2.30 \times 10^{-2}$	$2.89 \times 10^{-2}$	$5.11 \times 10^{-2}$	$5.86 \times 10^{-2}$	$2.93 \times 10^{-2}$	$3.65 \times 10^{-2}$
13	$3.62 \times 10^{-2}$	$4.00 \times 10^{-2}$	$2.26 \times 10^{-2}$	$2.80 \times 10^{-2}$	$4.96 \times 10^{-2}$	$5.55 \times 10^{-2}$	$2.78 \times 10^{-2}$	$3.50 \times 10^{-2}$
16	$3.13 \times 10^{-2}$	$3.32 \times 10^{-2}$	$2.13 \times 10^{-2}$	$2.48 \times 10^{-2}$	$4.37 \times 10^{-2}$	$4.65 \times 10^{-2}$	$2.71 \times 10^{-2}$	$3.30 \times 10^{-2}$
19	$2.75 \times 10^{-2}$	$3.17 \times 10^{-2}$	$1.98 \times 10^{-2}$	$2.24 \times 10^{-2}$	$3.89 \times 10^{-2}$	$4.13 \times 10^{-2}$	$2.59 \times 10^{-2}$	$2.94 \times 10^{-2}$

In SIR<sub>2</sub>,  $E_s$  is lower and  $K_{opt}$  is higher.  $E_s$  for  $N=1023$  is higher than that for  $N=255$  except for the lowest values of  $K$ , i.e.  $K=1$  or 3, in each SIR model. In previous tables,  $K_{opt}$  has the same value for both  $N=255$  and 1023. But in Table 5.18,  $K_{opt}$  is slightly higher for  $N=1023$  than for  $N=255$  in SIR<sub>2</sub> with  $\beta = 4$ . Compared to a very slow fading environment,  $E_s$  is lower for all values of  $K$  because of higher BKER. The optimal value of  $K$  is also higher for all SIR models.

With FEC,  $E_s$  for different  $K$ ,  $N$  and  $\beta$  is shown in Table 5.19, with AWGN at  $\frac{E_b}{N_o} = 40$  dB.

It can be seen that the optimal value of  $K$  with  $\beta = 4$  for  $N=1023$  bits is slightly higher than for  $N=255$  bits in  $SIR_2$  and  $SIR_3$ . Compared to no FEC,  $K_{opt}$  is reduced in all cases. However, in previous sections,  $K_{opt}$  with FEC is not reduced in all cases because in some cases,  $K_{opt}$  in no FEC is the lowest value of  $K$ . For  $K < K_{opt}$  in Table 5.18,  $E_s$  with no FEC is lower than that with FEC because  $P_s$  is increased substantially with FEC. But, for  $K \geq K_{opt}$ ,  $E_s$  is higher with no FEC because  $P_s$  is nearly equal to 1 even with no FEC. Compared to a very slow fading environment,  $E_s$  is lower for FEC and no FEC because the higher fading rate results in a lower  $P_s$ .

**Table 5.19: The spectrum efficiency,  $E_s$ , in an omnidirectional antenna system with FEC in a fading environment for  $f_d T_m \approx 1$ .**

$K$	$N=255$ bits				$N=1023$ bits			
	$\beta = 4$		$\beta = 3$		$\beta = 4$		$\beta = 3$	
	$SIR_2$	$SIR_3$	$SIR_2$	$SIR_3$	$SIR_2$	$SIR_3$	$SIR_2$	$SIR_3$
1	$\sim 0$	$3.93 \times 10^{-2}$	$\sim 0$	$3.57 \times 10^{-3}$	$\sim 0$	$4.24 \times 10^{-2}$	$\sim 0$	$6.53 \times 10^{-4}$
3	$2.38 \times 10^{-2}$	$9.52 \times 10^{-2}$	$1.16 \times 10^{-2}$	$4.52 \times 10^{-2}$	$3.70 \times 10^{-2}$	0.141	$7.62 \times 10^{-3}$	$6.97 \times 10^{-2}$
4	$4.28 \times 10^{-2}$	$7.32 \times 10^{-2}$	$1.78 \times 10^{-2}$	$4.59 \times 10^{-2}$	$6.86 \times 10^{-2}$	0.147	$2.20 \times 10^{-2}$	$8.00 \times 10^{-2}$
7	$4.21 \times 10^{-2}$	$4.93 \times 10^{-2}$	$2.72 \times 10^{-2}$	$3.82 \times 10^{-2}$	$7.60 \times 10^{-2}$	$8.73 \times 10^{-2}$	$4.66 \times 10^{-2}$	$6.53 \times 10^{-2}$
9	$3.69 \times 10^{-2}$	$3.93 \times 10^{-2}$	$2.68 \times 10^{-2}$	$3.27 \times 10^{-2}$	$6.54 \times 10^{-2}$	$7.04 \times 10^{-2}$	$4.64 \times 10^{-2}$	$5.66 \times 10^{-2}$
12	$2.90 \times 10^{-2}$	$2.95 \times 10^{-2}$	$2.38 \times 10^{-2}$	$2.60 \times 10^{-2}$	$5.22 \times 10^{-2}$	$5.39 \times 10^{-2}$	$4.16 \times 10^{-2}$	$4.63 \times 10^{-2}$
13	$2.69 \times 10^{-2}$	$2.73 \times 10^{-2}$	$2.26 \times 10^{-2}$	$2.48 \times 10^{-2}$	$4.88 \times 10^{-2}$	$4.99 \times 10^{-2}$	$4.00 \times 10^{-2}$	$4.34 \times 10^{-2}$
16	$2.21 \times 10^{-2}$	$2.23 \times 10^{-2}$	$1.94 \times 10^{-2}$	$2.10 \times 10^{-2}$	$4.04 \times 10^{-2}$	$4.07 \times 10^{-2}$	$3.45 \times 10^{-2}$	$3.72 \times 10^{-2}$
19	$1.87 \times 10^{-2}$	$1.86 \times 10^{-2}$	$1.73 \times 10^{-2}$	$1.80 \times 10^{-2}$	$3.42 \times 10^{-2}$	$3.43 \times 10^{-2}$	$3.06 \times 10^{-2}$	$3.21 \times 10^{-2}$

The spectrum efficiency for  $f_d T_m \approx 5$ ,  $N=255$  bits and AWGN at  $\frac{E_b}{N_o}=40$  dB with no FEC and with FEC is tabulated in Table 5.20. The value of  $f_d$  is set to be 100 Hz. It can be seen that  $K_{opt}$  is reduced greatly by using FEC. For  $\beta=3$  with no FEC, the optimal value of  $K$  is higher than 19. For  $K < K_{opt}$  with no FEC,  $E_s$  with no FEC is lower than with FEC. However, for  $K \geq K_{opt}$ ,  $E_s$  with no FEC is higher again. A comparison of Tables 5.19 and 5.20 shows that the system performance degrades with higher Doppler frequency and  $K_{opt}$  is increased.

**Table 5.20: The spectrum efficiency,  $E_s$ , in an omnidirectional antenna system in a fading environment for  $f_d T_m \approx 5$ .**

K	No FEC				FEC			
	$\beta=4$		$\beta=3$		$\beta=4$		$\beta=3$	
	SIR <sub>2</sub>	SIR <sub>3</sub>						
1	~0	$6.08 \times 10^{-6}$	~0	$6.08 \times 10^{-7}$	~0	$1.19 \times 10^{-3}$	~0	$3.57 \times 10^{-5}$
3	$2.03 \times 10^{-4}$	$1.42 \times 10^{-2}$	$2.03 \times 10^{-6}$	$2.03 \times 10^{-4}$	$8.33 \times 10^{-3}$	$8.33 \times 10^{-2}$	$5.95 \times 10^{-4}$	$3.21 \times 10^{-2}$
4	$1.52 \times 10^{-3}$	$1.52 \times 10^{-2}$	$7.60 \times 10^{-4}$	$1.52 \times 10^{-3}$	$3.26 \times 10^{-2}$	$7.72 \times 10^{-2}$	$6.47 \times 10^{-3}$	$3.57 \times 10^{-2}$
7	$1.04 \times 10^{-2}$	$3.91 \times 10^{-2}$	$1.30 \times 10^{-3}$	$7.38 \times 10^{-3}$	$4.59 \times 10^{-2}$	$5.04 \times 10^{-2}$	$2.17 \times 10^{-2}$	$3.98 \times 10^{-2}$
9	$2.30 \times 10^{-2}$	$4.02 \times 10^{-2}$	$3.71 \times 10^{-3}$	$8.44 \times 10^{-3}$	$3.87 \times 10^{-2}$	$3.95 \times 10^{-2}$	$2.50 \times 10^{-2}$	$3.43 \times 10^{-2}$
12	$2.68 \times 10^{-2}$	$3.70 \times 10^{-2}$	$6.08 \times 10^{-3}$	$1.09 \times 10^{-2}$	$2.90 \times 10^{-2}$	$2.96 \times 10^{-2}$	$2.54 \times 10^{-2}$	$2.80 \times 10^{-2}$
13	$2.81 \times 10^{-2}$	$3.55 \times 10^{-2}$	$6.32 \times 10^{-3}$	$1.33 \times 10^{-2}$	$2.73 \times 10^{-2}$	$2.75 \times 10^{-2}$	$2.37 \times 10^{-2}$	$2.63 \times 10^{-2}$
16	$2.77 \times 10^{-2}$	$3.13 \times 10^{-2}$	$8.16 \times 10^{-3}$	$1.41 \times 10^{-2}$	$2.23 \times 10^{-2}$	$2.23 \times 10^{-2}$	$2.10 \times 10^{-2}$	$2.19 \times 10^{-2}$
19	$2.58 \times 10^{-2}$	$2.77 \times 10^{-2}$	$1.02 \times 10^{-2}$	$1.46 \times 10^{-2}$	$1.88 \times 10^{-2}$	$1.88 \times 10^{-2}$	$1.82 \times 10^{-2}$	$1.86 \times 10^{-2}$

#### 5.4.2 Directional Antenna System

In this section, the spectrum efficiency for SIR<sub>5</sub> is obtained. Table 5.21 shows  $E_s$  for

different  $K$ ,  $N$ ,  $\beta$  and  $f_d$  with AWGN at  $\frac{E_b}{N_o} = 40$  dB.  $K_{opt}$  is 3 for  $f_d T_m \approx 1$ , but is higher for  $f_d T_m \approx 5$  because  $P_s$  is lower for higher values of  $f_d$ . Compared to a very slow fading environment,  $E_s$  is decreased significantly and  $K_{opt}$  is increased.

**Table 5.21: The spectrum efficiency,  $E_s$ , in a directional antenna system (SIR<sub>s</sub>) in a fading environment.**

$K$	$N=1023$ bits		$N=255$ bits			
	$f_d=5$ Hz		$f_d=20$ Hz		$f_d=100$ Hz	
	$\beta = 4$	$\beta = 3$	$\beta = 4$	$\beta = 3$	$\beta = 4$	$\beta = 3$
1	0.135	$9.02 \times 10^{-2}$	$9.12 \times 10^{-2}$	$6.69 \times 10^{-2}$	$1.22 \times 10^{-2}$	$6.08 \times 10^{-4}$
3	0.173	0.111	0.127	$8.10 \times 10^{-2}$	$6.04 \times 10^{-2}$	$1.32 \times 10^{-2}$
4	0.149	0.102	0.110	$7.60 \times 10^{-2}$	$6.99 \times 10^{-2}$	$1.90 \times 10^{-2}$
7	0.116	$7.67 \times 10^{-2}$	$7.25 \times 10^{-2}$	$5.64 \times 10^{-2}$	$6.51 \times 10^{-2}$	$2.82 \times 10^{-2}$
9	$8.37 \times 10^{-2}$	$6.57 \times 10^{-2}$	$5.91 \times 10^{-2}$	$4.90 \times 10^{-2}$	$5.61 \times 10^{-2}$	$3.07 \times 10^{-2}$
12	$6.75 \times 10^{-2}$	$5.41 \times 10^{-2}$	$4.66 \times 10^{-2}$	$3.90 \times 10^{-2}$	$4.56 \times 10^{-2}$	$2.81 \times 10^{-2}$
13	$6.31 \times 10^{-2}$	$5.07 \times 10^{-2}$	$4.36 \times 10^{-2}$	$3.69 \times 10^{-2}$	$4.25 \times 10^{-2}$	$2.78 \times 10^{-2}$

With FEC, the  $E_s$  values are shown in Table 5.22. It can be seen that  $K_{opt}$  is reduced in all cases. For  $K \leq K_{opt}$  with no FEC,  $E_s$  is improved by using FEC. However, compared to the very slow fading case in Table 5.17,  $E_s$  is reduced significantly. From Tables 5.18 to 5.22 for  $N=255$  bits, it can be seen that with no FEC, the  $E_s$  values for  $f_d=20$  Hz is higher than for  $f_d=100$  Hz for all  $K$ . But with FEC,  $E_s$  for  $f_d=20$  Hz is lower than for  $f_d=100$  Hz for  $K > K_{opt}$  obtained from  $f_d=100$  Hz. The reason is that with no FEC, the BKER for  $f_d=20$  Hz is lower than for  $f_d=100$  Hz for the SIR values corresponding to the values of  $K$  considered. However, with FEC, the BKER for

$f_d=100$  Hz is reduced by a greater amount than for  $f_d=20$  Hz because as  $f_d$  increases, the bit errors tend to less bursty.

**Table 5.22: The spectrum efficiency,  $E_s$ , in a directional antenna system (SIR<sub>5</sub>) with FEC in a fading environment.**

$K$	$N=1023$ bits		$N=255$ bits			
	$f_d=5$ Hz		$f_d=20$ Hz		$f_d=100$ Hz	
	$\beta =4$	$\beta =3$	$\beta =4$	$\beta =3$	$\beta =4$	$\beta =3$
1	0.228	0.163	0.143	0.107	$9.28 \times 10^{-2}$	$2.68 \times 10^{-2}$
3	0.181	0.152	0.108	$8.62 \times 10^{-2}$	0.114	$7.14 \times 10^{-2}$
4	0.156	0.129	$8.58 \times 10^{-2}$	$7.27 \times 10^{-2}$	$8.85 \times 10^{-2}$	$7.67 \times 10^{-2}$
7	$9.25 \times 10^{-2}$	$8.54 \times 10^{-2}$	$5.06 \times 10^{-2}$	$4.74 \times 10^{-2}$	$5.10 \times 10^{-2}$	$4.98 \times 10^{-2}$
9	$7.24 \times 10^{-2}$	$6.92 \times 10^{-2}$	$3.96 \times 10^{-2}$	$3.81 \times 10^{-2}$	$3.97 \times 10^{-2}$	$3.93 \times 10^{-2}$
12	$5.44 \times 10^{-2}$	$5.31 \times 10^{-2}$	$2.97 \times 10^{-2}$	$2.91 \times 10^{-2}$	$2.94 \times 10^{-2}$	$2.96 \times 10^{-2}$

## 5.5 Consideration of the Co-channel Interferers in the Second Tier

In previous sections, the spectrum efficiency was determined considering only first-tier co-channel interferers. In this section, the influence of the second-tier co-channel interferers on  $E_s$  and  $K_{opt}$  is investigated for an omnidirectional antenna system with SIR<sub>3</sub>. There are six co-channel interferers in each tier. The mobile receiver are assumed to be received with equal power by all the interferers in each tier. From SIR<sub>3</sub> in Chapter 2, it can be found that the distances from the mobile to the first-tier interferers and the second-tier interferers are  $D$  and  $2D\cos(\frac{\pi}{6})$  respectively.

$E_s$  for different values of  $K$ ,  $\beta$  with  $N=255$  bits and AWGN at  $\frac{E_b}{N_o}=40$  dB in a non-fading

environment is shown in Table 5.23. The corresponding SIR for each  $K$  is obtained from Tables 2.3 and 2.5. The results for a very slow fading environment are shown in Table 5.24.

**Table 5.23:  $E_s$  in a non-fading environment for  $N=255$  and  $\frac{E_b}{N_o}=40$  dB.**

$K$	SIR <sub>3</sub>			
	No FEC		FEC	
	$\beta =4$	$\beta =3$	$\beta =4$	$\beta =3$
1	$3.95 \times 10^{-2}$	$3.04 \times 10^{-4}$	0.126	$5.35 \times 10^{-2}$
3	0.203	0.161	0.119	0.117
4	0.152	0.152	$8.92 \times 10^{-2}$	$8.92 \times 10^{-2}$
7	$8.68 \times 10^{-2}$	$8.68 \times 10^{-2}$	$5.10 \times 10^{-2}$	$5.10 \times 10^{-2}$
9	$6.75 \times 10^{-2}$	$6.75 \times 10^{-2}$	$3.97 \times 10^{-2}$	$3.97 \times 10^{-2}$
12	$5.06 \times 10^{-2}$	$5.06 \times 10^{-2}$	$2.97 \times 10^{-2}$	$2.97 \times 10^{-2}$

With FEC,  $E_s$  is improved for  $K=1$  only. For other values of  $K$ ,  $E_s$  is lower. Compared to the results in Tables 5.1 and 5.4,  $E_s$  is smaller for  $K \leq 3$  because the BKER is higher with 2 tier co-channel interferers (see Section 4.5.2). But for  $K=1$  and  $\beta =3$  with FEC,  $E_s$  is higher than the value in Table 5.4, because the corresponding SIR value for  $K=1$  and  $\beta =3$  is very low, (-0.62 dB), and the BKER with only 1 tier interferers and 2 tier interferers are then equal to 1. However, the BKER after FEC for 2 tier interferers is lower than for 1 tier interferers due to a reduced burstness. For  $K > 3$ ,  $E_s$  has the same value because  $P_s$  is nearly equal to 1.

**Table 5.24:**  $E_s$  for  $SIR_3$  in a very slow fading environment for  $N=255$  and  $\frac{E_b}{N_o}=40$  dB.

$K$	No FEC		FEC	
	$\beta = 4$	$\beta = 3$	$\beta = 4$	$\beta = 3$
1	0.136	$6.38 \times 10^{-2}$	0.134	$7.49 \times 10^{-2}$
3	0.161	0.114	$9.93 \times 10^{-2}$	$8.11 \times 10^{-2}$
4	0.134	0.107	$8.28 \times 10^{-2}$	$7.07 \times 10^{-2}$
7	$8.31 \times 10^{-2}$	$7.16 \times 10^{-2}$	$4.96 \times 10^{-2}$	$4.59 \times 10^{-2}$
9	$6.57 \times 10^{-2}$	$5.88 \times 10^{-2}$	$3.90 \times 10^{-2}$	$3.65 \times 10^{-2}$
12	$4.97 \times 10^{-2}$	$4.61 \times 10^{-2}$	$2.94 \times 10^{-2}$	$2.80 \times 10^{-2}$

From Table 5.24, it can be seen that the FEC used does not improve the spectrum efficiency for any value of  $K$  (except for  $K=1$  and  $\beta=3$ ). The value of  $K_{opt}$  is the same for the non-fading and the very slow fading cases. Compared to Tables 5.9 and 5.12,  $E_s$  is lower for all values of  $K$  due to greater interference. As a general comment, if the second tier co-channel interferers are considered, the spectrum efficiency decreases somewhat, but the optimal value of  $K$  remains unchanged.

## Chapter 6 Conclusions

In this thesis, a simulation model of a communication system with multiple co-channel interferers using NCFSK modulation was developed. This model has been thoroughly tested and validated. The error performance of a cellular *packet data* communication system (in the outbound direction) with multiple co-channel interferers was first investigated. The spectrum efficiency for a number of different SIR models was then evaluated. Finally, the optimal cluster size to maximize the spectrum efficiency for different system configurations and parameters was examined.

The BER and BKER simulation results were presented. In a non-fading channel, the BER was found to increase with the number,  $n_I$ , of co-channel interferers for SIR values above about 2 dB. The BER curves converge to the theoretical curve given by (2.4) in which  $N_o$  is replaced by  $N_{o+i}$ . Therefore, as  $n_I$  increases, the interference signal can be modeled as Gaussian noise of the same PSD value. It was also found that the BKER increases with  $n_I$  for all SIR values considered and are upperbounded by the “theoretical” BKER curve given by (2.7). If we assume that the interference signal is modeled as Gaussian for BKER, the results are pessimistic. Analysis of the CDF and  $P(M,N)$  showed that the burstiness of errors decreases with  $n_I$ .

In a very slow Rayleigh fading channel, the BER is more or less independent of  $n_I$  and is well approximated by (2.14) in which the PSD of the interference signal is assumed to be equal to that of the Gaussian noise. As  $n_I$  increases, the BKER increases towards the theoretical BKER given in (2.16) with  $N_o$  replaced by  $N_{o+i}$ . For large SIR values, the interference signal can be modeled as Gaussian for BKER. With random error correction, the improvement in packet

decoding success rate increases with  $n_I$  because the channel becomes less bursty.

The spectrum efficiency,  $E_s$ , and optimal cluster size,  $K_{opt}$ , in a non-fading (NF), a slow fading (SF) and a very slow fading (VSF) environment were studied. In interference-limited cases, it was found that  $E_s$  tends to increase with the propagation loss exponent,  $\beta$ .  $K_{opt}$  is usually lower for  $\beta=4$  than for  $\beta=3$ . The value of  $K_{opt}$  is not very sensitive to the block length  $N$  for  $N=255$  and 1023 bits, although the  $E_s$  values with  $N=1023$  are always higher than those with  $N=255$ .

In a VSF channel,  $E_s$  is lower than that in a NF channel for all SIR models considered. For both NF and VSF in an omnidirectional antenna system,  $K_{opt}$  is 3, 4 or 7, depending on  $\beta$  and SIR models. In a directional antenna system,  $K_{opt}$  is equal to 1 regardless of the system configurations and parameters. The optimal value of  $E_s$  in the directional antenna system is at least three times more than that in the omnidirectional antenna system. Although the rate 3/4 BCH error correcting code reduces BKER, it does not generally improve the spectrum efficiency in the SIR models considered. However, it tends to lower  $K_{opt}$ .

The SF results show a large degradation in  $E_s$ . As the fading rate increases,  $E_s$  decreases and  $K_{opt}$  increases. In this situation,  $E_s$  can be improved substantially (and  $K_{opt}$  reduced) by using FEC.

Among the related topics for further study are the following:

- (1) To analyze the near-far effect by assuming that a mobile is uniformly distributed in a cell.

- (2) To improve the spectrum efficiency by applying diversity.
- (3) To obtain empirical formulas based on simulation results to estimate the BKER [40]. The

parameters involved are  $f_d$ ,  $\frac{E_b}{N_o}$ ,  $N$  and  $n_I$ .

- (4) To extend the present study to other modulation schemes.

## Glossary

AWGN	- Additive White Gaussian Noise
BKER	- Block Error Rate
BER	- Bit Error Rate
$B_i$	- Bandwidth of interference signal
$B_n$	- Equivalent noise bandwidth
CDF	- Cumulative Distribution Function
$D$	- Minimum distance between two co-channel cells
$E_b$	- Energy per bit
$E_s$	- Spectrum Efficiency
FEC	- Forward Error Correction
$f_d$	- Doppler frequency
$I_o$	- PSD of interference signal
$K$	- Cluster size
NF	-Non-Fading
$N_e$	- Equivalent bandlimited Gaussian noise power
$N_o$	- One-sided PSD of Gaussian noise
$N_{o+i}$	- Sum of $N_o$ and $I_o$
$n_I$	- Number of co-channel interferers
pdf	- Probability Density Function
PSD	- Power Spectral Density
$P_s$	- Probability of successful packet reception

$P(M,N)$	- The probability of more than $M$ bits error in a block of $N$ bits
$R$	- Radius of a cell
$R_b$	- Bit rate
SF	-Slow Fading
SIR	- Signal-to-interference power ratio
VSF	-Very Slow Fading
$\beta$	- Propagation loss exponent
$\gamma$	- Equal to $\frac{E_b}{N_o}$

## Bibliography

- [1] R. Schneiderman, *Wireless Personal Communications*, Piscataway: IEEE Press, 1994.
- [2] R. H. Clarke, "A statistical theory of mobile-radio reception", *Bell System Tech. Journal*, vol. 47, pp. 957-1000, July-Aug. 1968.
- [3] W. C. Y. Lee, *Mobile Communications Engineering*, New York: McGraw-Hill, 1982.
- [4] J. M. Wozencraft and I. M. Jacobs, *Principles of Communication Engineering*, New York: Wiley, 1965.
- [5] H. Suzuki, "A statistical model for urban radio propagation", *IEEE Transactions on Communications*, vol. COM-25, no. 7, pp. 673-680, July 1977.
- [6] A. J. Viterbi and J. K. Omura, *Principles of Digital Communication and Coding*, New York: McGraw-Hill, 1979.
- [7] A. Kegel, W. Hollemans and R. Prasad, "Performance analysis of interference and noise limited cellular land mobile radio", *IEEE 41st Vehicular Technology Conference*, St. Louis, MO, pp. 817-821, May 1991.
- [8] R. Prasad and A. Kegel, "Spectrum efficiency of microcellular systems", *IEEE Vehicular Technology Conference*, St. Louis, MO, pp. 357-361, May 1991.
- [9] R. Prasad and A. Kegel, "Improved assessment of interference limits in cellular radio performance", *IEEE Transactions on Vehicular Technology*, vol. VT-40, no. 2, pp. 412-419, May 1991.
- [10] M. Kerkhoff, J. M. G. Linnartz and R. Prasad, "Spectrum efficiency of packet switched data in mobile cellular networks", *Archiv fur Elektronik und Ubertragungstechnik*, Vol. 48, No. 3, pp. 145-152, May 1994.
- [11] A. Kegel, H. J. Wesselman and R. Prasad, "Bit error probability for fading DPSK signals in microcellular land mobile radio systems", *Electronics Letters*, vol. 27, no. 18, pp. 1647-1648, August 1991.
- [12] Y. D. Yao and A. U. H. Sheikh, "Bit error probabilities of NCFSK and DPSK signals in microcellular mobile radio systems", *Electronics Letters*, vol. 28, no. 4, pp. 363-364, Feb. 1992.
- [13] R. Prasad, A. Kegel and J. Olsthoorn, "Spectrum efficiency analysis for microcellular mobile radio systems", *Electronics Letters*, vol. 27, no. 5, pp. 423-425, Feb. 1991.

- [14] P. P. S. Carter and A. M. D. Turkmani, "Performance evaluation of Rayleigh and log-normal GMSK signals in the presence of cochannel interference", *IEE Proceedings. Part I: Communications, Speech & Vision*, vol. 139, no. 2, pp. 156-164, April 1992.
- [15] A. M. D. Turkmani and P. P. S. Carter, "Software investigation of co-channel interference in a digital cellular radio system", *International Conference on Antennas and Propagation*, York, UK, pp. 169-172, April 1991.
- [16] W. C. Y. Lee, *Mobile Cellular Telecommunications Systems*, New York: McGraw-Hill, 1990.
- [17] C. Leung and R. Gerhards, "Reuse cluster size selection for a mobile packet radio system", *IEEE Pacific Rim Conference*, Victoria, B. C., pp. 230-234, May 1995.
- [18] R. E. Ziemer and W. H. Tranter, *Principles of Communications*, 3rd edition, Boston: Houghton Mifflin, 1990.
- [19] V. H. Macdonald, "The cellular concept", *Bell System Tech. Journal*, vol. 58, pp. 15-41, Jan. 1979.
- [20] W. C. Y. Lee, "Mobile cellular systems conserve frequency resource", *Microwave System News & Comm. Tech.*, vol. 15, no. 7, pp. 139-150, June 1985.
- [21] R. E. Eaves and A. H. Levesque, "Probability of block error for very slow Rayleigh fading in Gaussian noise", *IEEE Transactions on Communications*, vol. COM-25, no.3, pp. 368-374, Mar. 1977.
- [22] J. S. Bird, "Error performance of binary NCFSK in the presence of multiple tone interference and system noise", *IEEE Transactions on Communications*, vol. COM-33, no. 3, pp. 203-209, Mar. 1985.
- [23] J. E. Padgett, C. G. Gunther, and T. Hattori, "Overview of wireless personal communications", *IEEE Communications Magazine*, pp. 28-41, vol. 33, no. 1, Jan. 1995.
- [24] K. S. Shanmugam, *Digital and Analog Communication Systems*, New York: Wiley, 1985.
- [25] W. C. Jakes, Jr., *Microwave Mobile Communications*, New York: Wiley, 1974.
- [26] J. J. Jones, "FSK and DPSK performance in a mixture of CW tone and random noise interference", *IEEE Transactions on Vehicular Technology*, vol. COM-19, no.10, pp. 693-695, Oct. 1970.
- [27] W. C. Y. Lee, *Mobile Communications Design Fundamentals*, 2nd edition, New York: Wiley, 1993.
- [28] A. M. D. Turkmani and M. Ladki, "A study of the error distributions in the wideband mobile radio channel", *IEEE Vehicular Technology Society 42nd VTS Conference*, Denver, CO,

- vol. 1, pp. 355-358, May 1992.
- [29] B. Maranda and C. Leung, "Block error performance of noncoherent FSK modulation on Rayleigh fading channels", *IEEE Transactions on Communications*, vol. COM-32, no.2, pp. 206-209, Feb. 1984.
- [30] M. Abramowitz and I. A. Stegun, *Handbook of Mathematical Functions*, New York: Dover Publications, Inc., 1972.
- [31] J. G. Proakis, *Digital Communications*, 2nd edition, New York: McGraw-Hill, 1989.
- [32] J. K. Cavers and J. Varaldi, "Cochannel interference and pilot symbol assisted modulation", *IEEE Transactions on Vehicular Technology*, vol. VT-42, no. 4, pp. 407-413, Nov. 1993.
- [33] ComDisco System, Inc., *SPW<sup>TM</sup> - The DSP Framework<sup>TM</sup> User's Guide and Tutorial*, Document Version 3.0, Sept. 1992.
- [34] ComDisco System, Inc., *SPW<sup>TM</sup> - The DSP Framework<sup>TM</sup> Designer/BDE<sup>TM</sup> User's Guide*, Document Version 3.0, Sept. 1992.
- [35] L.W. Couch II, *Digital and Analog Communication Systems*, 4th edition, New York: Macmillan, 1993.
- [36] ComDisco System, Inc., *SPW<sup>TM</sup> - The DSP Framework<sup>TM</sup> DSP & BOSS<sup>TM</sup> Communications Library Reference*, Document Version 3.0, Sept. 1992.
- [37] K. Pahlavan and A. H. Levesque, *Wireless Information Networks*, New York: Wiley, 1995.
- [38] S. Lin and D. J. Costello, *Error Control Coding*, New York: Prentice-Hall, 1983.
- [39] A. B. Carlson, *Communication Systems*, 3rd edition, New York: McGraw-Hill, 1986.
- [40] C. Leung and J. Ng, "Estimation of Block Error Rates for NCFSK Modulation on a VHF/UHF Mobile Radio Channel", *IEEE Transactions on Communications*, vol. COM-38, no. 2, pp. 46-49, May 1989.
- [41] L. Wang, "Error Probability of a Binary Noncoherent FSK System in the Presence of Two CW Tone Interferers", *IEEE Transactions on Communications*, vol. COM-22, no. 4, pp. 1948-1949, Dec. 1974.
- [42] C. Sunderg, "Block Error Probability for Noncoherent FSK with Diversity for Very Slow Rayleigh Fading in Gaussian Noise", *IEEE Transactions on Communications*, vol. COM-29, no. 1, Jan. 1981.
- [43] F. G. Stremler, *Introduction To Communication Systems*, 2nd edition, Massachusetts: Addi-

son-Wesley, 1982.

[44] W. Beyer, *CRC Standard Mathematical Tables*, 27th edition, Florida: CRC Press, 1984.



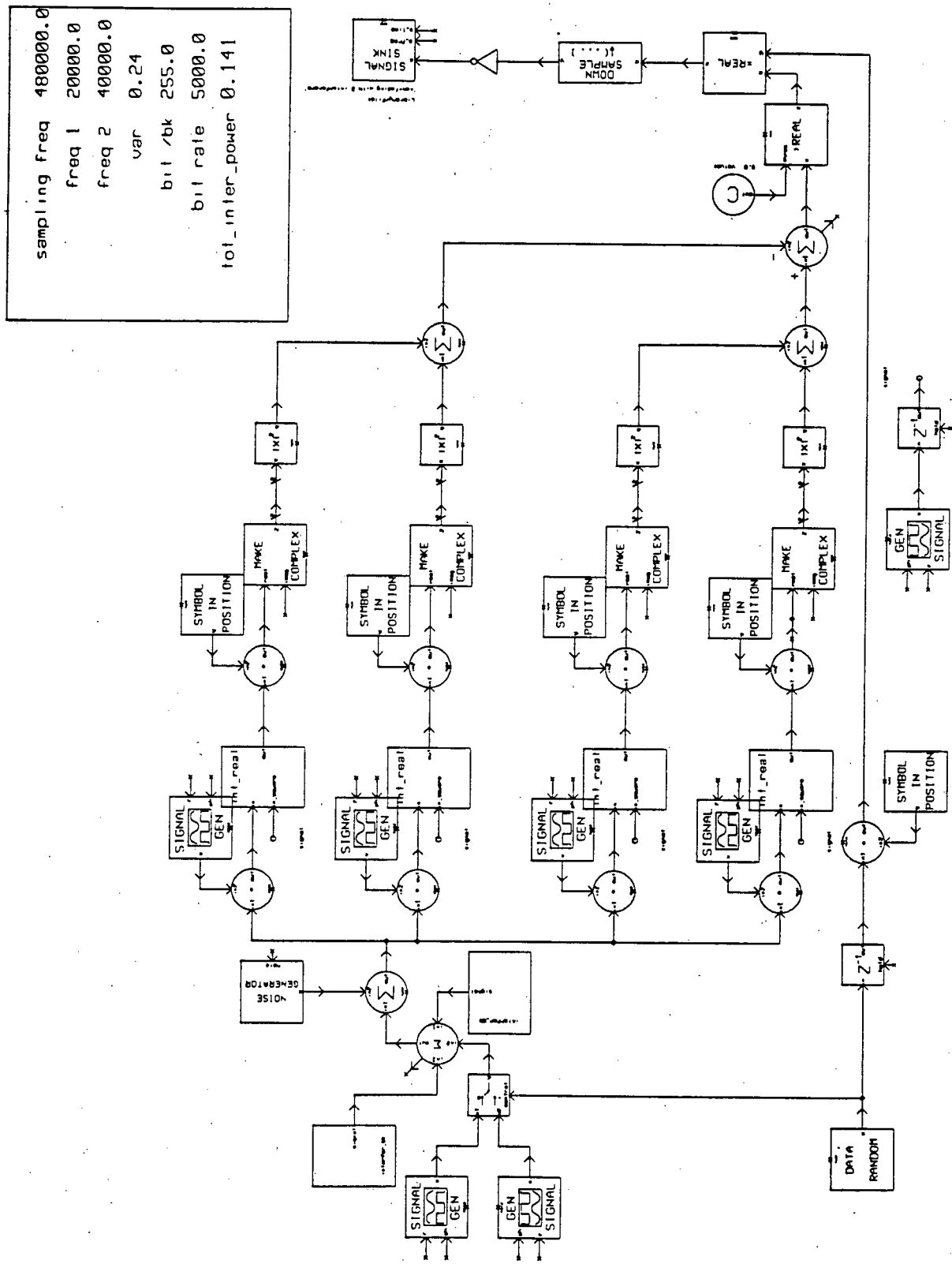


Figure A.2 Communication model with 2 co-channel interferers in a non-fading environment.



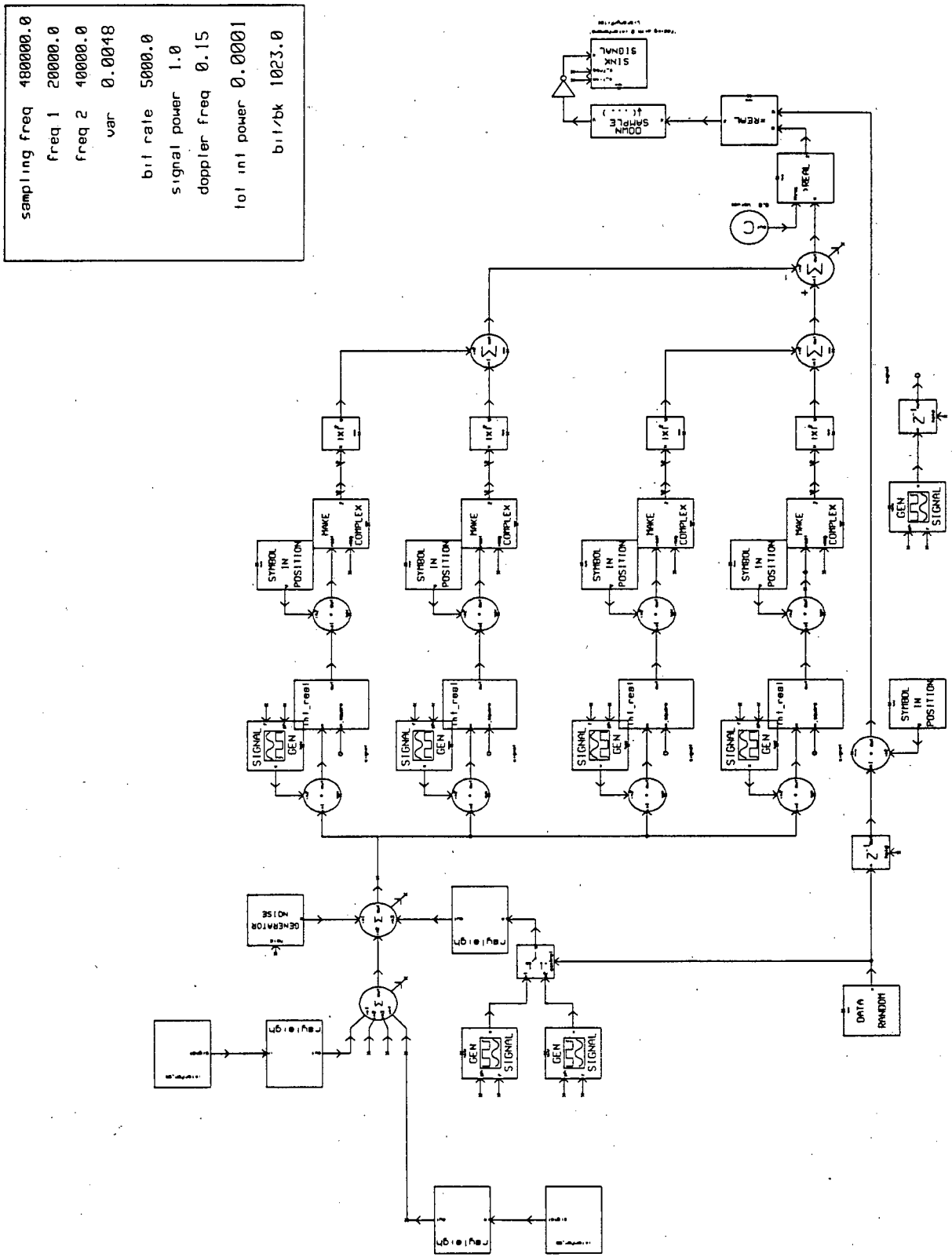


Figure A.4 Communication model with 2 co-channel interferers in a Rayleigh fading environment.

## Appendix B Derivation of BER in Rayleigh Fading

The BER equation in slow Rayleigh fading with an arbitrary number of co-channel interferers is derived. Assume that the co-channel interference signals are bit synchronized with the desired signal and no background noise. In a slow fading environment, the amplitude and phase of the signals do not vary substantially during a bit time duration and the signals add vectorially. Since both desired and interference signals have a complex Gaussian distribution, vector addition of the signals results in a sum signal with a Rayleigh amplitude distribution and an exponential power distribution. Thus, the power at the output of the detector in each channel has an exponential distribution and the pdf for the instantaneous power,  $p_i$ , is

$$f_{P_i}(p_i) = \frac{1}{\mu_i} e^{-\frac{p_i}{\mu_i}} \quad \text{for } i=0 \text{ or } 1, \quad (\text{B.1})$$

where  $\mu_0$  and  $\mu_1$  are the mean powers at the output of detector for channel '0' and channel '1' respectively. Without loss of generality, assume that the desired signal sent is a '1'. The probability of error is defined as

$$Pr(\text{error} \mid \text{desired signal is '1'}) = \sum_l Pr(\text{error} \mid l \text{ interferers send '0'}) Pr(l), \quad (\text{B.2})$$

where  $Pr(l)$  is the probability that  $l$  co-channel interferers send a '0' and is given by

$$Pr(l) = \binom{n}{l} 2^{-n} \quad (\text{B.3})$$

where  $n$  is the total number of co-channel interferers.

Then  $Pr(\text{error} \mid l \text{ interferers send a '0'})$  is given by

$$Pr(\text{error} \mid l \text{ interferers send a '0'}) = Pr(P_0 > P_1)$$

$$\begin{aligned} &= \int_0^{\infty} \int_0^{\infty} f_{p_1} f_{p_0} dp_0 dp_1 \\ &= \frac{1}{\mu_0 \mu_1} \int_0^{\infty} e^{-\frac{p_1}{\mu_1}} \int_0^{\infty} e^{-\frac{p_0}{\mu_0}} dp_0 dp_1 \\ &= \frac{1}{\mu_1} \int_0^{\infty} e^{-p_1 \left( \frac{1}{\mu_1} + \frac{1}{\mu_0} \right)} dp_1 \\ &= \frac{\mu_0}{\mu_1 + \mu_0} \left[ -e^{-p_1 \left( \frac{\mu_1 + \mu_0}{\mu_1 \mu_0} \right)} \right]_0^{\infty} \\ &= \frac{\mu_0}{\mu_1 + \mu_0}. \end{aligned} \tag{B.4}$$

Let  $\mu_i$  and  $\mu_d$  be the mean power of the interference signal and the desired signal respectively.

Then,  $\mu_0 = l\mu_i$  and  $\mu_1 = \mu_d + (n-l)\mu_i$  and (B.4) becomes

$$Pr(\text{error} \mid l \text{ interferers send '0'}) = \frac{l\mu_i}{\mu_d + n\mu_i}. \tag{B.5}$$

The probability of error in (B.2) becomes

$$\begin{aligned} Pr(\text{error} \mid \text{desired signal is '1'}) &= \sum_{l=0}^n \frac{l\mu_i}{\mu_d + n\mu_i} \times \binom{n}{l} 2^{-n} \\ &= \frac{\mu_i}{\mu_d + n\mu_i} 2^{-n} \sum_{l=0}^n l \binom{n}{l} \end{aligned}$$

$$\begin{aligned}
&= \frac{\mu_i}{\mu_d + n\mu_i} 2^{-n} n \sum_{l=0}^n \binom{n-1}{l-1} \\
&= \frac{\mu_i}{\mu_d + n\mu_i} 2^{-n} n \sum_{m=0}^{n-1} \binom{n-1}{m} \\
&= \frac{\mu_i}{\mu_d + n\mu_i} 2^{-n} n 2^{n-1} \\
&= \frac{\mu_i}{\mu_d + n\mu_i} \times \frac{n}{2} \\
&= \frac{1}{2 + 2 \times \frac{\mu_d}{n\mu_i}}.
\end{aligned} \tag{B.6}$$

where  $\frac{\mu_d}{n\mu_i}$  is the average desired signal-to-interference signal power ratio (SIR). Since

$$Pr(\text{error} \mid \text{desired signal is '0'}) = Pr(\text{error} \mid \text{desired signal is '1'}), \tag{B.7}$$

the average probability of error is given by

$$Pr(\text{error}) = \frac{1}{2 + 2 \times SIR}. \tag{B.8}$$

(B.8) shows that for a given SIR value, the BER does not depend on  $n$ . This agrees with the observation in Section 4.3.1. As discussed in Section 4.3.1, the BER with (unsynchronized) co-channel interference signal in a Rayleigh fading environment can be approximated by (2.14) in which  $N_o$  is replaced by  $N_{o+i}$ . For the case of no background noise, the BER can be approximated by

$$P_e = \frac{1}{2 + \frac{E_b}{I_o}}. \tag{B.9}$$

The simulation results for (1) one synchronized and (2) one unsynchronized co-channel interferer are shown in Figure B.1 and compared with the results obtained from (B.8) and (B.9). It can be seen that the BER for one synchronized interferer agrees closely with (B.8). The BER for one unsynchronized interferer can be approximated by (B.9). The BER with an synchronized interferer is slightly higher than with an unsynchronized interferer.

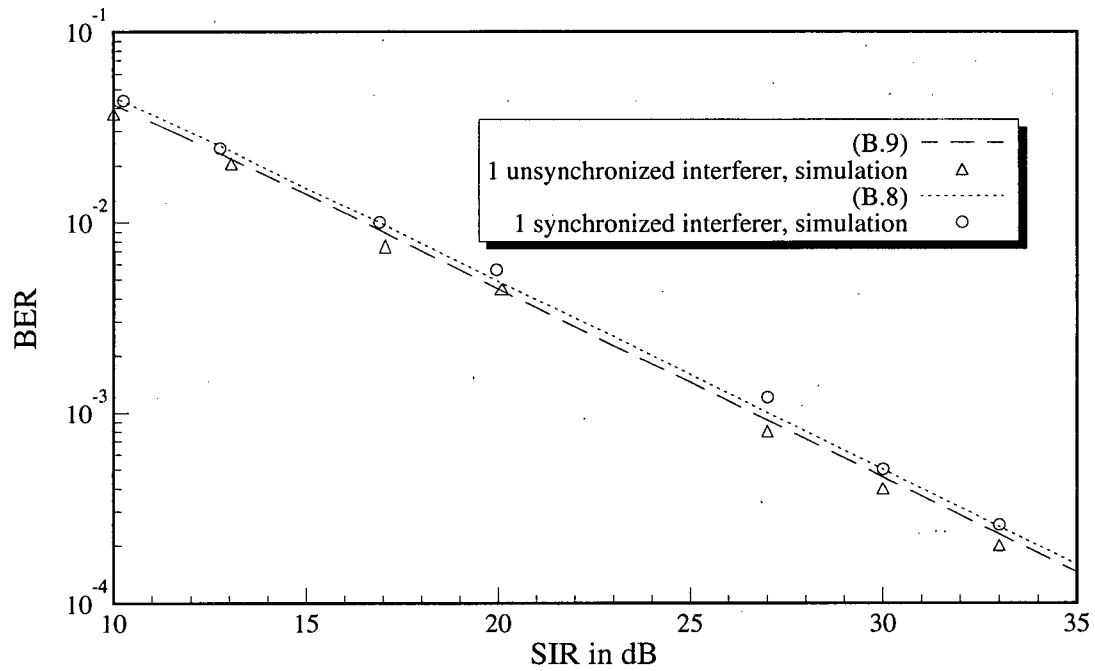


Figure B.1 The BER for one synchronized and unsynchronized co-channel interferer in a slow Rayleigh fading channel with no background noise.